Durham E-Theses

Electrons in the cosmic radiation

Xinyu Chi

How to cite:

Chi, Xinyu (1990) Electrons in the cosmic radiation. Doctoral thesis, Durham University.

Use policy

Electrons in the Cosmic Radiation

by

Xinyu Chi
B. Sc., M. Sc.

A thesis submitted to the University of Durham
for the Degree of Doctor of Philosophy

September, 1990

Abstract

The nature of cosmic ray electrons and their radiation in the Universe has been studied. A convection associated diffusion model is proposed to describe the main characteristics of the large-scale distribution of cosmic ray electrons in the Galaxy: (1) a small Galacto-centric radial gradient; (2) spectral flattening with Galactic latitude; and (3) an extensive halo above the Disk.

A new derivation of the interstellar radiation field indicates the existence of an inverse Compton γ-ray halo. This γ-ray halo can contribute up to 60% of the observed diffuse Galactic γ-ray flux at intermediate latitudes and also accounts for the spectral flattening with latitude. This result leads to a new estimate of the extragalactic γ-ray background flux.

An energy equipartition theory is proposed for the global correlation between radio power and far-infrared luminosity for spiral galaxies, in which the dynamical role of cosmic rays in galactic evolution is implied. The model successfully explains the non-unity slope of the correlation and predicts the escape of cosmic ray electrons from our Galaxy.

The interstellar flux of MeV cosmic ray electrons is derived from γ-ray data. The flux is found to be surprisingly high and a new type of source is required. The lower hybrid plasma instability initiated by stellar winds is suggested to be the acceleration mechanism. This high flux of electrons is sufficient to account for the interstellar ionization and heating in HI regions.

Features of the local Galactic magnetic field are revealed by analysing pulsar rotation measure data. The large scale regular field is found to be in a bisymmetric configuration and to be stronger in the interarm region (3 μG) than in the arm region (1 μG). The derived small-scale irregular field is shown to have a dominant strength of 6 μG.

i

Preface

The work presented in this thesis was carried out between 1988 and 1990 while the author was a research student under the supervision of Professor A.W. Wolfendale, F.R.S., in the Physics Department at the University of Durham. None of the material here has been submitted previously for a degree at this or any other university. Although the original ideas of the work were contributed by both the author and his colleagues (mainly Professor Wolfendale), the calculation and interpretation have been performed almost entirely by the author.

Some of the results presented here have been published as follow:

Chi, X. et al.: 1989, *Inverse Compton Contribution to Medium-latitude Galactic Gamma-ray Emission*, J.Phys. G: Nucl. Part. Phys. **15**, 1495.

Chi, X. and Wolfendale, A.W.: 1989, *Extragalactic Gamma-rays*, J. Phys. G: Nucl. Part. Phys. **15**, 1508.

Chi, X. and Wolfendale, A.W.: 1990, *Implications of the Correlation between Radio Continuum and Far Infrared Emission for Spiral Galaxies*, Mon. Not. R. astr. Soc. **245**, 101.

Chi, X. and Wolfendale, A.W.: 1990, *Features of the Local Galactic Magnetic field*, J. Phys. G: Nucl. Part. Phys. **16**, 1409.

Chi, X. and Wolfendale, A.W.: 1990, *Ionization and heating of the interstellar HI regions by low energy cosmic ray electrons*, in Proc. IAU 144. Symposium on The Interstellar Disk-Halo Connection in Galaxies, ed. H. Bloemen, Kluwer Academic Publishers, Dordrecht, in press.

Chi, X. and Wolfendale, A.W. 1990, *The Interstellar Radiation Field*, in Proc. IAU 144. Symposium on The Interstellar Disk-Halo Connection in Galaxies, ed. H. Bloemen, Kluwer Academic Publishers, Dordrecht, in press.

Contents

Chapter 1

Introduction

The discovery of cosmic rays ranks among the greatest events that have happened in Physics during the first quarter of this century. In 1912, Victor Hess, for the first time, made convincing balloon borne measurements of gas ionization in the atmosphere. He observed that the ionization rate first decreased slightly and then increased rapidly with altitude, persisting up to the highest altitude (5 km). This result clearly showed the ionization agent to be coming from extraterrestrial space. At the time, the highly penetrating cosmic rays were believed to be γ-rays, which were the most penetrating radiation then known.

It was not until the late 1920s that the identification of cosmic rays was achieved by the application of new techniques. Skobeltzyn (1927) applied the cloud chamber to cosmic ray research and observed tracks of charged particles. Bothe and Kolhörster (1928) used Geiger-Müller counters to identify charged particles which penetrated two or more counters. These experiments unambiguously demonstrated the charged-particle nature of cosmic rays. Meanwhile, the latitude effect of cosmic rays, observed by Clay (1927), provided further evidence for their charged nature. Later, the observations of the east-west asymmetry of cosmic rays (Johnson, 1933; Rossi, 1934) led to the conclusion that the majority of the primary cosmic radiations consisted of positively charged particles, mainly protons.

From the 1930s to the 1950s, the significance of cosmic ray studies lay mainly in its high energy physics aspect, cosmic rays were used as a source of energetic particles in searches for new particles. Indeed, cosmic ray physics experienced a splendid period, many important discoveries were made in cosmic ray experiments. Anderson (1932), using a cloud chamber, discovered the first anti-particle—the positron—which had been predicted by Dirac's theory of Quantum Electrodynamics, in cosmic rays. In 1937, two groups working independently (Neddermeyer and Anderson, 1937; Street and Stevenson,

1937), discovered the intermediate mass particles—the mesons. In the following years, a series of experiments were carried out to study the nature of these mesons. Lattes, Occhialini and Powell (1947), from several events in emulsion experiments, found proof for the existence of two different kinds of meson: the π-meson and the μ-meson. Immediately afterwards, another important discovery came about: Rochester and Butler (1947) found two events of V-particles, now known as 'strange particles'. In the early 1950s, the study of strange particle properties was a central topic in Cosmic Ray Physics.

From the middle of the 1950s, however, the significance of cosmic ray study turned gradually towards the astrophysical aspect, largely the problem of the origin of cosmic rays. The reasons for this are two-fold: firstly, the development of space techniques made it possible to directly measure the primary cosmic ray spectrum and composition above the atmosphere and the relevant astronomical information on the interstellar medium was already available; secondly, laboratory accelerators began to operate and the particle beams had the great advantage of comprising particles of unique type and energy unlike the cosmic ray particle beams; Cosmic rays had therefore to give way to the accelerators in particle physics experiments, except perhaps, at the very highest energies.

The birth of cosmic ray astrophysics was marked by the establishment of a connection between cosmic radio emission and cosmic rays. Kiepenheuer(1950) and Ginzburg(1951) suggested that the Galactic radio emission was a result of the synchrotron emission of relativistic electrons (the electron component of cosmic rays) moving in the Galactic magnetic field. It is this connection that determines one of the most important aspects of the astrophysical nature of the subject. Cosmic ray astrophysics possesses the characteristic of astrophysics, *i.e.* the solution to problems is to start with the observational data and carry out an analysis using a combination of all the information obtained by different methods. Here, radio astronomy provides an important approach to the solution of the origin of cosmic rays; by considering cosmic radio emission it is possible to establish certain properties of cosmic rays both in the Galaxy and in the Universe as a whole. A prominent example is the interpretation of the Galactic radio emission data in terms of a cosmic ray halo (Ginzburg, 1953).

Since the electron component of cosmic rays is observed to exist universally from radio observations—in supernova remnants, in the Galaxy in general and in other galaxies—it is natural to suppose that the nuclear component is also generated by the same sources and exists universally. In the 1950s and 1960s, a variety of experimental methods were developed to measure the spectrum and composition. The balloon and satellite-borne ioniza-

tion calorimeters were designed for direct measurements; the ground-based extensive air shower arrays, Cerenkov light detectors and the underground muon-detectors were designed for indirect measurements. The results from all these experiments consistently suggested a power-law spectrum for the primary cosmic rays, while the direct measurements registered the presence of nuclei of all the elements (at low energies) from hydrogen to uranium, as well as the electron and the positron.

The interpretation of these observational results needs astronomical and physical information. Firstly, what kind of astrophysical objects could generate high energy particles? Secondly, what is the structure of the Galactic magnetic field and the distribution of the interstellar medium through which the particles pass? Thirdly, what is the mechanism by which cosmic rays interact with interstellar gas nuclei and photons? The answers to these questions are difficult. They have been pursued for decades, and the search still continues.

One of the earliest speculations about the origin of cosmic rays came from F. Zwicky in 1933 (no formal publication), who suggested that cosmic rays were generated in supernova explosions. Based on their balloon-borne measurements of the energy spectrum, which at that time consisted of several knees at the energies corresponding to the rest energies of light nuclei, Millikan et al. (1942) proposed that cosmic rays come from the spontaneous annihilation of nuclei, such as carbon, nitrogen and oxygen. Klein (1944) pursued this idea further and proposed that the energy released from the annihilation of galaxies and antigalaxies (composed of antimatter) could produce cosmic rays. Hoyle (1947) studied the possibility of converting potential energy into kinetic energy in supernova outbursts and suggested that the energy released might account for the energy density of cosmic rays. However, the discovery of heavy nuclei in primary cosmic rays (Bradt and Peters, 1948; Freier et al., 1948a,b) ruled out the possibility of cosmic rays being produced in violent process such as mass annihilation. Moreover, the measured element abundance of cosmic ray nuclei was found to be similar to the Galactic abundance, indicating that the generation of cosmic rays occurs in ordinary parts of the Galaxy, rather than requiring extraordinary conditions. Unfortunately, the existence of the Galactic magnetic field seriously hampers the problem. Direct tracing of a charged particle to its source is impossible, since, in the presence of a magnetic field (particularly a disordered field), the charged particle does not travel along a straight line but along a tortuous path. We will return to this question later when discussing the propagation problem.

In view of the observed ejection of high energy particles from solar flares, a solar origin of cosmic rays was proposed by Richtymer and Teller (1949).

However, the acceleration mechanism appears unable to generate particles with energies higher than 10^{11} eV and the total energy output from all stars in the Galaxy is far less than that required to give the observed energy density of cosmic rays. In an attempt to explain the power law spectrum, Fermi (1949) proposed a stochastic acceleration mechanism, in which a charged particle gains energy by repeated collisions with magnetic clouds. Detailed calculations show that the efficiency of this process—a process termed second-order Fermi acceleration—is too low to achieve the required energy density of cosmic rays. There is the same efficiency problem with the betatron acceleration theory given by Alfvèn (1950). Before the 1970s, no working mechanism for Galactic cosmic ray acceleration was proposed, although the supernova origin was a promising one from the energetics point of view.

As an alternative to the Galactic origin of cosmic rays, one could propose an extragalactic origin. The observations of strong extragalactic radio sources, particularly the radio galaxies, supported this suggestion. Burbidge (1956) showed that the acceleration efficiency per unit volume in a number of strong radio sources seems to be as high as that of the Crab Nebula. From energetics considerations, the extragalactic cosmic rays could contribute a fraction of the nuclear component of the observed cosmic rays, at least to the high energy part as observed by the extensive air shower arrays (Fujimoto, 1964), extragalactic electrons are excluded from the Galaxy by the 2.7 K cosmic microwave background. If cosmological evolution is included, as in some models (*e.g.*, Hillas, 1968), the contribution of the extragalactic cosmic rays will increase.

As mentioned earlier, the propagation process has to be accounted for in the exploration of the origin of cosmic rays because of the existence of the Galactic magnetic field and the nature of the interstellar medium. When cosmic rays propagate in interstellar space, their intensity, elemental composition and spectral shape will all be changed with respect to that at injection. The gyroradius of a proton of a few GeV in a magnetic field of a few μG is only $\sim 10^{-6}$ pc, much smaller than the presumed scale of the interstellar field, so that the motion of the bulk of cosmic rays is along the field lines. The inhomogeneities in the field act as scattering centres and change the direction of particle motion. This process can be approximated as spatial diffusion. At the same time, cosmic ray particles interact with the interstellar medium. Cosmic ray nuclei collide with gas nuclei and fragment into lighter nuclei; whilst the electrons suffer energy loss from bremsstrahlung, synchrotron radiation and inverse Compton scattering. In view of the observed near-isotropy of arrival direction, cosmic ray propagation can be described in term of 3-dimensional diffusion (Ginzburg and Syrovatskii, 1964). The propagation equation includes a source function term, a spatial diffu-

4

sion term and fragmentation (for nuclei) or energy loss (for electrons) term, together with boundary conditions.

The interaction process is better known than the spatial diffusion process. The data on nuclear fragmentation cross-sections are available from accelerator experiments, and the energy loss rate of electrons can be calculated directly from the formulae of Quantum Electrodynamics. Such knowledge was available in the 1960s.

The 1970s saw many great achievements in cosmic ray astrophysics. The launch of the SAS-II γ-ray satellite in 1972 opened a new window on the Universe. γ-ray astronomy is closely related to cosmic ray astrophysics because the diffuse Galactic γ-rays mainly result from the interactions of cosmic rays with the interstellar matter and the photon fields (the Galaxy is transparent to γ-rays). Dodds *et al.* (1975) derived a galacto-centric radial gradient of cosmic ray intensity from the SAS-II data. This result rules out the hypothesis that cosmic rays in the GeV range are universal, as had been advanced by Brecher and Burbidge (1972). Also from the SAS-II data, Fichtel *et al.* (1978) found an indication for the existence of a Galactic γ-ray halo.

Cosmic ray propagation in the magnetized interstellar medium was widely studied. Many propagation models were proposed to account for a number of observational facts such as the power law spectrum, the low anisotropy and the abundances of primary and secondary nuclei. These models can be classified as: (a) the closed model; (b) the leaky-box model; (c) the pure diffusion model; (d) the dynamical halo model; and (e) the continuous acceleration model. The leaky-box model was a popular one at that time.

The physical background for diffusion in the leaky-box model was extensively investigated. To diffuse cosmic rays efficiently, the process should work on the scale comparable to their gyroradius. A 'collective effect' was formulated by Wentzel (1974) as the working model, in which cosmic rays are resonantly scattered off self-excited Alfvén waves in a magnetized plasma. The same mechanism was also used to explain the self-confinement of cosmic rays by Skilling (1971), a physical realization of the leaky-box model. In this model, due to the large scale density gradients at the borders of the Galactic Disk, the outward streaming of cosmic rays can excite Alfvén waves, these waves in return scatter off cosmic ray particles from the outward stream.

As an alternative to the self-confinement theory, it was proposed that there is diffusion due to an interstellar spectrum of hydromagnetic waves generated by other sources. If a spectrum of hydromagnetic waves exists, it could force cosmic rays to stream at a velocity less than the Alfvén velocity, so that the instability discussed above would not occur. Lee and Jokipii (1976) speculated that a Kolmogorov spectrum of hydromagnetic waves may exist in the interstellar medium, with scales extending from $10^{11} \sim 10^{19}$ cm.

The cosmic ray diffusion coefficient would then vary with particle energy as $D \propto E^{1/3}$.

The escape of cosmic rays from the Galaxy is determined by the boundary conditions, *i.e.* the configuration of the Galactic magnetic field above the Disk. Piddington (1972) suggested that if the Galactic magnetic field results from the compression of an extragalactic field of 10^{-2} μG, the two fields would still be connected. Therefore, cosmic rays would escape from the Galaxy along the continuous magnetic lines. Parker (1973) argued that a field of such configuration is unstable, and suggested that the field should be mainly parallel to the Galactic Disk and the field lines be closed. The route for cosmic ray escape would then be through magnetic bubbles which are inflated by cosmic ray pressure (Jokipii and Parker, 1969).

Different pictures of cosmic ray escape from the Galaxy are provided by the Galactic wind model and the dynamical halo model. Ipavich (1975) tackled the problem of cosmic ray escape with outward flows from the Galaxy. He found that the cosmic rays could transfer sufficient outward momentum to the gas to drive a Galactic wind. In this model, cosmic rays are assumed to be constrained to stream at the Alfvèn velocity by the self-generated waves and the waves are assumed to be dissipated slowly, so that cosmic rays propagate in a convective way. Jokipii (1976) proposed a dynamical halo model which combines the main features of Parker's bubble model and Ipavich's wind model, and so allows a comparison with observational facts. In this one-dimensional model, cosmic rays are generated in the Disk and diffuse along the Galactic magnetic field lines. In the halo, the scattering centres responsible for the diffusion are convected outwards, the cosmic ray intensity falling to zero at the boundary.

A particularly important result was the achievement of cosmic ray lifetime measurements. The life-time is a crucial parameter for the judgement of cosmic ray confinement and escape. The measurements of the abundance of the unstable isotope ^{10}Be in the cosmic ray nuclear composition led to an estimate of the life-time $\sim 2 \times 10^7$ yr (Garcia-Munoz *et al.*, 1977). This result rules out the closed model of propagation (Rasmussen and Peters, 1975) since the cosmic ray life-time (10^7 yr) is much smaller than the life-time of the Galaxy (10^{10} yr). However, it has to be stated that the homogeneous model is used in determining the life-time and in fact could be changed by a factor of up to 5 if other models are used.

In the later 1970s, a promising model involving acceleration by supernova remanent shock waves was formulated (Axford *et al.*, 1977; Bell, 1978a,b; Blandford and Ostriker,1978). In this mechanism, fast particles gain energy from the crossings between upstream and downstream regions of a shock front. The particles are prevented from streaming away upstream by scat-

tering off Alfvèn waves which they themselves generate, and from streaming away downstream by scattering off turbulent hydromagnetic waves in the shock wake. The resultant energy spectrum is a power law with a differential index close to 2 (actually a little higher). This acceleration process is efficient for particles gaining energy, and is called first-order Fermi acceleration. Taking the energetics of supernovae into account, this mechanism can be responsible for the origin of the Galactic cosmic rays in the energy range $10^9 \sim 10^{14}$ eV (above 10^{14} eV, it is incapable of accelerating particles because of the limited scale of shock waves).

Continuing into the 1980s, further achievements were made in cosmic ray astrophysics. Observationally, the nuclear composition of cosmic rays was measured up to an energy of a few hundred GeV per nucleon, from light nuclei to Fe in a number of experiments. Beyond this directly measurable energy range ($> 10^{14}$ eV), a total particle spectrum is given by the extensive air-shower measurements, and a mixed origin model was gradually established which incorporates both propagation effect and contributions from different sources (*e.g.*, Gawin *et al.*, 1984; Fichtel and Linsley, 1986; Wdowzcyk and Wolfendale, 1989). This model is supported by the measurements of muon content in extensive air showers (Blake *et al.*, 1990). The relationship between traversed grammage and particle energy was established (Garcia-Munoz *et al.*, 1987). A few hundred extremely high energy events ($> 10^{19}$ eV) were accumulated from extensive air shower experiments in both the northern and southern hemispheres. The all sky radio survey at 408 MHz was completed (Haslam *et al.*, 1981a,b). An analysis of the data revealed a radio halo above the disk (Phillipps *et al.*, 1981). The γ-ray data from the COS-B satellite yielded many interesting features of cosmic ray intensity variation in the Galaxy. The Galacto-centric radial gradient of cosmic ray intensity seen by the SAS-II satellite was confirmed, most importantly for the proton component (Bhat *et al.*, 1986). The spectrum of the diffuse γ-rays was found to be flatter in the Outer Galaxy than in the Inner Galaxy (Bloemen, 1987). Further evidence for the γ-ray halo was established (Chi *et al.*, 1989).

In the theoretical area, a solution to the dynamical halo model was derived to explain the spectral shape of cosmic ray electrons, particularly the bending point at about 10 GeV, and the spectrum in the halo (Lerche and Schlickeiser, 1982). An implication of the cosmic ray halo is that it may be supported by cosmic ray pressure against gravity (Chevalier and Fransson, 1984; Hartquist and Morfill, 1986).

The idea of the continuous acceleration of cosmic rays by supernova remnants in the interstellar space was considered by Blandford and Ostriker (1980), and developed by a number of workers (*e.g.*, Wandel *et al.*, 1987;

Letaw *et al.*, 1987; Giler *et al.*, 1989). This process can give an elegant explanation of both the smoothness of the cosmic ray spectrum and the energy dependence of the secondary to primary ratio in the observed nuclear composition.

In the above brief review, all the components of the cosmic radiation were considered together, not distinguishing the electron component. We now focus on the electron component. As mentioned earlier, the existence of the electron component was demonstrated by radio observations in the early 1950s, but the direct registration of primary cosmic electrons did not come until 1961 when two groups independently recorded electrons in their balloon experiments (Earl, 1961; Meyer and Vogt, 1961). The first charge separation of cosmic ray electrons into 'negatrons' and positrons was achieved in 1964 (De Shong *et al.*, 1964). Since then both direct measurements (balloon and satellite experiments) and indirect measurements (radio and γ-ray observations) have been carried out extensively to obtain the intensity, spectrum and charge ratio e^+/e^- (see *e.g.*, summaries by Webber, 1983; Müller and Tang, 1987).

The measured electron flux in the energy range above 0.1 GeV is only about three percent of the total cosmic ray flux. The positron flux is 10% of the total electron flux and these particles are thought to be mainly secondary particles produced in the nuclear interactions of cosmic ray nuclei with the interstellar gas nuclei. As a component of cosmic rays, the electrons are, quite reasonably, assumed to be accelerated in the same process and to propagate in the same way as those nuclei with the same rigidity. Therefore the acceleration mechanism and propagation models discussed above are applicable to the electrons. However, being high charge to mass ratio particles, electrons lose their energy easily. In the interstellar environment, the energy loss time is comparable to the life-time of confinement for GeV electrons, so that the energy loss processes have to be taken into account. It is just from these energy loss processes that nonthermal radiations appear, and provide important information on the origin of cosmic rays. Various aspects of the nature of cosmic ray electrons comprise the main topics in the following chapters. Here we briefly summarize the experimental results:

1. Data from direct measurements show a power law spectrum with differential index 3.3 above 10 GeV and 2.4 below 10 GeV, with increased uncertainty below 1 GeV.

2. The e^+/e^- ratio is a function of energy: it decreases from 40% to 5% with energy increasing from 0.1 GeV to 4 GeV, and then increases again.

8

3. Radio data indicate a power law spectrum; below 400 MHz the differential power spectrum index is 0.62, above this frequency the index is 0.8.

4. γ-ray data indicate that the spatial distribution of cosmic rays in the Galaxy is fairly smooth.

Nearly 80 years have passed since the discovery of cosmic rays. The effort towards understanding these energetic particles in the Universe is far from finished and a new era is just opening with the forthcoming launch of NASA's Gamma Ray Observatory. In this thesis the role of electrons in the cosmic nonthermal radiation is presented, together with recent work in this field by the author and his colleagues. Chapter 2 discusses the Galactic electrons above 100 MeV. A new propagation model involving diffusion and convection is proposed and the electron distribution in the Galaxy is derived. The resultant spectral variations of synchrotron radiation and γ-rays are explained. Chapter 3 deals with Galactic electrons below 100 MeV. An acceleration mechanism is suggested to account for the low energy electron excess implied by observations of diffuse low energy γ-rays. The implications of this model for interstellar heating, ionization and chemical reactions are discussed.

Chapter 4 discusses the problem of electron escape from the Galaxy and its implication for extragalactic γ-rays and for γ-rays in the halo. Chapter 5 discusses the problem of electrons in other galaxies. An energy equipartition model is put forward to explain the widely existing correlation between radio power and far infrared luminosity for spiral galaxies. The implication of this phenomenon is discussed. Chapter 6 analyses the features of the local Galactic magnetic field. As an application, the propagation of the highest energy cosmic rays is discussed. Finally, in Chapter 7 conclusions and prospects for the future are given.

Chapter 2

Galactic Electrons above 100 MeV

In this chapter we first make a brief review of the key observational results pertaining to cosmic ray electrons in this energy range, then focus on their generation and propagation in the Galaxy, and finally discuss their interactions with the Galactic magnetic field and the interstellar radiation field which result in radio synchrotron emission and γ-ray emission, respectively.

2.1 The observational results

Particles in this energy range are those usually referred to as cosmic rays in the usual sense; they are relatively well measured and the results from different measurements are in good agreement. Direct measurements have already covered the electron energy spectrum from 100 MeV up to 2000 GeV. Below several GeV the measured flux near the Earth is, however, rather uncertain due to the effect of solar modulation; above 2000 GeV the incoming flux is too low to obtain a sufficient counting rate. Figure 2.1 gives a summary of the results from different experiments. The integral flux of the electrons constitutes only about one per cent of the total cosmic ray flux and the energy density is 0.012 eVcm^{-3}, about 3% of the total. A distinctive feature of this spectrum is that above 10 GeV it drops much faster than that of any nuclear species and can be fitted with a differential power-law with index 3.3. No convincing explanation for this spectral steepening has been put forward despite some attempts in terms of energy loss, of acceleration deficiency and of an excess of secondary electrons.

Measurements of the positron fraction, $e^+/(e^- + e^+)$, cover only a limited energy range, from 0.1 GeV to 30 GeV. Figure 2.2 shows the experimental data. The results of different groups are consistent below 4 GeV but diverse above this energy. Compared to model predictions, an excess appears in the

low energy range (below 1 GeV).
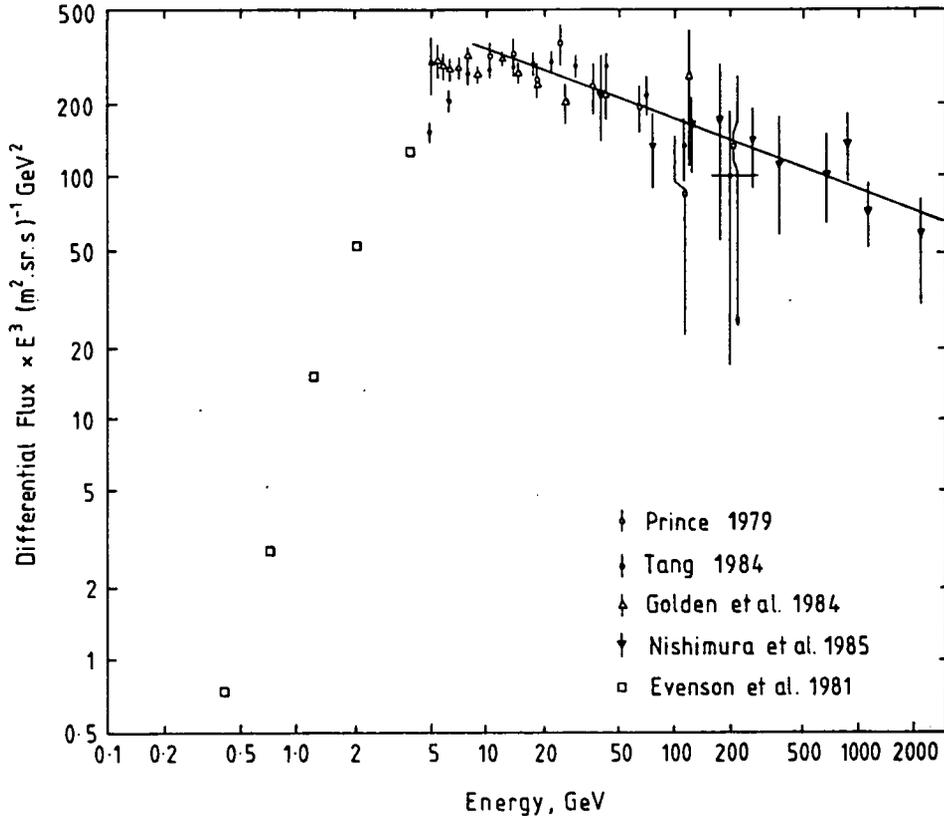
Figure 2.1 Cosmic ray electron spectrum from direct measurements near the Earth.

Indirect results from radio observations of the Galactic diffuse synchrotron emission are consistent with the direct measurements of the electron flux and spectrum. The radio emission in the frequency range generally used, 20 MHz ~ 10 GHz, are produced by electrons in the energy range 1 GeV~ 20 GeV assuming 5 μG for the effective strength of the Galactic magnetic field (see Chapter 6). In a similar fashion to the electron spectrum observed near the Earth, the interstellar electron spectrum derived from radio data also contains a spectral index variation in this energy range. Radio spectral index maps have been published for most parts of the sky (Lawson et al., 1987).

The γ-ray surveys by the SAS-II (35 MeV—200 MeV) and the COS-B (70 MeV—5 GeV) satellites cover most part of the sky. Analyses of the data

show that a substantial fraction of the Galactic diffuse γ-radiation is contributed by cosmic ray electrons; specifically those γ-rays in the energy range below 70 MeV are thought to result mainly from the electron bremsstrahlung process. Since the distributions of the interstellar gas (at least HI) and of the interstellar radiation field are known, it is feasible to derive the cosmic ray distribution from γ-ray data. A large scale radial gradient of cosmic rays has been derived from the radial gradient of γ-ray emissivity discovered from both SAS-II data (Dodds *et al.*, 1975) and COS-B data (Bhat *et al.*, 1986b). On the other hand, γ-rays can be used as a probe, together with an assumed cosmic ray distribution, to detect the interstellar gas distribution which is difficult to measure by other astronomical methods. An example is the derivation of H_2 mass in the Galaxy from γ-ray data (Bhat *et al.*, 1985). The low energy electron intensity derived from γ-ray data is higher than that both from radio data and from direct measurements.

Figure 2.2. Positron fraction of cosmic ray electrons measured near the Earth.

2.2 Acceleration mechanisms

The acceleration mechanism for cosmic ray electrons is usually assumed to
be the same as that for cosmic ray nuclei, *i.e.* diffusive shock acceleration by
supernova remnants. The resultant differential energy spectrum is a power
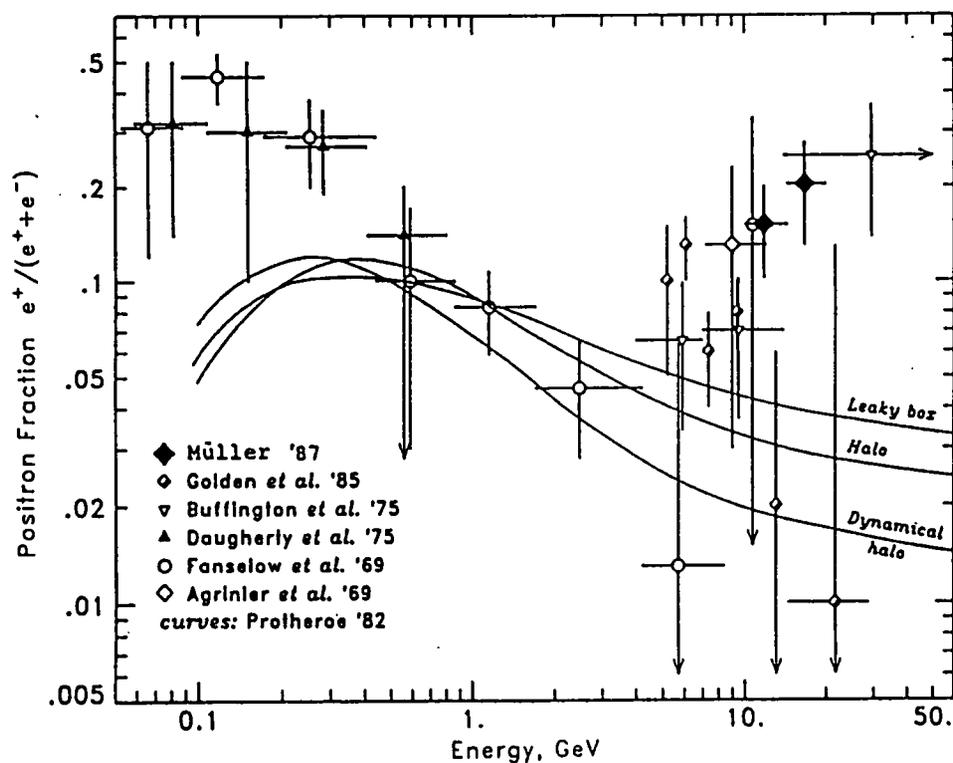law, $E^{-(2+\delta)}$, where $\delta \simeq 0.2 - 0.3$ determined by details of the acceleration
mechanism (Völk *et al.*, 1988). Bell (1978b) has considered the situation of
electron injection and pointed out that due to their smaller gyroradius the
injected electrons must have initial energies much greater than the thermal
energy of electrons in shock waves so that they can cross the shock front
easily. By assuming an equal injection temperature for both electrons and
protons, he calculated the energy spectra and showed a significantly lower
spectrum for electrons at high energies compared with that for protons, being
consistent with the observational result of $e/p \sim 1\%$ at energies above a few
GeV.

However, there is a problem with suprathermal injection. Asarov *et al.*
(1990) noted that the electron thermal temperature T_e is considerably lower
than ion thermal temperature T_i in the environment of supernova shocks.
This means that the efficiency for electron acceleration is lower and the total
energy gained by electrons is thus lower than that by protons. In fact, the
derived hard X-ray spectrum, which they intended as an explanation of the
hard X-ray excess in the radiation spectrum of young supernova remnants,
is lower than the observed. Nevertheless, the predicted power law spectrum
remains unchanged.

A further problem arises from the observed dispersion in radio spectral
indexes of supernova remnants. Radio observations show that although the
mean value of the indexes is 0.5, as theoretically predicted, there is a dis-
persion about this mean beyond theoretical prediction. Dröge *et al.* (1987)
explained this phenomenon by invoking second-order Fermi acceleration, in
addition to first-order Fermi acceleration.

There is also a problem related to electron diffusion in shock waves. In
diffusive shock acceleration, the acceleration time is proportional to the com-
ponent of the diffusion tensor normal to the shock front. The conventional
estimate of the diffusion coefficient based on diffusion parallel to the mag-
netic field appears to be smaller than required for some applications. For
example, the steepening of the electron spectrum at high energies may be
caused by a too small diffusion coefficient. To find a way out, Drury (1987)
has examined another possibility for electron acceleration—the shock drift
mechanism. He showed that shock acceleration can occur at perpendicular
or quasi-perpendicular shocks if the particles are strongly scattered.

In summary, the standard theory of diffusive shock acceleration, which

works well for nuclei acceleration, is unsatisfactory for electron and many problems remain unsolved. Nevertheless, this mechanism does qualitatively fit the observational data, it can give the right energetics and also the right spectrum. A statistical study by Cavallo (1982) showed that the total relativistic electron output as a function of supernova remnant radius is in agreement with the theoretical prediction, and Bhat *et al.* (1986b) have found a similar result for both electrons and protons.

Apart from supernova remnants, there are other candidates for the progenitors of cosmic rays, particularly those objects which show strong radio synchrotron emission, such as pulsars, binary-star systems, OB stars and Cygnus X-3 like objects. Accordingly, the acceleration mechanisms may be different from the standard theory.

Turning to positrons, these particles are generally thought to be secondary products of cosmic ray collisions with gas nuclei in the interstellar medium, *i.e.* $p + p \rightarrow \pi^{\pm} + X \rightarrow \mu^{\pm} + X' \rightarrow e^{\pm} + X''$. Another type of source is the radionuclei in supernova ejecta; the energetic decay positrons (~ 1 MeV) are most likely subsequently accelerated by supernova remnant shocks (Ellison *et al.*, 1990).

2.3 The distribution of electrons in the Galaxy

2.3.1 General remarks on diffusion and convection

Cosmic ray electrons in the Galaxy are certainly of Galactic origin and their distribution is determined by the source distribution, the propagation process and the boundary conditions. Theoretically, the distribution can be derived by solving the propagation equation. As mentioned in the Introduction, many propagation models have been proposed for solving this problem with varying degrees of success, although there is a problem with the spectral steepening. Observationally, information from direct measurements, radio astronomy, γ-ray astronomy and related fields imposes constraints on the theoretical description.

An important clue to the propagation of cosmic ray protons is the observation of anisotropy in the arrival directions. Sufficient data have been accumulated from extensive shower experiments in the last 30 years. The observed anisotropy is low below 10^{14} eV and above this energy it increases with increasing energy, up to 10^{20} eV where the first harmonic amplitude becomes essentially unity. This result indicates that the motion of the bulk of cosmic rays ($\leq 10^{14}$ eV) is mainly of diffusive character within a few pc of the solar system and it is probable that this diffusive character holds for

electrons as well.

The case is likely to be true for general regions in the Galactic Disk (but not for the halo where the physical condition is different). The smooth distribution of radio synchrotron emission and γ-ray emission supports the concept of diffusive motion of cosmic rays in the Galaxy.

There are two physical mechanisms which can generate the diffusive motion. The first one is the resonant scattering of the streaming cosmic rays with self-excited Alfvén waves; and the second is the scattering by inhomogeneities in the Galactic magnetic field. Although a sharp distinction between these two mechanisms is unable to be made to see what actually happens, due to the incapability of observations, theoretical considerations can indicate different features for different mechanisms.

The resonant scattering could be very efficient at low energies ($\sim 10^9$ eV) where the number of particles is dominantly large and they carry most of the cosmic ray momentum; but the efficiency is very low at higher energies ($> 10^{11}$ eV) where the streaming speed required to lead to resonant scattering would exceed the speed of light. This feature results in a strong energy dependence of the diffusion coefficient, approximately $D \propto E^2$.

For the scattering by inhomogeneities in the magnetic field, the diffusion is determined by the scale sizes of the inhomogeneities. The diffusion coefficient is also energy dependent and the dependence varies with the spectrum of turbulence, for example, $D \propto E^{1/3}$ for the Kolmogorov spectrum and $D \propto E^{1/2}$ for the Kraichnan spectrum. Recent observations show that the interstellar medium is highly turbulent and in particular that the interstellar magnetic field is highly irregular (see Chapter 6). If the scale of irregularity in the magnetic field ranges from 10^{13} cm to 10^{20}cm, the diffusive motion of cosmic rays in the energy range 10^9 eV—10^{18} eV can be easily explained.

To conclude the above discussion, we would like to suggest that the diffusive propagation of cosmic rays does not occur in the same way throughout the whole energy range and that the two diffusion mechanisms are complementary. The resonant scattering may be dominant at low energies, while the scattering by tangled magnetic fields may be dominant at high energies.

Turning to the convection of cosmic rays, the idea of a Galactic wind has drawn more and more attention in recent years. However, the key question still remains unsolved: where does the wind energy come from ? Originally, Ipavich (1975) and Jokipii (1976) proposed that the wind could be driven by cosmic rays. Indeed, cosmic rays must transfer some outward momentum to the interstellar gas as they are escaping from the Galaxy, but whether this momentum is sufficient to power a Galactic wind or not depends on the pressure balance between the cosmic rays, the gas thermal motion and the magnetic field. Recent analyses of pulsar rotation measure data (see Chapter

6) lead to the conclusion that the magnetic field pressure is dominant in the Galactic Disk, being greater than that of the cosmic rays and the thermal pressure of gas. The conclusion implies that the cosmic ray pressure is almost certainly insufficient to power a Galactic wind in the Disk (although it could work in the halo).

As an alternative to a cosmic ray driven wind, a wind driven by supernova blast waves was proposed by Hayakawa (1979), in which cosmic rays and gas are convected away from the Disk by the blast waves. If this mechanism works, the convection speed would be very high and the distribution of cosmic rays in the Galaxy would be highly inhomogeneous due to the rareness of supernova explosion events. In fact an upper limit to the wind speed of 16 km·s^{-1} has been set using the age distribution of cosmic rays (Giler *et al.*, 1979). Here, we have combined theoretical justifications and observational facts to propose a Galactic wind which is powered mainly by supernova remnants and early type stars (particularly Wolf-Rayet stars) and which convects gas and cosmic rays into the halo. The strength of the wind is weak in the Disk so that it could more properly be called a 'breeze'.

In the halo, a different propagation process will be present because the physical conditions are changed. The magnetic field becomes weaker and so does its pressure. The gas there is at a high temperature, of low density, and is ionized. The cosmic rays escaping from the Disk, together with convecting gas flow, could blow a Galactic wind since the cosmic ray pressure becomes overwhelming in this circumstance (the case for a low magnetic field in the halo is given in Chapter 6). If the magnetic field lines are originally perpendicular to the outwards streaming, they will be blown up and cosmic rays will thereby escape from the Galaxy. If the field lines are parallel to the streaming, resonant scattering by self-excited Alfvén waves will occur and cosmic rays will diffuse and therefore be confined for longer. The author considers that the interstellar medium in the halo is also turbulent and the magnetic field there is very irregular so that cosmic ray diffusion by irregularities is expected to occur.

A dynamical description of the cosmic ray driven Galactic wind has been given by McKenzie and Völk (1982). These authors gave a set of equations for the halo dynamics in terms of thermal gas fluid, cosmic ray fluid and magnetic waves. In the one-dimensional case, the Galactic wind solutions can be solved numerically (Breitschwerdt *et al.*, 1987). An interesting feature of these solutions is that the strength of the magnetic waves reaches its peak at 8 kpc above the Disk, which might be considered as the boundary for cosmic ray confinement. It is necessary to point out that the Galactic wind is mainly driven by the dominant nuclear component of the cosmic rays which thereafter undergoes the convection process, in addition to the

diffusion process, in the halo. Nevertheless, it is natural to assume that the electron component propagates in association with the nuclear component and therefore undergoes the same processes.

2.3.2 A synthetic analysis of radio data and γ-ray data

In order to derive information on the cosmic ray distribution in the Galaxy to the fullest extent, it is necessary to use both radio and γ-ray data in the analysis. This is because each kind of data has its own merit (and shortcomings) in tracing cosmic rays. Radio synchrotron radiation is produced by a single species of cosmic rays—electrons moving in the magnetic field—and therefore traces these electrons only. The uncertainty here is the Galactic magnetic field, for which the spatial distribution is not well known and the thermal contamination of free-free emission from HII regions. The diffuse Galactic γ-ray radiation is a mixture of different components, including electron bremsstrahlung, electron inverse Compton scattering and proton-matter interaction. The related distribution of interstellar gas and the radiation field are known. It is necessary to note that the vertical scale height of the radio emission is much larger (about ten times) than that of the γ-ray emission.

Starting the analysis with the radio data, the emissivity distribution in the Galaxy is found, by applying an unfolding method (Phillipps et al., 1981; Beuermann et al., 1985), to have an exponential radial scale length of 4 kpc. If this variation is contributed equally by both the cosmic ray electrons and the Galactic magnetic field, each of them will have a scale length of 8 kpc. The derivation of the vertical scale height is more difficult because the solar location lies within the Galactic Disk and thus it is hard to see the vertical variation. The absolute value of local emissivity, or equivalently the absolute values of the cosmic ray intensity and the strength of the magnetic field are required. We have tackled the problem very recently and found the best estimate of the scale height to be 2 kpc (see the next Section).

The variation of the radio spectral index across the Galaxy provides an extremely important clue to the propagation of cosmic rays. If cosmic ray sources are confined to the Disk, there should be a variation of the radio spectral index with Galactic latitude. Indeed, radio data show a spectral flattening with increasing latitude in both the Galactic Centre (GC) direction and the Anti-Centre (AC) direction (Lawson et al., 1987; Reich and Reich, 1988). The change in the radio spectral index is about 0.2—0.25, corresponding to a change of 0.4—0.5 in the electron spectral index. However, there is a slight difference of the spectral variation between GC and AC, the spectrum is flatter in AC than in GC by about 0.1. Furthermore,

the spectral index shows a flattening and an interesting variation in the local spiral arm region ($60^0 < l < 90^0$), as noticed by Rogers *et al.* (1988): it first decreases with latitude and then rises again. Considering the location of the solar system being on the edge of the local spiral arm, this flattening may contribute part of the spectral flattening seen in the AC direction.

If the propagation of cosmic rays is pure diffusion, as described by Ginzburg and Syrovatskii (1964), the electron spectrum should steepen due to energy dependent diffusion and energy loss via both synchrotron emission and inverse Compton emission as the electrons diffuse away from the Galactic Plane. Accordingly, the radio spectrum should steepen with increasing latitude. However, this is not the case and the radio data show the opposite trend. It is certain that there is some process producing this flattening of the electron spectrum above the Disk Plane. The author suggests that convection plays this role, as described by the Galactic wind model (Lerche and Schlikeiser, 1982), in which the electron spectrum below the characteristic energy E_D will be become flatter above the Disk Plane.

The situation with γ-ray data is similar but more complicated. A large scale radial gradient has been established (Dodds *et al.*, 1975; Bhat *et al.*, 1986b; Strong *et al.*, 1988) with an energy dependent scale length which can be fitted with a power-law form as $L = 8(E_\gamma/300\text{MeV})^{0.2}$ kpc (van der Walt and Wolfendale, 1988). The spectral index variation across the Galaxy is intriguing. In order to make the situation less complicated only the higher energy γ-rays were used in the spectral analysis since it was believed that cosmic ray protons are the predominant contributor to the γ-rays above 300 MeV. The results can be summarized as follows:

1. the ratio of the inner Galaxy intensity to that in the outer Galaxy falls with increasing energy and the difference in power-law spectral index is 0.4 at energies above 300 MeV (Bloemen, 1987).

2. the spectrum flattens with increasing latitude in the outer Galaxy, but steepens with latitude in the inner Galaxy at energies above 300 MeV (Bloemen *et al.*, 1988).

The interpretation of these results underwent a difficult evolution. If the cosmic rays are of Galactic origin and produced by supernova remnants (SNR), there should be a radial gradient in their spatial distribution due to a very strong gradient in the SNR surface density. The earliest conclusion of the presence of a gradient at lower energies derived from the SAS-II data was confirmed by COS-B data. However, at higher energies the conclusion became diverse. The COS-B group (Bloemen *et al.*, 1984) misinterpreted the data and claimed no radial gradient of γ-ray emissivity above 300 MeV

in the outer Galaxy. Therefore they moved towards an extragalactic origin of cosmic rays to explain this phenomenon as well as the small gradients at lower energies. The problem with an extragalactic origin is that an excess of extragalactic γ-ray flux will result. The Durham group (Bhat *et al.*, 1986a) analysed the same COS-B data but with their own estimates of the distribution of the important H_2 component and consistently claimed the presence of a gradient at all energies in the outer Galaxy. The final conclusion of the COS-B group (Strong *et al.*, 1988) has come to agreement with that of the Durham group.

The small gradient of cosmic rays cannot be simply attributed to extensive diffusion of the particles from the inner Galaxy into the outer Galaxy. Bloemen and Dogiel (see the review by Bloemen, 1989) have made such an attempt but failed. By using a large diffusion coefficient ($D \sim 10^{29} \text{cm}^2 \cdot \text{s}^{-1}$) and an extensive halo ($h = 15 \sim 20$ kpc), so as to achieve a very effective mixing of cosmic rays, together with the assumption of the source distribution being that of SNR, the solution to the propagation equation they obtained has a much larger gradient than that observed. It seems that the only way out is the assumption of an increase of the cosmic ray life-time with increasing galacto-centric distance, as suggested by Wolfendale (1986). Here, the author would like to develop this idea and provide a physical picture.

As is well known, the life-time of cosmic rays against escape is a function of the diffusion coefficient D and scale height H, *i.e.* $\tau = H^2/(2D)$. Radio data show a nearly constant scale height for the Galactic synchrotron emission over a large Galacto-centric distance range. This result indicates that the life-time variation should be due to the variation of the diffusion coefficient—the diffusion coefficient decreasing with the Galacto-centric distance. What is the physics behind this? Recent observations reveal that the interstellar medium is highly inhomogeneous and contains so called 'worms and bubbles', which are produced by stellar expansions. The lines of the Galactic magnetic field are also deformed and aligned with these structures. In this way, many vertical magnetic fluxes should be generated and cosmic rays should diffuse (and convect) away from the Galactic Disk quickly along these vertical structures. Since more stellar explosions occur in the inner Galaxy there should be more vertical magnetic fluxes which lead to quicker diffusion (and convection, we will return to this aspect later). In the outer Galaxy, however, the situation is the opposite: slow diffusion and slow convection.

For the interpretation of the spectral variation, it is imperative to point out here that the flattening (steepening) of the γ-ray spectrum does not necessarily mean a flattening (steepening) of the cosmic ray spectrum, because the γ-rays comprise multi-components. Unfortunately, this point has

been missed by some workers. Bloemen (1987) simply attributed the γ-ray spectral flattening in the outer Galaxy to a spectral flattening of cosmic ray protons and used a diffusion-convection transition model to explain it. However, this model requires that the spectral flattening occur within the thin gas disk, which is difficult to fulfil in term of the standard diffusion-convection model (Lerche and Schlikeiser, 1982). In a later work (Bloemen *et al.*, 1988), when Bloemen and collaborators applied this simple model to both radio data and γ-ray data, they had to make *ad hoc* assumptions that the convection is faster in the outer Galaxy than in the inner Galaxy and that the radio spectral flattening with latitude is due to thermal emission at intermediate latitudes from hot ionized gas. The first assumption is physically unreasonable because it is impossible for the energy input per unit area for the convection to be greater in the outer Galaxy than in the inner Galaxy. The second assumption is in contradiction with recent observations (IAU Symp. 144, Leiden, 1990) which exclude a large filling factor for the hot ionized gas in the Galaxy.

Rogers *et al.* (1988) have proposed an interesting alternative model in which the γ-ray spectral flattening in the outer Galaxy is due to the solar location being on the inner edge of the local Orion arm. Within the arm acceleration mechanisms are at work so as to give a flatter cosmic ray spectrum in the arm region than in the interarm region. This model depends on the geometrical size of the spiral arm: in other words, how much γ-ray flux can be contributed by the arm due to the increase in the source number above that of the interarm region. Insofar as the γ-ray data are concerned it could be a successful explanation, but it has difficulty coping with the radio emission, which extends far above the spiral arms.

The working model should explain both the radio data and γ-ray data, together. Here, the author makes such an attempt and proposes a qualitative model. The model includes the following assumptions:

1. the bulk of cosmic rays ($\leq 10^{14}$ eV) are of Galactic origin and are accelerated by SNR in the Galactic Disk;

2. cosmic rays propagate away from the Galactic Plane through both diffusion and convection so as to achieve a spectral flattening above the Disk; the diffusion coefficient and convection speed increase with decreasing galacto-centric distance as to achieve a small radial gradient;

3. cosmic rays have a flatter spectrum in the spiral arm regions than in the interarm regions.

With assumptions 1 and 2, the radio data can be naturally explained: the radial gradient is due to the cosmic ray life-time increasing with galacto-

centric distance and the spectral flattening above the Disk is due to a transition between diffusion and convection.

In addition, with assumption 3, the γ-ray data can be also naturally understood. The observed γ-ray flux in the energy range 35 MeV — 6 GeV is a mixture of several components: (i) γ-rays produced by electron bremsstrahlung which have a steep spectrum and are distributed in the gas Disk; (ii) γ-rays produced by electron inverse Compton scatterings which have a flat spectrum and form a γ-ray Halo; (iii) γ-rays produced by proton-matter interactions which have a spectral index in between the above two and are distributed in the gas Disk; and (iv) γ-rays from unresolved point sources which have a flat spectrum and are located in the Disk Plane.

As with the radio results, the small gradient in the γ-ray emissivity is a result of the cosmic ray propagation effect, the propagation being quick in the inner Galaxy and slow in the outer Galaxy. The spectral difference between the inner Galaxy and the outer Galaxy is caused by both the solar location on the inner edge of the local Orion arm and the presence of the inverse Compton Halo. Possibly the Halo may have a greater characteristic height (at which the spectral flattening occurs) in the inner Galaxy than in the outer Galaxy. The spectral flattening with increasing latitude in the outer Galaxy is caused by the existence of the inverse Compton Halo which contributes a considerable fraction (up to 60%) of the total flux at intermediate latitudes. The spectral steepening with latitude in the inner Galaxy is due to the presence of the unresolved point sources in the Disk which are estimated to contribute a substantial fraction ($\sim$ 35%) of the total flux towards the inner Galaxy.

2.3.3 A convection associated diffusion model

A complete description of the propagation of cosmic ray electrons in the Galaxy should include propagation both in the Disk and in the Halo. In general the propagation equation has a 3-dimensional form with a certain boundary condition. Here we suggest the expression,

$$\nabla \cdot (D\nabla n) - V\frac{\partial n}{\partial z} + \frac{1}{3}\frac{\partial V}{\partial z}E\frac{\partial n}{\partial E} + \frac{\partial}{\partial E}(bn) = q(E, R, z)$$
$$n|_{\Sigma} = 0 \qquad (2.1)$$

where Σ stands for the boundary.

In this equation, the first term on the left-hand side stands for diffusion, the diffusion coefficient depends on both energy and position, and can be written as $D = D_0(R, z)E^{\alpha}$. $D_0(R, z)$ decreases with increasing R and possibly increases with z, as discussed in the above subsection; α is a function

21

of the turbulence spectrum, theoretically, $\alpha = 0.3$ if a Kolmogorov spectrum is assumed and $\alpha = 0.5$ if a Kraichnan spectrum is adopted, while observationally $\alpha = 0.4 - 0.7$.
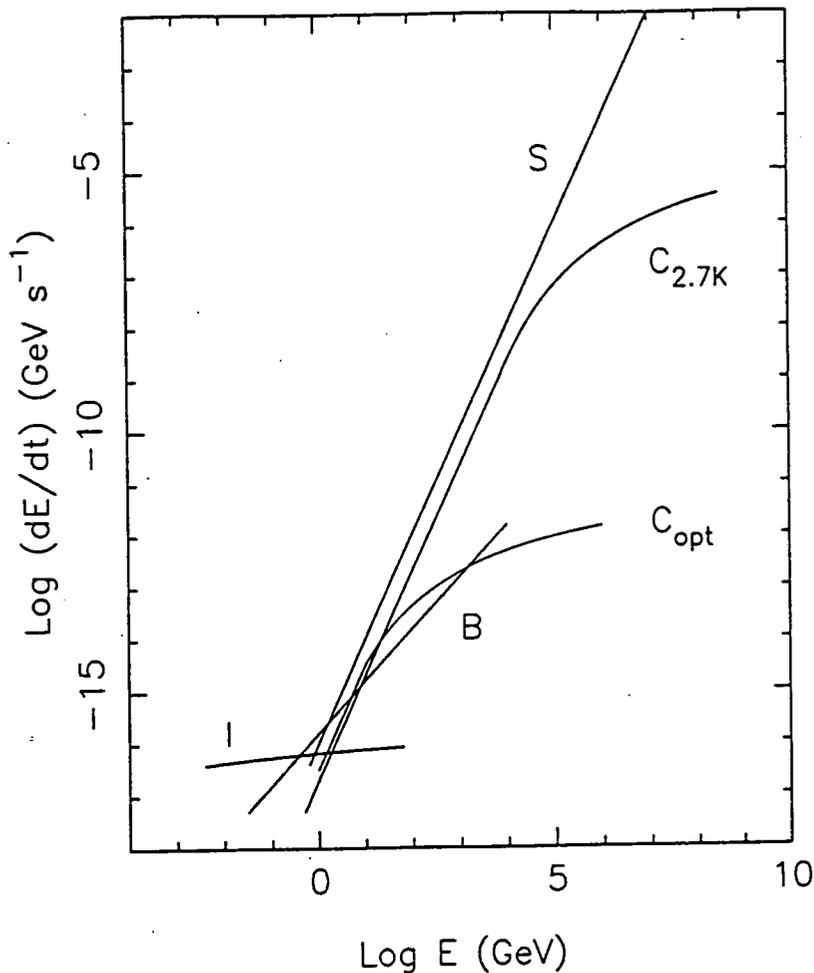
Figure 2.3. Energy loss rate of electrons as a function of electron energy in the interstellar medium. S: synchrotron loss in a magnetic field of $B_\perp = 5\mu G$; $C_{2.7K}$: inverse Compton scattering with the 2.7K microwave background photons (of energy density 0.24 eV·cm^{-3}); C_{opt}: inverse Compton scattering with optical photons (of energy density 0.41 eV·cm^{-3}); B: bremsstrahlung with gas (of density 0.2 H-atom·cm^{-3}); I: ionization loss with gas (of density 0.2 H-atom·cm^{-3}).

The second term stands for convection, which occurs only in the direction perpendicular to the Disk. The convection speed V is a function of position (R and z), V decreases with increasing R but increases with z as $V = 3V_1 z$—a common assumption, where V_1 is the velocity divergence.

The third term stands for adiabatic deceleration, which will play an important role when the cosmic ray pressure is dominant. The last term stands for energy loss; at energies above GeV the energy loss is dominated by synchrotron radiation and inverse Compton scattering, and thus the energy loss rate b is a function of R, z and E as $b = a(R, z)E^2$. Figure 2.3 shows the energy loss rates in various astronomical processes. Finally, the right-hand side term stands for the source function and has the form $KE^{-\Gamma}e^{-z/z_0}\sigma_{SNR}(R)$, where $\sigma_{SNR}(R)$ is the supernova surface density.

The solution to the problem is almost impossible to achieve analytically, so the numerical method has to be applied although the work is of considerable amount and therefore can be called an 'industry'. As a good approximation, some workers have tried to use the one-dimensional solution to approach the problem under certain simplified boundary conditions. Owens and Jokipii (1977) used a Monte-Carlo approach and a free escape boundary condition to calculate the electron spectrum in the halo. Lerche and Schlickeiser (1982) derived an analytical solution to the Galactic wind model by using an infinite boundary condition. Van der Walt (1990) used a Monte-Carlo method to examine the spectral variation with different input parameters.

Here, instead of solving the equation, the author would like to investigate the relation between the diffusion coefficient D and convection speed V over the whole Galaxy, to see how these two parameters change the electron spectrum from place to place. Following the work of Lerche and Schlikeiser (1982), the characteristic energy E_D is defined as $E_D = V_1/(bd)$ with $V = 3V_1 z$ and $D = D(E)d(z)$; and the characteristic height μ is defined as $\mu = (4D(E)/((6 + \alpha)V_1))^{1/2}$. Coming from the outer Galaxy to the inner Galaxy, V_1, b and D are increasing with decreasing R. If the increasing rate of V_1 is comparable to that of b, the characteristic energy E_D will not change significantly from the outer Galaxy to the inner Galaxy. However, the increasing rate of D is likely to be higher than that of V_1, then the characteristic height μ will increase from outer Galaxy to the inner Galaxy. This variation is what we require and is probably the actual case.

2.4 Synchrotron radiation from electrons

Since radio synchrotron radiation is an important probe of the cosmic ray

distribution in the Galaxy and in other galaxies, it is necessary to look into the production and characteristics of this radiation in some detail. As an application, the vertical distribution of the Galactic synchrotron emission is derived and accordingly the scale heights of the magnetic field and cosmic ray electrons are discussed.

The emissivity of synchrotron radiation from isotropic relativistic electrons in a random magnetic field is given by (e.g., Ginzburg and Syrovatskii, 1964)

$$q_\nu = a(\Gamma)\frac{e^3}{mc^2}(\frac{3e}{4\pi m^3 c^5})^{(\Gamma-1)/2}B_\perp^{(\Gamma+1)/2}K_e\nu^{-(\Gamma-1)/2} \qquad (2.2)$$

where K_e and Γ are the coefficient and spectral index of the power law electron spectrum, respectively. $a(\Gamma)$ is a function of Γ and its numerical values are given by Ginzburg and Syrovatskii (1964), for example $a(2.5) = 0.0852$ and $a(3) = 0.0742$. If we substitute the electron charge, e, electron mass, m, and the light speed, c, with their numerical values in cgs units, equation (2.2) gives

$$q_\nu = 1.35 \times 10^{-22}a(\Gamma)K_e B_\perp^{(\Gamma+1)/2}(\frac{6.26 \times 10^{18}}{\nu})^{(\Gamma-1)/2}$$

$$\text{erg} \cdot \text{cm}^{-3} \cdot \text{sec}^{-1} \cdot \text{sr}^{-1} \cdot \text{Hz}^{-1} \qquad (2.3)$$

The maximum in the synchrotron radiation spectrum for a single electron occurs at the frequency

$$\nu_\text{m} = 1.2 \times 10^6 B_\perp(\frac{E}{mc^2})^2\text{Hz} \qquad (2.4)$$

where $B_\perp$ is in Gauss. This expression is important and usually interpreted as an approximate relation between synchrotron radiation frequency and the corresponding electron energy.

The energy loss rate of a relativistic electron by synchrotron radiation is given by

$$-(\frac{dE}{dt})_\text{syn.} = 0.98 \times 10^{-3}B_\perp^2(\frac{E}{mc^2})^2 \text{ eV} \cdot \text{sec}^{-1} \qquad (2.5)$$

A number of analyses have been made of synchrotron radiation from the standpoint of deriving the dependence of synchrotron emissivity as a function of Galactocentric distance, R (radial), and height above the Galactic Plane z (vertical). The all-sky radio survey data at 408 MHz of Haslam (1981a,b) have been frequently used for this purpose. In these analyses, a model of the Galactic magnetic field is needed.

Phillipps et al. (1981a,b) determined the emissivity distribution by applying an unfolding method to the data inside the solar circle. They found that the radial component of the emissivity variation for $3.6 < R < 10$ kpc

24

can be represented by a power law, $q_\nu \propto R^{-1.9}$, or equally well by an exponential function $q_\nu \propto e^{-R/3.9}$, or by a Gaussian function $q_\nu \propto e^{-(R/7.8)^2}$ (with R in kpc in both cases). The vertical variation of the emissivity can be represented by a gaussian function $q_\nu \propto e^{-(z/0.75)^2}$ for $|z| \leq 1$ kpc and a linear fall down to zero at $z = 16.7$ kpc. This interpretation indicates an extended halo above the Galactic Disk. An imperfection of their analysis is the assumption of a compression of the regular magnetic field component (rather than an enhancement of the irregular component) in the spiral arms, which appears to be contrary to the recent results on the the magnetic field (see Chapter 6).

Beuermann *et al.* (1985) performed a similar analysis of the 408 MHz data. They interpreted the data in term of a two-disk model, comprising thin and thick disks. Assuming exponential variations in both R and z, the parameters in the spatial distribution of the emissivity can be determined. For the thin disk, the radial scale length was found to be 3.3 kpc, the vertical scale height increases with R and equals 0.27 kpc in the solar vicinity. For the thick disk, the radial scale length is 3.9 kpc, the vertical scale height increases with R and equals 2.6 kpc in the solar vicinity.

The recognition of a correlation between the Galactic thermal radio emission and the Galactic far infrared emission (Haslam and Osborne, 1987) enables an improvement in the interpretation of the radio data, insofar as the thermal contamination to the synchrotron emission can be removed by using the far infrared data from the IRAS survey. Broadbent (1989) made a detailed analysis of the technique for subtraction of the thermal component from the radio data and revised the previous analyses. Instead of using an unfolding method, she used a model fitting method—modelling both the Galactic magnetic field and the electron distribution in the Galaxy, to derive the structure of synchrotron emission in the Galaxy. The magnetic field model includes a radial variation as a gaussian function with scale length 13.2 kpc, and a vertical variation as a result of spiral shock wave compression in the Disk ($|z| \leq 0.5$ kpc). The electron density distribution contains no radial variation but a vertical variation (an extended halo) with the scale height being a function of R. An important achievement of this analysis is the determination of the spiral pattern of radio emission, which matches the optical spiral pattern in the Galaxy.

Since the radio emissivity is the product of two quantities—cosmic ray electron density and magnetic field energy density (or, more exactly, $B^{(\Gamma+1)/2}$), if we know one of them we can derive the other. Information from other astronomical fields may help find the solution to the problem. Recent results on the Galactic magnetic field (see Chapter 6) provide a better understanding of the Galactic radio emission. Here, as an application to cosmic ray

25

astrophysics we examine the electron distribution as a function of z. Two alternative situations can be identified, as follows:

(i) *Equipartition of energy between cosmic ray particles and magnetic field energy.* A commonly used model, despite no real justification, has equipartition between the field energy density and the cosmic ray proton energy density. It is assumed that the electron to the proton ratio (usually taken to be 1:100) does not depend on z; this is reasonable for the electrons under consideration here which, like the protons, are thought to mainly escape from the Galaxy without suffering catastrophic losses. Adopting the measured brightness temperature of 12.3 K at 408 MHz towards the Northern Galactic Pole, the locally measured electron spectrum $N(E) = 80E^{-2.6}$ m^{-2}s^{-1}sr^{-1}GeV^{-1} and the effective magnetic field $B_\perp = 5$ μG, we find an exponential scale height $z_{1/2} = 3.4$ kpc for both the electron density and the magnetic field energy density.

(ii) *Decoupling of field and particles.* The alternative assumption is that the cosmic rays and the field are decoupled above the Galactic Disk. This is likely to be the real physical situation and one in which the cosmic ray scale height is greater than that of the magnetic field because the cosmic rays escaping from the Galaxy require a higher pressure than the magnetic field pressure in the halo. If we set an exponential scale height of $z_{1/2} = 2$ kpc for the magnetic field energy density, we obtain an electron scale height of more than 5 kpc.

Finally, it is interesting to note that the study of the Galactic synchrotron radiation has an importance for cosmological observations. Banday *et al.* (1990) point out that the observed fluctuations of the cosmic microwave background at 10 GHz do not comprise a genuine cosmological signal but rather the fluctuation in the Galactic synchrotron radiation; they conclude that genuine signals will not appear until much higher frequencies.

2.5 γ-rays from electrons via bremsstrahlung and inverse Compton scattering

Cosmic γ-ray studies have the great advantage of receiving signals directly from sources without suffering substantial losses and they therefore probe large distances in the Universe. It is interesting to note that while contributing to the longest wavelength part of the cosmic electromagnetic radiation spectrum—radio synchrotron radiation, cosmic ray electrons also contribute to the shortest wavelength part of the electromagnetic spectrum—γ-rays. In interstellar space there are two γ-ray production processes: bremsstrahlung and inverse Compton scattering.

2.5.1 γ-rays from bremsstrahlung

Bremsstrahlung is the radiation emitted by a charged particle accompanying deceleration in the Coulomb field of another charge. In the case of cosmic ray electrons moving in the interstellar medium, the deceleration is caused by the Coulomb fields of gas nuclei (and to a lesser extent, electrons). The cross sections for γ-ray production from bremsstrahlung are derived in Heilter's book (Heilter, 1954) and have been developed to give more accurate results by a number of workers (see the reviews by, Koch and Motz, 1959; Blumenthal and Gould, 1970). Following the work of Sacher and Schönfelder (1984), here we use accurate production cross sections for electrons with energies above 10 keV. This topic is treated in some detail because the expressions will be needed later.

The symbols used in the following formulation are:

k—the photon energy in units of electron rest energy mc^2;

T—the kinetic energy of the electron in unit of mc^2;

p, p'—the momentum of the electron before and after collision in units of mc;

E, E'—the total electron energy before and after collision in units of mc^2;

β, β'—the velocity of the electron before and after collision in units of c;

Z—the atomic charge number;

r_0—the classical electron radius, $r_0 = e^2/(mc^2) = 2.82 \times 10^{-13}$ cm;

σ_T—the Thompson cross section, $\sigma_T = (8\pi/3)(e^2/mc^2)^2 = 6.65 \times 10^{-25}$ cm^2;

α—the fine structure constant, $= 1/137$.

For the purposes of accuracy, bremsstrahlung production in three different energy intervals is considered, respectively, as following:

(i) 10 keV $< T <$ 200 keV. In this energy range the production cross section is given by

$$d\sigma_{\text{br}} = f_E \times d\sigma_{\text{KM}} \qquad (2.6)$$

where $d\sigma_{\text{KM}}$ is the cross section of Koch and Motz (1959),

$$d\sigma_{\text{KM}} = \frac{2\alpha Z^2 \sigma_T}{\pi} (\frac{dk}{k}) \frac{1}{p^2} ln \mid \frac{p + p'}{p - p'} \mid \qquad (2.7)$$

27

and f_E is the Elwert factor, a correction to the Born approximation at non-relativistic energies,

$$f_E = \frac{\beta(1 - exp(-2\pi\alpha Z/\beta))}{\beta'(1 - exp(-2\pi\alpha Z/\beta'))} \qquad (2.8)$$

(ii) 200 keV $< T <$ 2 Mev. In this case the cross section is

$$d\sigma_{br} = g \times f_E \times d\sigma_{KM} \qquad (2.9)$$

where

$$d\sigma_{KM} = \frac{3\alpha Z^2 \sigma_T}{8\pi}(\frac{dk}{k})\frac{p'}{p}\{\frac{4}{3} - 2EE'\frac{p^2 + p'^2}{(pp')^2} + \frac{\epsilon_0 E}{p^3} + \frac{\epsilon E}{p'^3} - $$
$$\frac{\epsilon\epsilon_0}{pp'} + L[\frac{8}{3}\frac{EE'}{pp'} + k^2\frac{E^2E'^2 + p^2p'^2}{p^3p'^3} $$
$$+\frac{k}{2pp'}((\frac{EE' + p^2}{p^3})\epsilon_0 - \frac{EE' + p'^2}{p'^3} + \frac{2kEE'}{p^2p'^2})]\} \qquad (2.10)$$

is the cross section of Koch and Motz (1959) (valid only for electron-nucleus collisions) with the following abbreviations:

$$L = 2ln(\frac{EE' + pp' - 1}{k}),$$
$$\epsilon_0 = ln(\frac{E + p}{E - p}),$$
$$\epsilon = ln(\frac{E + p'}{E - p'}) \qquad (2.11)$$

where f_E is again the Elwert factor and g is a linear interpolation factor defined by

$$g = 1 + \frac{T(keV) - 200}{1800} \qquad (2.12)$$

This factor takes account of the increasing impact of electron-electron collisions. Below a kinetic energy of 200 keV the influence of electrons in the target atoms can be neglected (Brown, 1971). At T=2 MeV the electron-electron cross section is comparable to the electron-nucleus cross section (Gould, 1969).

(iii) 2 MeV$< T <$ 10 GeV. In this energy range the cross section depends on the screening effect of electrons around the atomic nucleus. The screening factor is defined by

$$\Delta = \frac{68.5k}{2E(E - k)Z} \qquad (2.13)$$

28

being proportional to the minimum momentum transfer in a collision. It is also a measure of the impact distance in the view of classical physics: the smaller the Δ value, the larger the impact distance and thus the greater the screening effect; and vice versa.

The bremsstrahlung cross section for the case of $\Delta < 1.5$ (complete screening) is

$$d\sigma_{\mathrm{br}} = \frac{3\alpha Z^2 \sigma_{\mathrm{T}}}{8\pi}(\frac{dk}{k})\left\{[1 + (\frac{E'}{E})^2]\phi_1(\Delta) - \frac{2}{3}(\frac{E'}{E})\phi_2(\Delta)\right\} \qquad (2.14)$$

where $\phi_1(\Delta)$ and $\phi_2(\Delta)$ are functions of Δ and their numerical values are tabulated in the work of Blumenthal and Gould (1970). For hydrogen atoms we cite those values of ϕ_1 and ϕ_2 from the above work and list them in Table 2.1

Table 2.1 The numerical values of functions $\phi_1(\Delta)$ and $\phi_2(\Delta)$.

Δ	0.0	0.05	0.10	0.20	0.50	1.0	2.0	5.0	10.0
ϕ_1	45.79	44.11	42.64	40.16	34.97	29.97	24.73	18.09	13.65
ϕ_2	44.46	43.65	42.49	40.19	34.93	29.78	24.34	17.28	12.41

For $1.5 < \Delta < 5$ (weak screening) the cross section is given by

$$d\sigma_{\mathrm{br}} = \frac{3\alpha Z^2 \sigma_{\mathrm{T}}}{\pi}(\frac{dk}{k})\,[1 + (\frac{E'}{E})^2 - \frac{2}{3}(\frac{E'}{E})][ln\frac{2EE'}{k} - \frac{1}{2}] \qquad (2.15)$$

For $\Delta > 5$ (very weak screening) the crossing section is obtained by multiplying Eq. (2.10) by a factor of 2.

The γ-ray emissivity via bremsstrahlung can be written in the form

$$q_{\mathrm{br}}(E_\gamma) = \int_{E_\gamma + mc^2}^{\infty} 4\pi K_e T^{-\Gamma} n_{\mathrm{H}} \frac{d\sigma_{\mathrm{br}}(E_\gamma, E)}{dE_\gamma} dE \qquad (2.16)$$

where $K_e T^{-\Gamma}$ is the cosmic ray number density and n_{H} is the atomic hydrogen gas density. At ultrarelativistic energies, the slope of the bremsstrahlung γ-ray spectrum is identical to the slope of the electron spectrum. Figure 2.4 shows the bremsstrahlung γ-ray spectrum from the locally measured electron spectrum in the range above 100 MeV.

For relativistic electrons, the bremsstrahlung cross section can be approximated as a linear function of electron energy E and may be written in the form

$$\sigma_{\mathrm{br}}(E, E_\gamma) = \frac{<M>}{<X>}\frac{E}{E_\gamma} \qquad (2.17)$$

29

where $< M >$ is the average mass of the target atoms in grams and $< X >$ is the average radiation length for the gas in grams per square centimeter. The radiation lengths for pure hydrogen and helium are

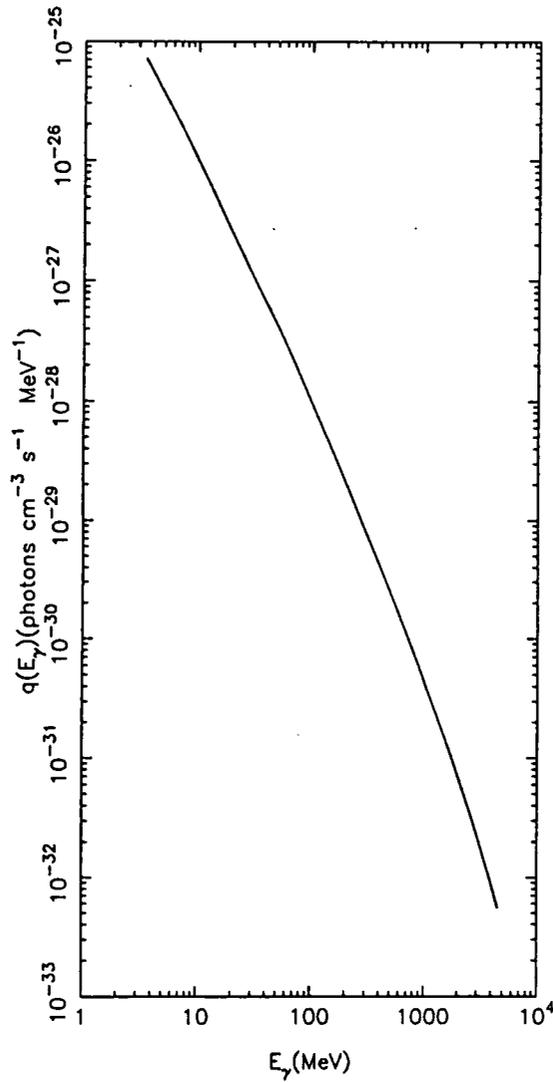$$X_H = 62.8 \text{ g/cm}^2,$$
$$X_{He} = 93.1 \text{ g/cm}^2 \tag{2.18}$$

Figure 2.4. Bremsstrahlung γ-ray spectrum calculated from the local measured electron spectrum with a gas density 0.2 H-atom·cm^{-3}.

30

Taking the percentages of these two constituents as weighting factors, 91% for hydrogen and 9% for helium, we obtain the average radiation length for interstellar matter

$$X = 65 \ \text{g/cm}^2 \tag{2.19}$$

2.5.2 γ-rays from inverse Compton scattering

Inverse Compton scattering is the relativistic form of Thompson scattering in which a photon scatters off an electron and changes its energy. In the case of astrophysical interest, a relativistic electron (cosmic ray electron) collides with a photon ε of the interstellar or intragalactic radiation field and transfers energy to the photon. For the condition $\gamma\varepsilon \ll mc^2$, on average the final photon energy ε' is

$$\langle \varepsilon' \rangle = \frac{4}{3}\varepsilon\gamma^2 \tag{2.20}$$

and the cross section can be simply taken as the Thompson cross section (Heilter, 1954),

$$\sigma_c = \sigma_T \tag{2.21}$$

In the other extreme $\gamma\varepsilon \gg mc^2$, the Klein-Nishina form of the cross section should be used, which is

$$\sigma_c = \frac{3}{8}\sigma_T(\frac{mc^2}{\varepsilon})[\frac{1}{2} + ln(\frac{2\varepsilon}{mc^2})] \tag{2.22}$$

and the final photon energy is

$$\varepsilon' \sim \gamma mc^2 \sim E \tag{2.23}$$

In the general case, the exact cross section (e.g., Jauch and Rohrlich, 1955) is given by

$$\frac{d\sigma}{d\Omega} = \frac{r_0}{2}(\frac{E_\gamma}{\varepsilon})^2 \, (\frac{\varepsilon}{E_\gamma} + \frac{E_\gamma}{\varepsilon} - sin^2\theta) \tag{2.24}$$

where θ is the scattering angle and is related to E_γ by

$$\frac{E_\gamma}{\varepsilon} = 1/[1 + \frac{\varepsilon}{mc^2}(1 - cos\theta)] \tag{2.25}$$

The emissivity of inverse Compton γ-rays depends on both the electron density $N(E)$ and photon energy density $u(\varepsilon)$; in the case of an isotropic

31

photon field and isotropic electron distribution it is (*e.g.*, Jones, 1968)

$$s(E_\gamma) = 2\pi r_0^2 (mc^2)^2 \int_0^\infty d\varepsilon \, \frac{u(\varepsilon)}{\varepsilon^2} \int_{E_{\min}}^\infty dE \frac{N(E)}{E^2}$$

$$\times \{2qlnq + (1+2q)(1-q) + \frac{(\Gamma_e q)^2(1-q)}{2(1+\Gamma_e q)}\} \qquad (2.26)$$

where the symbols are defined as follows:

$$
\begin{aligned}
\Gamma_e &= 4\gamma\varepsilon/mc^2, \\
E_1 &= E_\gamma/(\gamma mc^2), \\
q &= E_1/(\Gamma_e(1-E_1)), \\
E_{\min} &= (E_\gamma + \sqrt{E_\gamma^2 + (mc^2)^2 E_\gamma/\varepsilon})/2 \qquad (2.27)
\end{aligned}
$$

The interstellar photon field includes three components: (i) the universal 2.7 K microwave background, which has energy density 0.24 eVcm^{-3} and an average photon energy of 6×10^{-4} eV; (ii) optical and UV; and (iii) infrared. The determination of the latter two components has been a difficult task and a recent estimate has been made by the author and colleagues (see Appendix A). The results are characterized by a substantial energy density in the halo. Figure 2.5 shows the local inverse Compton γ-ray emissivities of cosmic ray electrons scattering with optical, FIR and 2.7 K microwave background photons, respectively.

Theoretical models have been extensively compared with γ-ray observations in the past and some differences in conclusions from different groups still remain. There are three physical processes contributing to the diffuse Galactic γ-ray emission, *i.e.* nuclear interaction, bremsstrahlung and inverse Compton scattering. It is generally accepted that the bremsstrahlung process is the dominant one for γ-ray energies below 70 MeV although there are uncertainties in calculating the absolute flux. The main uncertainty is the electron intensity distribution in the Galaxy, particularly the low energy electron intensity (below 1 GeV), which is even not well known in the solar vicinity. Turning to higher energies, the inverse Compton γ-rays are a significant contributor to the Galactic diffuse γ-ray emission above 70 MeV. The SAS-II group (Kniffen and Fichtel, 1981) claimed that more than 50% of the total diffuse γ-ray flux in the Disk is due to inverse Compton scattering; whereas the COS-B group (Bloemen, 1985) reached the opposite conclusion that the inverse Compton γ-ray flux is negligible ($\sim$ 5%) in the Disk. The Durham group (Riley and Wolfendale, 1984; Chi *et al.*, 1989) studied the problem in more detail by using the most accurate estimate of the photon field and the most reliable cosmic ray electron distribution in the Galaxy in their calculation. Their conclusion is that the inverse Compton emission

accounts for about 20% of the total γ-ray flux at low latitudes ($|b| < 10^0$) and up to 60% at intermediate latitudes. Later, in Chapter 4, we will return to this problem again and show the existence of an inverse Compton γ-ray halo.
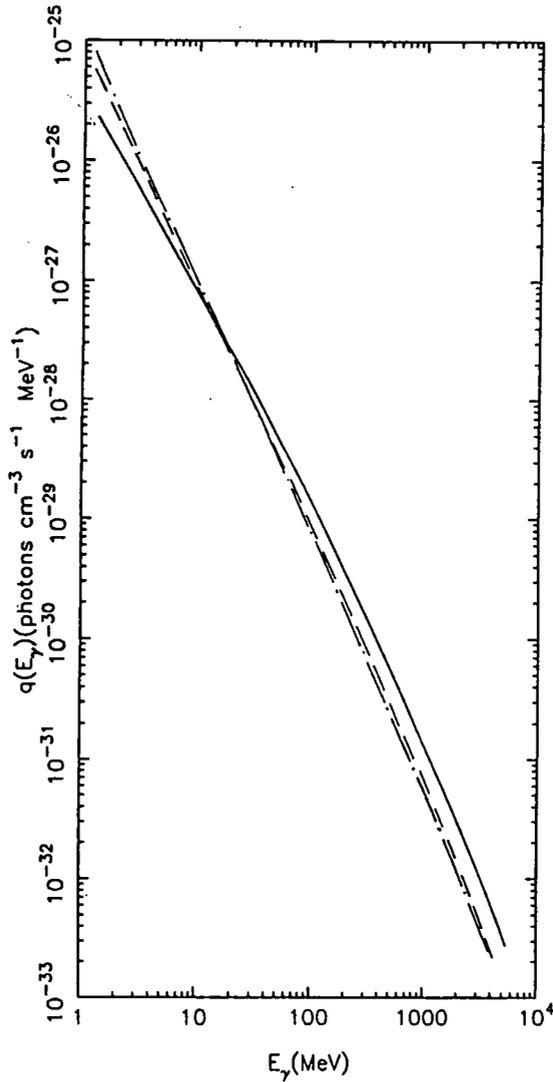

Figure 2.5. Inverse Compton γ-ray spectra of electrons scattering with the local interstellar radiation fields. Solid line: starlight (0.13 $\sim$ 8μm); dashed line: FIR (8 $\sim$ 1000μm); dot-dashed line: 2.7K cosmic microwave background.

Chapter 3

Galactic Electrons below 100 MeV

In this chapter we first analyse the evidence for an excess flux of cosmic ray electrons in this energy range from hard X-ray and low energy γ-ray data, then propose a model to account for their generation and propagation, and finally discuss the implications of this model to (1) cosmic γ-ray background, and (2) interstellar ionization, heating and support.

3.1 The evidence from hard X-ray studies

Particles in this low energy range are usually referred to as the 'seed' particle population. The direct measurements of the particles near the Earth are seriously influenced by the solar wind and the measured flux has been modulated dramatically from the interstellar level. Figure 3.1 shows a summary of the energy spectra measured by balloon and satellite experiments (after Evenson *et al.*, 1981). Moreover, at low energies, different sources of particles begin to contribute and the spectrum cannot be understood by a simple extrapolation of a Galactic population of cosmic rays to the seed population, diffusing into the heliosphere and being subjected to influences of the solar wind. Actually, a substantial flux of electrons in the solar system originates from the Jovian magnetosphere and it is quite possible that below 25 MeV most if not all the electrons observed at 1 AU are of Jovian origin (Eraker and Simpson, 1981). Although the spacecraft measurements have extended to 40 AU, the outer boundary of the modulating region of the heliosphere is far beyond this distance and likely to be about 100 AU where the electron flux represents the real local interstellar level. Therefore, indirect methods of estimating the spectrum are needed.

Apart from the method using γ-ray data, three other methods are possible in complementing direct measurements and we give a brief review in the

following:

1. Using the propagation equation in conjunction with the injection spectrum to calculate the ambient electron spectrum. In this approach, diffusion, convection and energy loss by ionization should be included in the solution for electrons with energies below 100 MeV. The uncertainty of this method mainly consists in the source function—whether the injection spectrum is a single power law as described by the standard diffusive shock acceleration mechanism, or another kind of source also contribute a substantial fraction of the low energy electrons. Protheroe and Wolfendale (1980) have made such an investigation by solving the diffusion equations and have shown that a single power-law injection spectrum is insufficient to account for the low energy part of the diffuse γ-ray radiation. Ip and Axford (1985) performed a similar calculation by employing a leaky-box model to both electrons and nuclei and found a consistent result for the electron spectrum with that of previous workers. These calculations clearly show that at low energies ionization loss is important and can reduce the electron spectrum by more than an order of magnitude.

2. To demodulate the low energy electron spectrum measured in the solar system to obtain the interstellar one. Estimates of the interstellar electron spectrum based on modulation of the electron spectrum observed by spacecraft at large distances (many AUs) should, in principle, give an upper limit to the interstellar flux (a fraction of the measured flux is due to Jovian particles). By assuming that the electron flux at 21.5 AU is of Galactic origin, Eraker and Simpson (1981) established an upper limit for the Galactic electron flux. Their result indicates that at 1 AU the Galactic flux is only about 1% of the measured total flux and the outer boundary of the modulating region of the heliosphere is probably at 70 AU.

3. To extrapolate the electron spectrum derived from radio synchrotron spectrum down to low energies. This method includes calculating the amount of free-free absorption which is important at low radio frequencies ($<$ 10 MHz) since the radio spectrum measurements have extended down to 0.1 MHz, and modelling the spatial distributions of the Galactic synchrotron emission and absorption. Cummings *et al.* (1973) derived the interstellar electron spectrum from the radio emission in the anti-galactic centre direction. In their model, the strength of the magnetic field is assumed to be 5 μG and the line of sight distance in the anti-centre direction to be 4 kpc. The obtained electron spectrum

35

is much higher than that measured near the Earth at solar minimum: at 12 MeV the ratio of the derived to the measured is 4×10^2. The uncertainty with this method comes from the estimation of the amount of free-free absorption. Lower estimates (Webber *et al.*, 1980) give an electron spectrum with an almost constant spectral index -2.1 down to 40 MeV and -1.3 below 40 MeV. Higher estimates of free-free absorption (Strong and Wolfendale, 1978) give an electron spectrum that increases above the extended -2.3 spectrum extrapolated from higher energies. Consequently, this ambient spectrum requires a new source or injection spectrum.
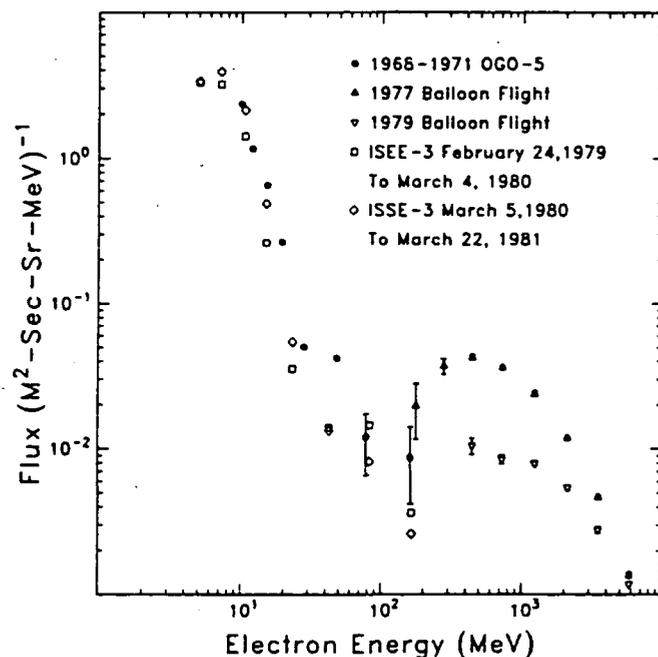
Figure 3.1. Low energy cosmic ray electron spectrum measured by balloon and satellite experiments near the Earth (after Evenson *et al.*, 1981).

The diffuse Galactic γ-ray data provides a superb probe of the cosmic-ray electrons since the low energy γ-rays are dominantly produced by electron bremsstrahlung with interstellar gas of which the distribution is relatively well known and the γ-rays do not suffer any attenuation in the Galaxy. The intermediate energy γ-ray data from both SAS-II (Fichtel *et al.*, 1978)

and COS-B (Paul *et al.*, 1978) show an unexpectedly large flux of diffuse Galactic γ-rays and a power law spectrum in the detected energy range (SAS-II: 35 MeV—200 MeV and COS-B: 50 MeV—6 GeV). Apparently, this power law spectrum cannot be accounted for only by the π^0-decay component from proton-matter interaction which falls down below 70 MeV. Here the contribution from electrons must come in, although there is an ambiguity between the contribution from bremsstrahlung and the contribution from inverse Compton scattering. Low energy γ-ray measurements from different experiments consistently show a high flux, which can be an extrapolation from the higher energy flux according to a power law. Figure 3.2 gives a compilation of γ-ray measurements for the Galactic Centre region. It should be be noted that since observations do not in general refer to the same region of sky, the uncertainty in the spectrum is quite large.
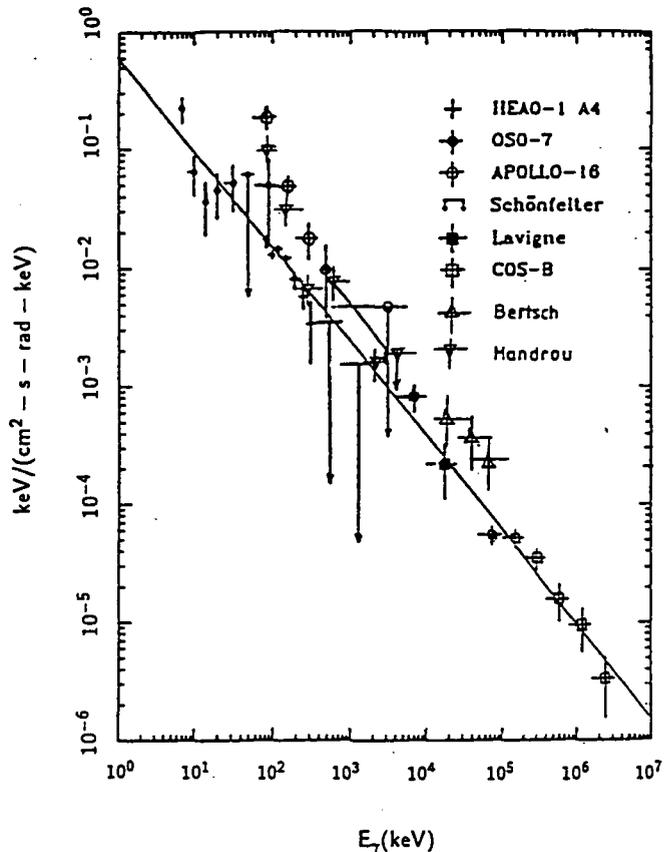

Figure 3.2. The diffuse Galactic γ-rays from the Galactic Center region (after Peterson *et al.*, 1990).

Cesarsky *et al.* (1978) modelled the diffuse γ-ray spectra measured by the COS-B satellite and concluded that a significant flux of electrons must be present in the interstellar medium, at least down to 50 MeV. This result is consistent with the derivations from radio data by Cummings *et al.* (1973) and by Strong and Wolfendale (1978). Coming down to lower energies, the balloon experiment by Lavigne *et al.* (1986) recorded a large γ-ray flux in the energy range 4 MeV—25 MeV from the Galactic Centre region. They interpreted the flux as due to electron bremsstrahlung and derived a power-law electron spectrum 159 $E^{-2.3}$ electrons $\cdot$ cm^{-2} $\cdot$ s^{-1} $\cdot$ sr^{-1} $\cdot$ MeV^{-1} in the energy range 12 MeV—75 MeV. Schönfelder *et al.* (1988) measured the γ-rays of 0.6 MeV—3 MeV from the Galactic Centre region and put an upper limit on the local interstellar electron spectrum in the energy range 1 MeV—10 MeV as 40 $E^{-1.8}$ electrons $\cdot$ cm^{-2} $\cdot$ s^{-1} $\cdot$ sr^{-1} $\cdot$ MeV^{-1}. The most reliable measurement of γ-ray data at even lower energies is given by the HEAO-1 experiment which covers an energy range of 90 keV—280 keV (Peterson *et al.*, 1990). This measurement not only indicates a large γ-ray flux from the Galactic Centre region, but also reveals an unusual profile of the galactic longitudinal distribution which is peaked at about $l = 50^0$ rather than at $l = 0^0$ as shown by the 100 MeV γ-ray data and is relatively low in the anti-centre direction.

In the present work, we derive the interstellar electron spectrum by using all the available γ-ray data below 70 MeV, together with the assumption that the low energy γ-rays are dominantly produced by electron bremsstrahlung with interstellar matter. For the distribution of interstellar matter, we consider the atomic hydrogen HI and molecular hydrogen H_2 separately, but neglect the ionized hydrogen. The HI distribution is taken to have a constant surface density and a constant scale height in the Galacto-radial range 4 kpc $\leq R \leq 15$ kpc,

$$n_{\text{HI}} = n_{\text{HI}}^0 \cdot exp(-\frac{z^2}{2(0.12)^2}) \tag{3.1}$$

where $n_{\text{HI}}^0 = 0.15$ atoms $\cdot$ cm^{-3}. While in the range $R < 4$kpc,

$$n_{\text{HI}} = n_{\text{HI}}^0 \cdot (R/4) \cdot exp(-\frac{z^2}{2(0.12)^2}) \tag{3.2}$$

The H_2 distribution is taken to depend on both R and z. The volume density function has the form

$$n_{H_2}(R, z) = n_{H_2}(R) \cdot exp(-\frac{z^2}{2\Delta_{H_2}}) \tag{3.3}$$

where the scale height Δ_{H_2} is a function of R: $\Delta_{H_2} = 0.025 + 0.003R$ in the Galacto-radial range $4 \text{ kpc} \leq R \leq 12 \text{ kpc}$. The surface density varies as follow:

$$\sigma_{H_2}/\sigma_{HI} = \begin{cases} 1, & 4\,\text{kpc} \leq R \leq 6\,\text{kpc} \\ 2 - R/6, & 6\,\text{kpc} < R \leq 12\,\text{kpc} \\ 0, & R > 12\,\text{kpc, or} R < 4\,\text{kpc} \end{cases} \qquad (3.4)$$

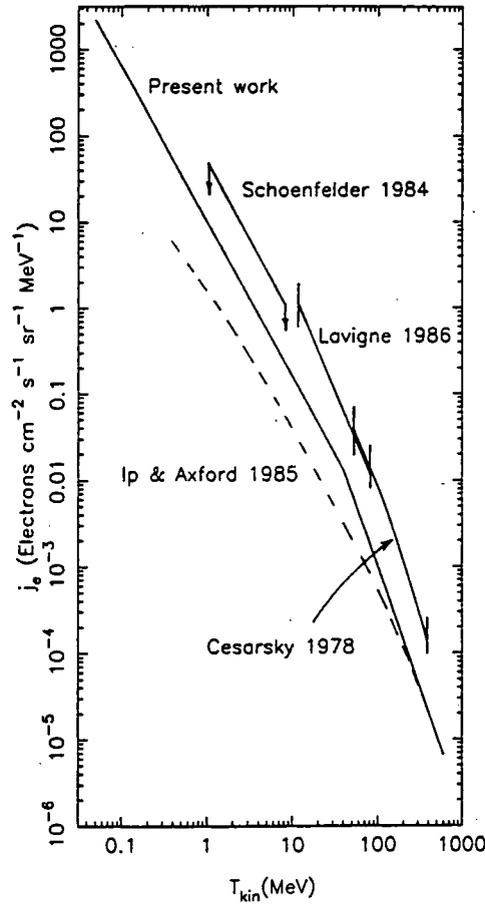Figure 3.3. The local interstellar electron spectrum estimated from γ-ray data.

For the electron distribution, we assume that the electron scale height is much larger than the gas scale height and therefore the electron distribution in the vertical direction can be taken as a constant. The Galacto-radial variation is assumed to be $j_e(R) \propto e^{-R/4}$ if $4 \text{ kpc} \leq R \leq 15 \text{ kpc}$ and $j_e(R) =$

$j_e(R = 4\,\text{kpc})$ if $R < 4$ kpc. The reason for this large radial gradient is that these low energy electrons are thought to be produced by stellar flares and winds and cannot reach too far (≤ 250 pc if only by diffusion) before losing most kinetic energy against ionization, so that they are fairly 'local'. The unusual longitudinal profile in the HEAO-1 γ-ray data (see Figure 1 of Peterson *et al.*, 1990) is an indication of this 'locality'. Nevertheless, they could be convected into the Galactic Halo by the Galactic wind.

Our estimated electron spectrum in local interstellar space is plotted in Figure 3.3, it can be fitted with two power-law functions,

$$j_e = 10E^{-1.8}\text{electrons} \cdot \text{cm}^{-2} \cdot \text{s}^{-1} \cdot \text{sr}^{-1} \cdot \text{MeV}^{-1} \tag{3.5}$$

in the energy range 100 keV—40 MeV, and

$$j_e = 400E^{-2.8}\text{electrons} \cdot \text{cm}^{-2} \cdot \text{s}^{-1} \cdot \text{sr}^{-1} \cdot \text{MeV}^{-1} \tag{3.6}$$

in the energy range 40 MeV—1 GeV.

For comparison we also draw the spectra of other workers derived from γ-ray data in Figure 3.3. It is apparent that our spectrum is lower than all the others. The difference is caused by different models of the electron distribution on large scale in the Galaxy, we use a large Galacto-radial gradient whereas others use a small one. Compared with theoretical predication calculated from a single power-law injection spectrum, our spectrum is much higher than the upper limit spectrum given by Ip and Axford (1985). This means that it certainly requires extra sources for generating these low energy electrons.

Finally, it is necessary to mention that towards the Galactic Centre region the contribution from inverse Compton scattering to the γ-rays below 70 MeV is small, less than 30% by our estimate.

3.2 Generation and propagation

Observations of particle acceleration at the Earth's bow shock provide an important clue to the problem of the mechanism for seed particle acceleration. The Earth's bow shock is stimulated by the solar wind passing by the magnetosphere of the Earth. At the radius of the Earth's orbit, typical values of the solar wind parameters are $\rho \sim 10^{-23}\text{g} \cdot \text{cm}^{-3}$, $T_e \sim 10^5$ K, $V \sim 400$ km·s^{-1}, $B \sim 3 \times 10^{-5}$ G, respectively. The Earth's magnetic field is approximately dipolar and so the magnetic pressure will decrease with distance r from the Earth $\propto r^{-6}$. The solar wind accelerates through a bow shock, when the magnetic pressure becomes comparable to the momentum flux of

the solar wind $\sim \rho V^2$ at $r \sim 10$ Earth radii. A fairly isotropic component of particles with energies ranging up to 100 keV have been detected on site.
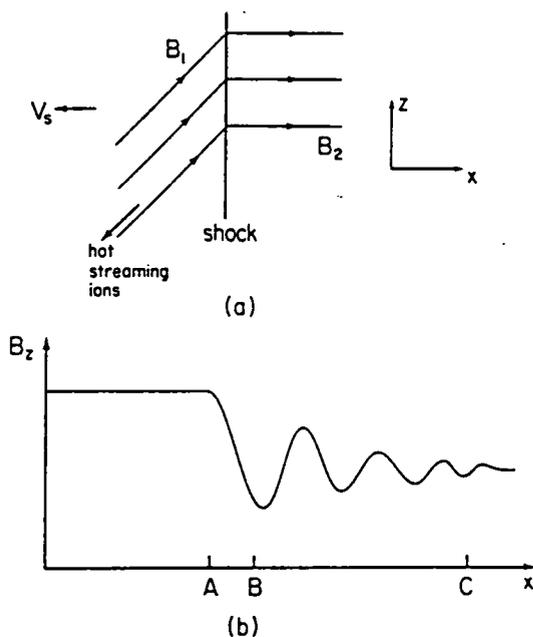
Figure 3.4. Schematic picture of a shock in the $x - z$ plane (after Kundu *et al.*, 1989), here assuming no magnetic field in the y direction. (a) The shock propagation at speed v_s in the negative x direction. A stream of hot ions is thought to run along the ambient upstream magnetic field. (b) The behavior of z-component of the magnetic field in a slow shock. For $x < A$, the plasma is undisturbed by the shock; for $A < x < B$, the main shock transition takes place; and for $B < x < C$, dispersive MHD waves phase stand in the shocked downstream plasma.

The understanding of particle-magnetic wave interaction in the bow shock region has been improved dramatically by the Prognoz satellite observations that streams of energetic particles are in association with low hybrid wave turbulence (Vaisberg *et al.*, 1983). The interpretation of the phenomenon is that the structure of the bow shock is governed by the reflection of a fraction of the incident ions at the shock front. Roughly one percent of the incident ions in the solar wind are reflected upstream in a beam with a speed of about 1000 km $\cdot$ s^{-1}, 2—3 times their incident speed. These ions form a cross-field beam which is unstable to lower hybrid waves (Wu *et al.*, 1984). It is well

known that lower hybrid waves propagating perpendicular to the magnetic field can efficiently accelerate electrons to relativistic energies in the context of type II solar bursts (Lampe and Papadopoulos, 1977), fast moving type IV solar bursts (Vlahos et al., 1982), and solar coronal mass ejection events (Kundu et al., 1989). This mechanism has three nice features: (1) it can extract electrons from the thermal population; (2) it only needs adequate currents (either electrons or ions) to drive it; and (3) it operate in both slow-mode and fast-mode shocks.

To show how it works, it is useful to discuss the detailed structure of these shocks. It is a well known fact that the stochastic acceleration by plasma instabilities requires high phase velocities in at least one direction. The low hybrid instability possesses such a property because the wave direction is nearly perpendicular to the magnetic field lines so that the parallel component of its phase velocity $\omega/k_\parallel$ can be very large and electrons moving along the magnetic field lines will be accelerated. Figure 3.4 shows the schematic picture of the shock structure (after Kundu et al., 1989). The structure consists of a supersonic to subsonic transition (A-B) and a following dispersive wave train (B-C).

The dispersion relation for lower hybrid wave can be solved analytically (McBride et al., 1972). If we neglect gradients in density n, magnetic field $\mathbf{B}$ and temperature T, assume electrostatic waves at long wavelengths $kr_e \ll 1$ (where $r_e = v_e/\Omega_e$ is electron gyroradius), frequency ω in the range $\Omega_i \ll \omega \ll \Omega_e$ (where $\Omega_{e,i}$ are electron and ion gyrofrequencies), and wave vector $\mathbf{k}$ nearly perpendicular to $\mathbf{B}$, the dispersion relation in the laboratory frame of reference is

$$1 - \frac{\Omega_H^2 \Theta^2}{2k^2 v_e^2 \theta^2}\left(\frac{\omega - \mathbf{k} \cdot \mathbf{U}_e}{2^{1/2} k v_e \theta}\right) - \frac{\Omega_H^2}{2k^2 v_i^2}\left(\frac{\omega - \mathbf{k} \cdot \mathbf{U}_i}{2^{1/2} k v_i}\right) = 0 \qquad (3.7)$$

where $\Omega_H = (\Omega_e \Omega_i)^{1/2}$ is the lower hybrid frequency, ω_i is the ion plasma frequency, $\Theta = \theta \omega_e/\omega_i$, $\theta = sin^{-1}(\mathbf{k} \cdot \mathbf{B}/kB)$, $v_{e,i} = (T_{e,i}/m_{e,i})^{1/2}$ are thermal velocities, and U_e and U_i are the electron and ion streaming speeds due to the current across $\mathbf{B}$ in the shock front.

The saturation level of the current-driven lower hybrid waves can be found analytically or by computer simulations (McBride et al., 1972). Its value is

$$\frac{W}{nT_e} = 5 \times 10^{-2}\left(\frac{\Omega_e}{\omega_e}\right)^2 \qquad (3.8)$$

where W is the energy density of the waves.

The effective temperature T_t of the accelerated electrons can be calculated by solving one dimensional diffusion equation. Following the formulation of

42

Vlahos *et al.* (1982), we calculate T_t at the bow shock. It turns out, compared with the thermal temperature, to be given by

$$\frac{T_t}{T_e} = 10^{-2}\Omega_H t_0 \tag{3.9}$$

where t_0 is the time of electron interacting with wave. For $B = 10^{-5}$G and $t_0 = 2.5 \times 10^2$ s, $T_t/T_e = 10^3$. Since the lower hybrid waves are saturated at $5 \times 10^{-2}(\Omega_e/\omega_e)$, by assuming that most of the wave energy goes into the electron kinetic energy, we can estimate the upper limit to the number of electrons accelerated:

$$\frac{n_t}{n_0} = 5 \times 10^{-2}(\frac{\Omega_e}{\omega_e})^2 \frac{T_e}{T_t} \tag{3.10}$$

where n_0 is the background thermal electron density. For $B = 10^{-5}$G and $n_e = 10$ cm^{-3}, we find $n_t/n_0 = 5 \times 10^{-11}$. However, the ratio will be several orders of magnitude higher at a stellar flare since there $n_0 = 10^8$ cm^{-3} and $B = 1$ G.

This acceleration mechanism, we suggest, could be operated efficiently by main sequence stars through stellar flares and winds, although they have difficulties in accelerating particles to the 'proper' cosmic ray energies (≥ 1 GeV). As observational evidence, the unusual longitudinal profile of the low energy γ-rays derived by Peterson *et al.* (1990) does match very well the longitudinal profile of the Population I-type stellar objects derived by Pandey *et al.* (1990). The termination shocks produced by stellar winds from Wolf-Rayet stars can release amounts of energy as high as 10^{41} ergs $\cdot$ s^{-1} in the Galaxy. A similar amount of energy is also available from the winds of OB stars, the flares on M and K stars, as well as the shocks of old supernova remnants. Therefore the energy budget (10^{41} ergs $\cdot$ s^{-1}) for the low energy cosmic ray electrons is sufficient in the Galaxy if about 20% of the above mentioned energy output goes into electrons.

Turning to the propagation of these electrons, the main process is diffusion since the speed of the Galactic wind, which leads to convection, is small $V_c \sim 16$ km$\cdot$s^{-1} (Giler *et al.*, 1979) in the Galactic Disk. The life-time of 100 keV electrons against ionization loss in the interstellar medium is $\tau \sim 10^{13}$ s, and the convection range is only $L_c \sim V_c \cdot \tau \sim 5$ pc. In contrast, the diffusion range is much larger and the actual value depends on the value of the diffusion coefficient. Here, although the diffusion coefficient for these low energy electrons is not well known by theoretical consideration or by direct measurement, we can infer it by extrapolation from higher energies. There are two working schemes: (1) the diffusion coefficient is energy dependent, $D \propto E^{0.5}$, and is set to be 10^{29} cm$^2 \cdot$ s^{-1} at $E = 1$ GeV, then $D = 10^{27}$ cm$^2 \cdot$ s^{-1} at $E = 100$ keV and the diffusion range is $(6D\tau)^{1/2} \simeq 80$ pc; (2)

the diffusion coefficient is assumed to be energy independent below 1 GeV and its value to be 10^{28} cm$^2 \cdot$ s^{-1} at $E = 100$ keV, then the diffusion range is $(6D\tau)^{1/2} \simeq 250$ pc. In any case, the diffusion range is larger than the average distance between OB stars, so that the electrons can be pervasive in the whole Galaxy.

3.3 Implication for the cosmic γ-ray background

A direct consequence of the presence of a large flux of electrons in the MeV energy range in the Galaxy is that normal galaxies could contribute a substantial fraction of the cosmic γ-ray background radiation in the hundred keV range. A compilation of measurements of the diffuse cosmic X-ray and γ-ray background is displayed in Figure 3.5. The flux of the isotropic background is fairly high in the energy region of a few hundred keV.
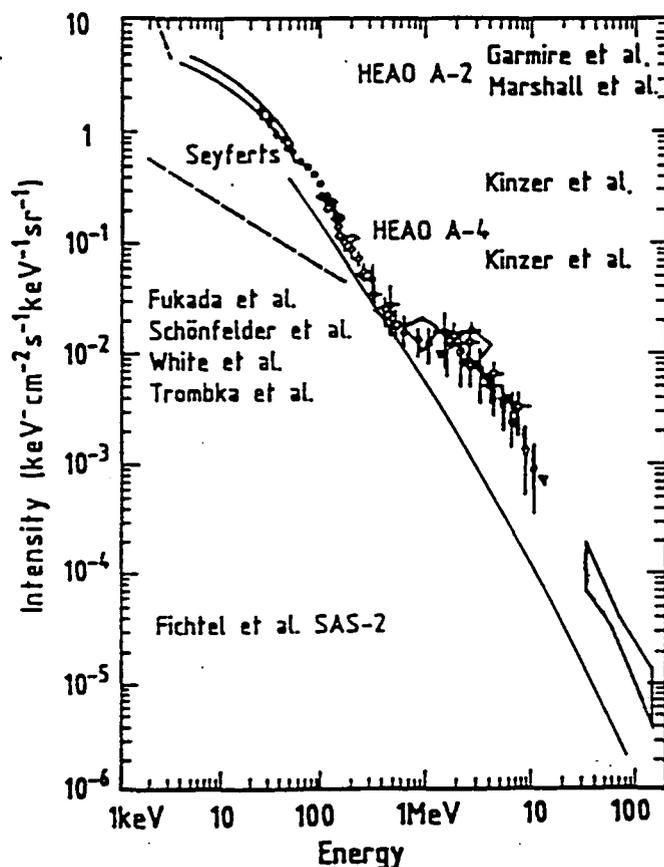

Figure 3.5. The extragalactic γ-ray background flux. The solid

line is the prediction from the normal galaxy model in the present work.

The origin of the background radiation in this energy range is not really understood yet. The mechanisms can be classified into two types: (1) unresolved active galaxies; and (2) thermal bremsstrahlung of intergalactic hot gas. The first type of modeling (*e.g.*, Rothschild, *et al.*, 1983) has usually found it inevitable to invoke a cosmological evolution in the number density, luminosity, and spectral shape of the candidate population; that is, the population has to be substantially different at early epochs than at the present epoch. Whether such a kind of cosmological evolution is true or not is not well known. The second type of modeling (*e.g.*, Marshall *et al.*, 1980) can fit the spectral shape in the energy range 2—50 keV by adjusting the gas temperature. However, it has difficulties with spatial density and evolution. Now, the recent measurement of cosmic microwave background by the COBE satellite certainly rules out the existence of the intergalactic hot gas— the spectral distortion, as predicted by the thermal electron Comptonization mechanism, is not seen.

Here, we propose a new model for the background radiation, in which individual normal galaxy makes a contribution. The γ-ray luminosity of our Galaxy can be calculated in a broad energy range from a few GeV down to a hundred keV by assuming a diffuse origin and a cosmic ray spectrum. Unlike the cosmic γ-ray spectrum which has a very flattened part in the energy range 100 keV—1 MeV, the spectrum of the total Galactic γ-ray luminosity varies only a little in the whole energy range, approximately, a power-law spectrum with index 2.8 above 1 MeV and a slightly flatter power-law with index 2.4 below 1 MeV. For the simplicity of calculation, we assume that all the normal galaxies have the same luminosity and the same spectral shape as our Galaxy. In a non-cosmologically evolutionary model, the cosmic γ-ray flux from normal galaxies at the epochs after galaxy formation is given as

$$I = \frac{cn}{4\pi H_0} \int_0^{z_{\max}} dz L_{\mathrm{G}} \left[(1+z)E\right]/[(1+z)(1+\Omega z)^{1/2}] \qquad (3.11)$$

where z is the redshift; H_0 is the Hubble constant; Ω is the cosmic matter density constant; L_{G} is the Galactic luminosity function; and n is the density of normal galaxies. Here we take $H_0 = 100 \ \mathrm{km \cdot s^{-1} \cdot Mpc^{-1}}$, $\Omega = 1$, $z_{\max} = 4$, and $n = 0.02 \ \mathrm{Mpc^{-3}}$; then the flux follows as

$$I = 75 E^{-2.4} \mathrm{photons \cdot cm^{-2} \cdot s^{-1} \cdot sr^{-1} \cdot keV^{-1}} \qquad (3.12)$$

for the energy range 100 keV—1 MeV, constituting 75% of the observed flux. It is the difference between the background spectrum and the Galactic

spectrum that enables the normal galaxies to contribute a dominant fraction of the low energy γ-ray background flux; whereas at higher energies (about 100 MeV) the contribution from normal galaxies is less than 10% (Strong *et al.*, 1976).

3.4 Implication for support of the interstellar medium

The large scale distribution of HI gas is found to have constant surface density and a constant scale height for the inner Galaxy 4 kpc < R < 10 kpc (Lockman, 1984). This constancy of the shape and the width of the HI layer is a great puzzle. According to the equilibrium formulation by Spitzer (1978), if only the thermal pressure is taken into account the scale height of the gas is a function of stellar mass density,

$$h \propto \sigma_v \rho_s^{-1/2}(R) \tag{3.13}$$

where h is the scale height, σ_v is the velocity dispersion of the gas and $\rho_s(R)$ is the stellar density at the Galactic Plane. This expression is only valid when the stellar scale height is greater than the gas scale height. From studies of HI gas in our Galaxy and in external galaxies, σ_v appears to be independent of R. Assuming an exponential distribution of stellar density with scale length 4 kpc (Bahcall *et al.*, 1983; Mathis *et al.*, 1983), we find that $\rho_s(4\text{kpc})/\rho_s(10\text{kpc}) \simeq 4$. In this way we would expect the HI scale height at $R = 4$ kpc to be half the local scale height. So extra pressure from other agents should come into play.

The pressure from the Galactic magnetic field seems not to be a contender as the radio synchrotron data indicate that the radial variation of the emissivity is small, accordingly the variation of the magnetic field towards the inner Galaxy is small and with it the cosmic ray gradient (cosmic rays above 1 GeV). Whereas the pressure from the normal cosmic rays is a strong contender. From γ-ray data we know that the cosmic ray intensity (≥ 1 GeV) in the inner Galaxy is 1.4 times the local value, *i.e.* 0.4 eV $\cdot$ cm^{-3} at $R = 10$ kpc and 0.56 eV $\cdot$ cm^{-3} at $R = 4$ kpc. So is the 'seed' population of cosmic rays, the distribution of the low energy electrons has an even larger radial gradient, the energy density is 0.05 eV $\cdot$ cm^{-3} at the local position but 0.22 eV $\cdot$ cm^{-3} at $R = 4$ kpc. This increase will certainly contribute to the pressure against gravity in the inner Galaxy and totally the increase of cosmic ray pressure toward the inner Galaxy is by a factor of 2, as required.

3.5 Implication for ionization and heating of HI regions

The presence of thermal free electrons in the interstellar medium is clearly revealed by the dispersion of pulsar signals and by wide spread diffuse H_α emission. When radio waves pass through an ionized plasma, their group velocity is slightly less than the velocity of light in vacuum and is a function of frequency. For a homogeneous isotropic medium, it can be shown that the group velocity has a simple expression (e.g., Ginzburg, 1970)

$$v_g = c(1 - \omega_p^2/\omega^2)^{1/2} \qquad (3.14)$$

where ω_p is the plasma frequency and ω is the wave frequency. The plasma frequency is given by

$$\omega_p^2 = 4\pi n_e e^2/m \qquad (3.15)$$

where n_e is the free electron density. For continuous signals the reduced velocity is of course unobservable, but the pulsed nature of pulsar emission makes it possible to evaluate the degree of dispersion from the difference in pulse arrival times at two different frequencies. It is straight forward to obtain the time delay, approximately to the first order in ω_p^2/ω^2:

$$t_2 - t_1 = \frac{2\pi e^2}{mc}(\omega_2^{-2} - \omega_1^{-2}) \int_0^d n_e dl \qquad (3.16)$$

where d is the distance from the observer to the pulsar. The column density of electrons in the path to the source, $\int_0^d n_e dl$ is usually defined as the dispersion measure DM.

The diffuse H_α ($\lambda = 6563$Å) is emitted in the process of an electron recombining with a proton. The observed H_α intensity is a linear integral along the line of sight (e.g., Spitzer, 1978),

$$I = 0.36 \int n_e^2 T_4^{-0.9} dl \ \text{Rayleighs} \qquad (3.17)$$

where T_4 is the temperature in units of 10^4 K and dl is the path length in pc. One Rayleigh is $10^6/4\pi$ photons $\cdot$ cm^{-2} $\cdot$ s^{-1} $\cdot$ sr^{-1}. In steady state, the H_α intensity is a measure of the ionization rate. For a constant temperature, the emission measure $EM = \int n_e^2 dl$ can be obtained. The unit of EM is cm^{-6} $\cdot$ pc.

Observations of the Galactic H_α emission sample only the local region within $2 \sim 3$ kpc of the Sun. The results provide strong evidence for widely spread regions of warm (10^4 K), nearly fully ionized hydrogen distributed throughout the Galactic Disk (Reynolds, 1983). The derived recombination rate is 4×10^6 cm^{-2} (Reynolds, 1984) and correspondingly the ionized gas

density is $\sim 0.1\text{cm}^{-3}$ (somewhat higher than the conventional 0.03 cm^{-3}. The scale height is ~ 600 pc (Reynolds, 1985).

Pulsar dispersion measures give a consistent result with that of the H$_\alpha$ emission measure. The measured dispersions, together with independently measured distances of about 30 pulsars have shown that the ionized gas has a spatially averaged density of 0.03 cm^{-3} near the middle plane and a scale height substantially larger than that of the HI layer (Manchester and Taylor, 1981). Accurate measurements of the scale height require the presence of pulsars far above the Disk Plane. The recent discovered pulsars in globular clusters provide such an opportunity. Reynolds (1989) used the dispersion data of 5 pulsars in four globular clusters and 33 pulsars in the Disk to determine the scale height, his best estimate is 1 kpc. Lyne (1990) made an independent analysis and obtained the same result.

The ionizing agent has been a mystery for more than three decades. Is it charged particles or photons ? It is very hard to distinguish by observations. The proposal of ionization by charged particles—cosmic rays was discussed in detail by Spitzer and Tomasko (1968). The derived minimum ionization rate from a demodulated cosmic ray proton spectrum down to 40 MeV is only 10^{-17} s^{-1}, apparently insufficient for HI regions. So they invoked 2 MeV cosmic ray protons which are assumed to originate from Type I supernova expansion shells at speed 2×10^4 km$\cdot$s^{-1}, to provide the ionization. However, as pointed out by Spitzer and Jenkins (1975), the short life-time of these low energy protons limit their range to far less than the average distance between Type I supernovae and makes them useless for ionizing large regions of the interstellar medium.

The alternative proposal—ionization by soft X-rays—was made independently by Silk and Werner (1969) and Sunyaev (1969). Werner *et al.* (1970) supposed two possibilities for the Galactic soft X-ray sources: (1) a weak, unresolved source model with a source density of $\sim 10^{-2}\text{pc}^{-3}$ and an average source luminosity of 10^{32}ergs $\cdot$ s^{-1} in soft X-rays below 0.25 keV; (2) a strong, discrete source model with a source density of $3 \times 10^{-8}\text{pc}^{-3}$ and a mean source luminosity of 3×10^{37}ergs$\cdot$s^{-1} in soft X-rays. However, in both models the requirement for source luminosity can hardly be fulfilled since observations show that very luminous sources are rare. A further difficulty comes from the short range of these photons. The cross-section for photo-nionization of hydrogen atom is $6 \times 10^{-18}(E_{\text{Ly}}/E)^3$ cm^2, where $E_{\text{Ly}} = 13.6$ eV is the Lyman edge; thus the low energy photons dominate ionization. A column density of 1.6×10^{17} cm^{-2} will attenuate photons at the Lyman edge significantly. Given the mean density of the ISM of $\sim 1\text{cm}^{-3}$, this column density is equivalent to a distance of only 0.06 pc. In this ionization scenario, the ionized gas density is not uniform, it is high near the sources but low far

away from the sources.

Very recently, a detailed study of the structure of the local ionized gas was carried out by Reynolds (1990a). He found that the ionization along two well-defined line segments to the pulsars PSR 0950+08 and PSR 0823+26 separated by 28^0 cannot be accounted for by HII regions surrounding nearby B stars or known hot white dwarf stars. The nearest O stars with Lyman continuum luminosities capable of producing the ionization are approximately $300 \sim 400$ pc from the line segments. So he concluded that there are three possibilities for the observational facts: (1) a different morphology for the interstellar HI, in which warm, low density 'extra medium' occupies most of the interstellar volume (Cox, 1989); (2) Lyman luminosities for early B or hot white dwarf stars are more than an order of magnitude larger than those currently accepted; or (3) an unrecognized source of ionization within the Galactic disk.

In the present work, we propose that the unrecognized source of ionization is the low energy cosmic ray electrons. If the electron spectrum derived in Section 3.1 is extrapolated down to 50 keV, it is sufficient to account for the ionization rate 1×10^{-15} H-atom$^{-1} \cdot$ s^{-1}. Although this idea was considered previously by a few workers, no working model has been built in term of electron acceleration and propagation. Pikel'ner and Tsytovich (1969) suggested that low energy cosmic rays could be accelerated by Langmuir turbulence and that the particles then ionize and heat the interstellar medium. The problem with their suggestion is that the acceleration process is of second-order Fermi type and its rate is insufficient to generate a large enough number of seed particles. Sacher and Schönfelder (1984) speculated on the possibility that a large flux of low energy electrons derived from an analysis of the γ-ray data could provide the interstellar ionization. However, they did not investigate the acceleration of these electrons but simply assumed the spatial distribution in the Galaxy to be the same as that of the interstellar gas. In this way, the Galacto-radial gradient of the electron distribution is very small and the local flux is very large (4 times as high as in this work).

Let us look at the details of ionization by electrons. This is a two-step process: (1) the incident electron collides with a hydrogen atom and knocks off a secondary electron; and (2) the secondary electron ionizes or heats the interstellar gas. The mean energy released by primary collisions of energetic electrons with hydrogen atoms is very difficult to determine either by theory or by experiment, here we take about 11 eV and 16 eV for the incident electrons of energy 10 keV and 100 keV, respectively. This mean energy is less than half that released in collisions of 2 MeV protons with hydrogen atoms (~ 36 eV) and hence there is a difference in ionization and heating by

49

primary electrons and by primary protons.

In a weakly ionized gas of atomic hydrogen ($n_e/n_H < 10^{-3}$), the secondary electron loses energy in ionization and excitation until its energy falls below 10.2 eV (Spitzer and Tomasko, 1968). The remaining energy must then be lost in elastic collisions. On average, therefore, a heating source of several eV (viz 11—16 eV minus 10.2 eV) is associated with each primary ionizing event. In a highly ionized gas of atomic hydrogen ($n_e/n_H > 10^{-1}$), the secondary electrons lose energy mostly in elastic collisions with the ambient electron gas and cause very little further ionization.

The situation in the interstellar HI regions is the latter case, where $n_e/n_H \simeq 0.03/0.15 \simeq 0.2$, only primary ionization occurs and secondary ionization does not happen. Here, it is interesting to notice that the energy going into ionization and the energy going into heating are almost in equal. Integrating over the whole Galaxy, both the ionization and the heating requires a total energy budget of $\sim 10^{41}$ ergs $\cdot$ s^{-1}. This amount of energy ($\sim 10^{41}$ ergs $\cdot$ s^{-1}) is capable of keeping the interstellar gas at a temperature $\sim 10^4$ K. Coincidentally, it is at this temperature that the energy loss rate of the ionized gas by recombination and by collisional cooling is at minimum (Reynolds, 1990b). It seems that the God is very *economical* in maintaining the Galaxy! Our model of electron ionization and heating is good one.

As a prediction of our model, the ionized gas density has a Galacto-radial gradient with a scale length of 4 kpc, there being more ionized gas in the inner Galaxy, due to a gradient in the electron intensity.

It can be remarked, finally, that it is unnecessary to postulate the decay products of dark matter particles as the source of the observed ionization, as has been suggested by Sciama (1990). It is also unnecessary to invoke the diffuse ionized gas as being *cool* as the interpretation of the inclination dependence of radio power at low frequency (57.5 MHz) observed in external spiral galaxies by Israel and Mahoney (1990). This inclination effect, we think, is caused by the absorption of HII regions. Furthermore, the single power-law extrapolation down to low frequencies used by Israel and Mahoney crucially depends on the assumption of a single power-law spectrum of GeV comic ray electrons, which is apparently in contradiction with the observed spectral variation in the GeV energy range.

Chapter 4

Electrons Escaping from the Galaxy

In this chapter we first examine the evidence for cosmic ray electrons in the GeV energy range escaping from the Galaxy, then discuss the consequences for γ-rays from the Galactic halo and for the extragalactic γ-ray background radiation.

4.1 Electrons in the halo

Grammage measurements of cosmic ray nuclei indicate that the average grammage traversed by the Galactic cosmic rays in the GeV energy range before arriving at the Earth is $N_g = 5$ g $\cdot$ cm^{-2} (assuming that all nuclei, including protons, come from the same sources). If the average density of the interstellar gas is taken to be $\bar{n} \simeq 1$ H-atom $\cdot$ cm^{-3}, we obtain the time of cosmic rays spent in the Galactic Disk

$$\tau_{\text{disk}} = N_g/(m_p n c) \simeq 3 \times 10^6 \text{yr} \tag{4.1}$$

The life-time measurements from the ^{9}Be/^{10}Be ratio give a value of 1.3×10^7yr for the cosmic ray nuclear component in the GeV energy range (Simpson, 1983), however. This difference means that the cosmic rays escape from the Galactic Disk and go into the halo before returning. In this way the mean density of the ISM 'seen' by cosmic rays is only $\bar{n} \sim 0.23$ atoms $\cdot$ cm^{-3}.

As shown in Chapter 2, we have enough reasons to assume the electron component to originate from the same type of source and to propagate in the same way as the nuclear component. Further, their life-time against energy loss (synchrotron radiation and inverse Compton scattering) is $\sim 2 \times 10^7$yr at an energy ~ 8 GeV, of the same order of magnitude as the life-time of the nuclear component. In this way, the electrons also escape from the disk and spend most of their life-time in the halo. The storage of cosmic

rays in the halo depends on its structure and stability. Important progress in understanding the halo dynamics has been made by Ko *et al.* (1990) very recently. Their numerical result shows that a static halo is unstable to overturning, and meanwhile the plasma pressure in the halo is a few orders of magnitude higher than the ambient intergalactic pressure. Therefore, the halo cannot be stationary and there will be a steady outflow, or Galactic wind rising outwards. Accordingly, the cosmic rays (both nuclear component and electron component) escape from the halo with the outward Galactic wind.

Cosmic ray electrons are often considered to be trapped in the magnetic fields within the Galactic disc and/or halo with a relatively small scale height. For example, Bloemen (1985) used an electron distribution of the form

$$f_e(R, z) = exp(-\frac{z}{z_0}) \tag{4.2}$$

Similarly, Fichtel *et al.* (1977) used

$$f_e(R, z) = exp(-\frac{1}{2}(\frac{z}{z_0})^2) \tag{4.3}$$

In both equations, a scale-height of $z_0 = 750$ pc was assumed.

However, recent observational results indicate that the CR electron halo may extend to several kiloparsecs above the Galactic plane. As shown in Chapter 2, the scale height of GeV cosmic ray electrons is likely to be ~ 5 kpc. A consistent result emerged from the study of the all-sky distribution of Galactic synchrotron emission by Phillips *et al.* (1981).

Another indication for a large electron halo has come from the study of the gas haloes of galaxies. The existence of such a halo in the Galaxy was predicted theoretically by Spitzer (1956), and observational evidence for it, using data from the IUE satellite, was given by Savage and de Boer (1979). They found hot ($\sim 10^5$ K), highly ionized, low density ($\sim 10^{-3} cm^{-3}$) gas several kiloparsecs away from the Galactic plane which is very probably supported by CR pressure. Static cosmic ray-supported halo models have been constructed (see, *e.g.* Chevalier and Fransson, 1984; Hartquist and Morfill, 1985). They require cosmic ray protons of GeV energies to extend several kiloparsecs above the Galactic disc in order to achieve theoretical halo gas densities in agreement with the observations. It would be surprising if CR electrons in the GeV energy range were not distributed in a similar manner. A dynamical cosmic ray supported halo model gives an even larger scale height (see, *e.g.* Völk, 1990).

4.2 Inverse Compton γ-rays from the halo

4.2.1 The question

The flux of diffuse cosmic γ-rays has considerable relevance to the origin of the cosmic radiation in that it derives from the interaction of cosmic ray particles (largely protons and electrons) with the gas and photon fields in the Galaxy. However, the relative contribution of electrons and protons as progenitors is not completely clear and, within the electron component, the respective fractions from electron bremsstrahlung on the gas in the Interstellar medium and inverse Compton (IC) interactions on the photon fields are also in doubt.

In the present work we look particularly at the last-mentioned topic, *viz.* the IC contribution, both as a function of the electron-induced flux and as a fraction of the total observed γ-ray flux.

There have been a number of previous studies of this problem and a brief summary is given in Table 4.1. Later Figures also give comparative estimates. Briefly, and for a typical situation: $l = 270° - 90°$ and $|b| \sim 10° - 20°$, estimates range from $< 10\%$ from Bloemen (1985) above 70 MeV to $\simeq 35\%$ from Riley and Wolfendale (1984) above 100 MeV. Clearly, further work is justified.

Table 4.1. Previous estimates of the IC contribution to γ-ray emission.

Author	% of total flux	Energy Range	latitude range
Kniffen and Fichtel (1981)	$> 50\%$	$10 - 100\,\mathrm{MeV}$	$|b| >$ few degrees
Riley and Wolfendale (1984)	35%	$> 100\,\mathrm{MeV}$	$|b| = 10° - 20°$
Bloemen (1985)	$< 5\%$	$> 70\,\mathrm{MeV}$	$|b| < 5°$
Bloemen (1985)	$< 10\%$	$> 70\,\mathrm{MeV}$	$|b| >$ few degrees

The ingredients for calculating the expected IC flux are, essentially, the electron intensity (and spectrum) and the photon energy density (as a function of wavelength), both at every point in the Galaxy but more particularly at rather large distances (z) above and below the Galactic Plane. It will be apparent that neither is known with any precision and there is considerable scope for argument.

A number of developments have occurred recently which make a new analysis timely. These are:

1. The spectral shape of the γ-ray spectrum at latitudes above $10°$ cannot

be understood in terms of the usual mixture of electron bremsstrahlung and pion production. An enhanced IC contribution is one possible explanation.

2. A new estimate of the production rate of γ-rays from proton-ISM collisions. We derive a smaller flux than accepted hitherto which means that the residual flux (total minus CR-ISM collision flux) is larger. Thus, the IC flux *could* be larger.

3. New calculations, by us (see Appendix A) of the energy density of starlight, which give higher values than those adopted by other workers.

4. A new analysis of gas and plasma at large z which indicate that the scale height of CR electrons could be significantly greater than assumed by others.

4.2.2 Analysis of the γ-ray Data

4.2.2.1 The spectrum of the excess emission

It is well known that the γ-ray emissivity above latitudes of a few degrees is significantly larger than that expected from the interaction of CRs with interstellar matter (see *e.g.*, Bloemen, 1989). We have evaluated the excess by fitting a longitude-dependent relation of the form

$$I_\gamma(\Delta E_\gamma, l, b) = \frac{A(\Delta E_\gamma, b)}{1 - R(\Delta E_\gamma, b)\cos l} \qquad (4.4)$$

to the total observed COS-B intensities. This relation adequately reproduces the general trend of the emission as a function of longitude l and greatly facilitates comparison of the data with the intensities expected from CR-ISM interactions.

The parameter A, equivalent to the intensity at $l = 90°$ predicted by the fit, was found to increase with increasing latitude b. The other parameter R, which allows for a variation of CR density with Galacto-centric radius, was estimated to be ~ 0.3 for $b = 10° - 20°$ and ~ 0.4 for $b = 4° - 10°$. However such a small change in R cannot originate in a CR gradient since this would imply a stronger gradient in the higher latitude band which is unlikely.

The expected intensities were derived from HI and CO emission data (see Section 4.2.2.2 for details) and from the γ-ray emissivities for CR nuclei calculated using the model of Dermer (1986) but with a (smaller) CR proton

spectrum consistent with that of Webber *et al* (1987). For $E_\gamma > 300\,\mathrm{MeV}$, where the electron bremsstrahlung contribution should be negligible, the ratio of observed (*i.e.*, predicted by the relation above) to expected intensities at $l = 90°(270°)$ and $b = 10° - 20°$ was found to be ~ 2.5; at lower latitudes the ratio was smaller, ~ 1.8.

A more detailed analysis of the observed and expected emissivity spectrum ($E_m^2 q/4\pi$, where $E_m^2 = E_1 E_2/(E_2 - E_1)$) for $10° < b < 20°$ is given in Figure 4.1. Also shown is the spectrum of the 'excess' (observed - expected).
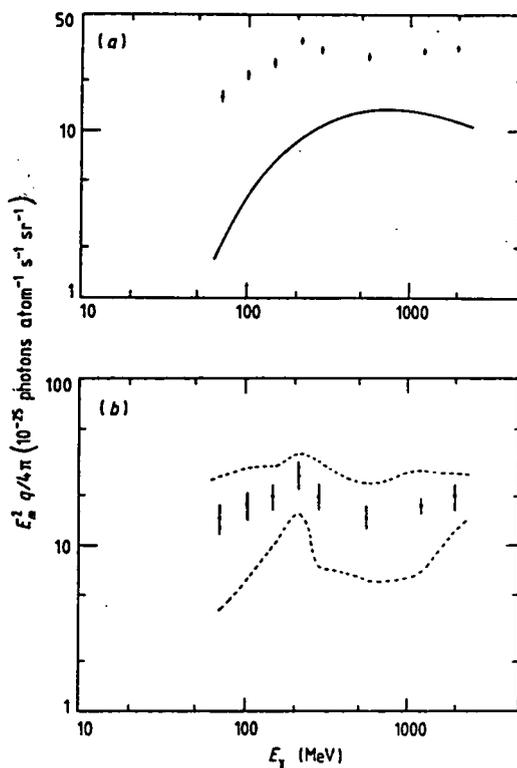
Figure 4.1. Emissivity spectra for $10° < b < 20°$ and $l = 90°$. For the energy interval $\Delta E_\gamma = E_2 - E_1$, $E_{m^2} \equiv E_1 E_2/\Delta E_\gamma$. (a) Points: 'observed'. Total emissivity derived using the intensity expressions and the gas data described in section 4.2.2. Error bars are statistical only. Full curve: expected. Emissivity for CR nuclei interacting with the ISM. (b) Total 'observed'— expected emissivity from (a) above. Errors include a contribution from the Dermer (1986) model used to compute the expected emissivity. Broken lines: Variation in residual emissivity when the COS-B isotropic background is changed by ±20%.

Electron bremsstrahlung has been ignored in deriving the spectrum of the excess emission since it affects only the low energy part ($< 300\,\mathrm{MeV}$) and has little impact on the results. It should be noted that the excess cannot arise from π° decay processes at all because there is a substantial dip in the spectrum around $500\,\mathrm{MeV}$ where π° decay produces a maximum. Agreement between the expected and observed spectra is not improved by modifying the CR spectrum $e.g.$, by making the CR spectrum flatter. In addition, if ionized gas constitutes a significant fraction of the ISM along the line of sight, then the dip at $500\,\mathrm{MeV}$ is even greater than that shown in Figure 4.1.

These spectral characteristics suggest that the only acceptable origin of the excess emission, apart from exotic mechanisms like photino-antiphotino annihilation (Rudaz and Stecker, 1988), is from IC interactions of electrons in the Galactic halo. However, an IC component should appear as a horizontal line when plotted in the manner of Figure 4.1 and it is necessary to argue that the COS-B isotropic background levels used in the present work (taken from Strong $et\ al.$ 1987) are incorrect. For example, if the background is uniformly reduced by $\sim 20\%$, the relative size of the $500\,\mathrm{MeV}$ dip is substantially reduced (see Figure 4.1). Additionally, if the background levels are also relatively incorrect by only modest amounts — say less than 10% — the peculiar spectral shape of the excess may disappear. Comparison of the background parameters quoted by Bloemen (1985), Strong $et\ al.$ (1987) and Bloemen $et\ al.$ (1988) suggest that the uncertainties in the isotropic COS-B background are at least of this order. For the standard COS-B background levels, Figure 4.1 implies that at $E_\gamma > 300\,\mathrm{MeV}$ and $l = 90^\circ$, the IC component is $\sim 60\%$ of the total emission. If the background levels are reduced by 20%, an even larger IC component is required ($\sim 80\%$).

4.2.2.2 The spatial variation of the excess emission

In order to compare the excess γ-ray flux with the IC model presented in section 4.2.4, we have re-derived it by subtracting from the total emission an estimated CR-ISM contribution which in this case includes a bremsstrahlung component. The proton-ISM emissivity has been assumed to be of the form

$$\frac{q_\mathrm{p}}{4\pi}(R, z, \Delta E_\gamma) = \frac{q_\mathrm{p}^\odot}{4\pi}(\Delta E_\gamma)\, f_\mathrm{p}(R, z)\, \mathrm{photons\, atom^{-1}\, s^{-1}\, cm^{-1}\, sr^{-1}} \qquad (4.5)$$

where the local emissivity, $q_\mathrm{p}^\odot$, follows from the calculation described in subsection 4.2.2.1 and $f_p(R, z)$ defines the variation of the proton intensity within the Galaxy. It has been assumed that CR electrons and protons are distributed in the same way i.e. $I_\mathrm{p}(\mathbf{r})/I_e(\mathbf{r}) = I_\mathrm{p}^\odot/I_e^\odot$. The contribution from

electron bremsstrahlung has been estimated approximately as

$$q_{br}(R, z, \Delta E_\gamma) = \alpha(\Delta E_\gamma)\, q_p(R, z, \Delta E_\gamma) \qquad (4.6)$$

with $\alpha = \langle q_{br}/q_p \rangle_{\Delta E_\gamma}$ estimated from the work of Bhat *et al.* (1986). The total CR-ISM contribution to the observed γ-ray intensity is

$$I_\gamma(\Delta E_\gamma) = (1 + \alpha)\, \frac{q_p^\odot}{4\pi}\, \langle f_p(\mathbf{r}) \rangle\, n_H \qquad (4.7)$$

for the neutral hydrogen (HI) and molecular (H₂) components of the ISM; $\langle f_p \rangle$ is the average of $f_p(\mathbf{r})$ along the line of sight.

Column densities of HI have been derived from the 21 cm radio surveys of Weaver and Williams (1973) and Strong *et al.* (1982) for $|b| \le 10°$, and Heiles and Cleary (1979) and Heiles and Habing (1974) for $|b| > 10°$. Molecular hydrogen is only significant at $|b| > 10°$ toward a few local giant molecular clouds. For these regions we have used the Columbia CO survey of Dame *et al.* (1987), converting to n_{H_2} with $n_{H_2} = 1.5 \times 10^{20}\, W_{CO}$ molecules cm^{-2} where $W_{CO} = \int T_{CO}\, dv$ is the velocity-integrated CO line-temperature.

4.2.3 The predicted flux of IC γ-rays

4.2.3.1 Statement of the problem

An estimate of Galactic IC γ-ray emission above 50 MeV requires knowledge of both the CR electron intensity and the radiation field throughout the CR halo. The ISM is opaque to starlight of $\lambda < 0.1\,\mu m$ because of photoelectric absorption by H and He. Thus γ-rays considered in this work ($E_\gamma > 50$ MeV) are produced by CR electrons of energy greater than 1 GeV. Solar-modulation effects make the local electron flux between 1 and 10 GeV rather uncertain and its behaviour elsewhere in the Galaxy is even less well-known. There is also uncertainty about the spatial variation of the photon energy density, though probably not to the same extent as for cosmic rays. In the rest of this subsection we discuss these points, and the adopted model, in more detail.

Having chosen the model for the distribution of CR electrons $I_e(E, \mathbf{r})$ and the energy density of the Galactic photon field $u_\lambda(\mathbf{r})$, the intensity of IC emission along a given line of sight (l, b) is calculated as

$$I(E_\gamma, l, b) = \int dE \int d\lambda \int_{LOS} ds\, \sigma_{IC}(E_\gamma, E, \lambda)\, I_e(E, \mathbf{r}_s)\, u_\lambda(\mathbf{r}_s) \qquad (4.8)$$

where σ_{IC} is the Klein-Nishina cross section for relativistic electrons (see Bloemen 1985 for references) and s denotes the distance along the line of sight from the observer.

4.2.3.2 The Galactic radiation field

Two recent estimates of the interstellar radiation field (ISRF) have been given by Kniffen and Fichtel (1981) and Bloemen (1985). In Appendix A our up to date estimate is presented and a comparison with previous works is given. Here, we only point out that the ISRF has a large scale height, which facilitates the γ-ray contribution from the halo.

4.2.3.3 The radial distribution of cosmic ray electrons

Two simple forms for the radial distribution of CRs have been used in the present work. In the first case, a uniform CR slab model of radius 20 kpc has been adopted i.e., $I_{CR}(R, z) = constant$ for $R \leq 20\,\mathrm{kpc}$, $|z| \leq 5\,\mathrm{kpc}$ and zero elsewhere. In the second case, the CRs vary as

$$I_{CR}(R, z) = \begin{cases} I_{CR}^{\odot}\, exp\left(-\frac{(R-R_{\odot})}{R_{CR}}\right) & R \leq R_{\odot} \\ I_{CR}^{\odot} & R_{\odot} < R < 20\,\mathrm{kpc} \\ 0 & 20\,\mathrm{kpc} \leq R \end{cases} \qquad (4.9)$$

for $|z| \leq 5\,\mathrm{kpc}$ and are zero elsewhere. Note that $R_{\odot} = 10\,\mathrm{kpc}$ has been adopted in this work. The radial scale-length (R_{CR}) is $\sim 7.2\,\mathrm{kpc}$ which produces a factor of two increase in I_{CR} between $R = 5$ kpc and $R = R_{\odot}$ as suggested by Bhat *et al.* (1986) for CRs in the disc of the Galaxy. In accordance with the idea of an extensive CR halo presented in Section 4.2.2, both the model distributions have a total width of 10 kpc. Of course, these two idealised models were chosen to simulate the presence or absence of large-scale gradients in the halo. Unfortunately, they can provide little information about CR variations in the gas disc because of the much smaller scale-height for the gas. The local CR electron spectrum is as given by Webber (1983).

4.2.4 Results and discussion

Figure 4.2 compares the predicted intensities of Bloemen (1985) with the present results for a uniform CR slab model of scale-height (half width) 1 kpc. It is apparent that Bloemen's estimate of the total intensity is smaller

than derived here by a factor of about 30% − 40% at $b = 15°$. For a half width of 5 kpc, the difference is considerably larger, almost a factor of 4.

Our predictions for a 10 kpc full width CR halo are given in Figure 4.3 for the two CR distributions. The 'observed' intensities have been calculated as in Section 4.2.2 and the predicted intensities for a ±20% variation of the isotropic background are also shown.

Inverse Compton emission derived from the model can account for a significant fraction (25% − 40% at $l = 90°$) of the observed excess. Between 150—300 MeV, the model can account for only ∼ 25% of the excess. It is interesting that there is a significant 'bump' in the spectrum of the total (and excess) emission at this energy. The reality of the bump is, of course, open to question since the isotropic background levels used in this analysis
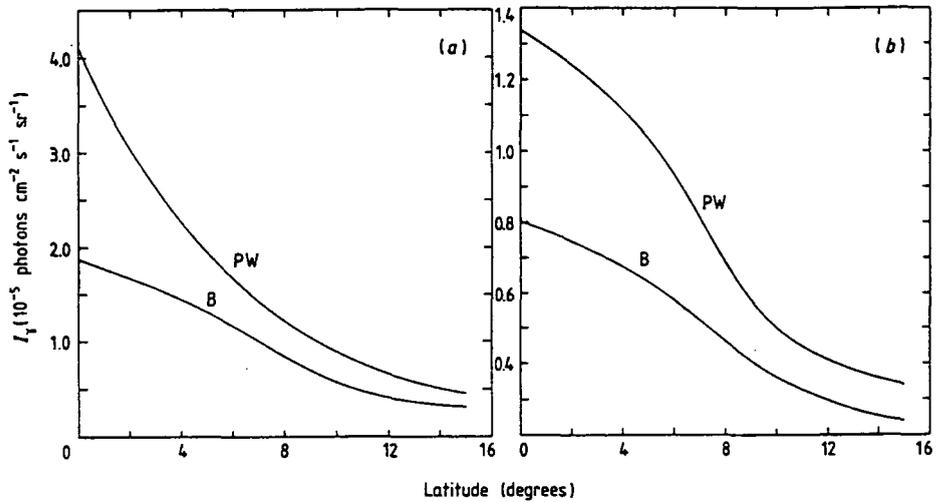

Figure 4.2. Intensity expected from IC emission between 70—150 MeV at (a) $l = 30°$ and (b) $l = 60°$ using our estimated radiation field and a uniform slab CR distribution of total width 2 kpc and radius 15 kpc. PW: present work; B: Bloemen (1985).

are subject to some uncertainty. Agreement between the model and observation is improved for a larger COS-B background in each energy band, but the spectral shape of the observed excess is relatively worse in this case (see Section 4.2.2) unless the background parameters are independently uncertain by substantial amounts. Of course, if the background levels are in fact too large, the model predictions are correspondingly too small.
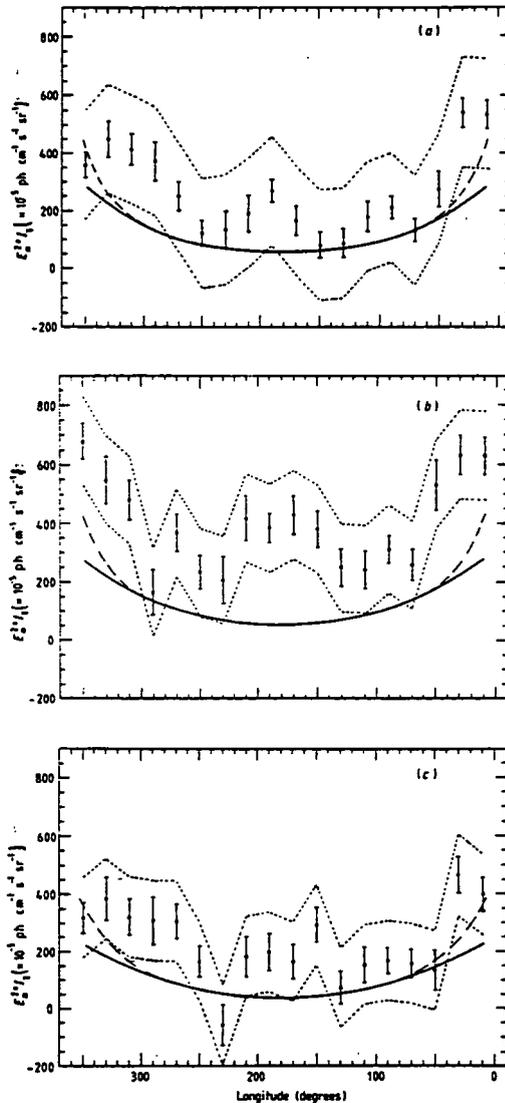
Figure 4.3. COS-B intensities between $|b| = 10° - 20°$ after subtraction of an estimated CR-ISM component (see text). The error bars account for statistical uncertainties only. For the energy interval $\Delta E_\gamma = E_2 - E_1$, $E_m^2 \equiv E_1 E_2/\Delta E_\gamma$. (a) 70—150 MeV. (b) 150—300 MeV. (c) 300—5000 MeV. Full curve: inverse Compton intensities predicted by the present work for a uniform slab CR halo of total width 10 kpc and radius 20 kpc. Broken curve: model IC emission as for the solid line except that a radial CR gradient in the halo has been assumed. Dotted lines: the observed excess emission for a ±20% variation in the standard COS-B isotropic background parameters.

4.2.5 A brief summary

Considering the uncertainties in the Galactic radiation field and, more importantly, in the distribution and spectral shape of CR electrons, the model calculations imply that the IC process is an important component of the observed excess emission. From the analysis in section 4.2.2, we suggest that it probably accounts for more than 50% of the total γ-ray emission above $b = 10°$ and provides a plausible explanation for the spectral shape of the excess emission. This conclusion contrasts with the analysis of Bloemen (1985) who argued that the IC process contributes less than 10% of the total emission at medium latitudes.

If the IC model does prove to be reasonable, there are important consequences for the analysis of the extra-galactic γ-ray background which has been estimated from SAS II data as $\sim 1.3 \times 10^{-5}\,\mathrm{photons\,cm^{-2}\,s^{-1}\,sr^{-1}}$ (see Thompson and Fichtel, 1982). In the diffusion-convection picture of CR propagation, the spectrum of CR electrons that 'escape' from a galaxy into the inter-galactic medium is steeper for a large halo than for a small one because of increased IC losses in the halo. Inverse Compton γ-rays from these escaped electrons and the extra-galactic photon field can contribute significantly to a diffuse background, but the spectral shape of the ambient electrons is a crucial factor.

The total luminosity of the Galaxy above 100 MeV from IC γ-rays becomes quite significant at more than $3 \times 10^{38}\,\mathrm{ergs\,s^{-1}}$ out of a total of $(1-2)\times 10^{39}\,\mathrm{ergs\,s^{-1}}$ for γ-rays as a whole assuming an $E_\gamma^{-1.8}$ spectrum. An IC contribution of this size may have some effect on previous large-scale correlation studies of γ-ray emission and tracers of inter-stellar gas, especially towards the inner Galaxy (*e.g.* Strong, 1985). Since the IC component varies rather slowly in both longitude and latitude, a significant under-estimate would probably manifest itself as an apparent increase in HI emissivity or isotropic background. The IC emission is not strongly correlated with molecular gas and is unlikely to influence estimates of the n_{H_2} to W_{CO} ratio, particularly in the Outer Galaxy where the flux variation is very small and where most medium-latitude molecular clouds are to be found.

A decisive test of the importance of the IC process at Galactic latitudes above $10°$ will be possible when the data from NASA's Gamma Ray Observatory, due for launch this November, become available. The USSR-France-Poland satellite Gamma-1 should also provide useful data.

4.3 Cosmic γ-ray background

4.3.1 The question

The diffuse extragalactic radiations have been puzzling astrophysicists for some time, because their origins are not clear, except for the 2.7 K microwave background which has been satisfactorily explained as the relic of the early universe. The problem of the diffuse extragalactic γ-ray background has come from the development of Gamma Astronomy in recent years. A derivation of the extragalactic diffuse γ-ray flux with energy above 35 MeV using SAS-II data by Fichtel *et al.* (1978) and Thompson and Fichtel (1982), gave a comparatively high value in the range (1.0 $\sim$ 1.3) $\times$ 10^{-5} photons cm^{-2} s^{-1} sr^{-1} above 100 MeV.

How should this diffuse γ-ray background be interpreted? The concept of unresolved sources contributing to diffuse γ-rays has been considered by Strong, Wolfendale and Worrall (1976); Bignami, Lichti and Paul (1978); Schönfelder (1978); Grindlay (1978) and Bignami *et al.* (1979). These sources include normal galaxies, radio galaxies, BL Lac objects, Seyfert galaxies and quasars. Among them, the normal galaxies dominate in number, but they contribute less than 10% of the total background for the energy range above 100 MeV, assuming all galaxies to emit the same flux of γ-rays as our Galaxy and without cosmological evolution (Strong, Wolfendale and Worrall 1976). Contributions from other kinds of galaxies are quite uncertain. According to the analysis of Bignami *et al.* (1979), radio galaxies and quasars contribute only several percent; whereas Seyfert galaxies and BL Lac objects may be strong contenders, possibly contributing up to 50%. However, a very recent analysis by Gao *et al.* (1990) shows that the contribution from active galaxies cannot be larger than 10% because the γ-ray spectra of active galaxies are very steep and cannot be derived by extrapolating their X-ray spectra, which are flat. Therefore, although the discrete source contribution may be significant it is very unlikely to be sufficient, without any cosmological evolution.

In the last section, we have reestimated the inverse Compton contribution to the Galactic γ-ray emission at medium latitudes using an electron halo model. The conclusion is that γ-ray emission via IC can contribute up to 60% of the Galactic diffuse γ-rays at medium latitudes. This will account for a certain fraction of the extragalactic γ-ray background, but some of the diffuse background still remains unexplained.

In this section, the extragalactic γ-ray background is reestimated using SAS-II data. We propose a new contribution to the diffuse γ-ray background:

γ-rays produced in inverse Compton interactions of escaped cosmic ray electrons from normal galaxies with the 2.7 K microwave radiation background in intergalactic space. We then go on to study the possibility of a cosmological increase of this component at early epochs and also the possible contribution from other cosmological phenomena.

4.3.2 A new estimate of the cosmic γ-ray background

Due to being essentially free of instrumental and radiation belt backgrounds, the SAS-II data may be used to directly estimate the extragalactic diffuse γ-ray background. Fichtel *et al.* (1978) show that the diffuse γ-ray flux observed by SAS-II in the energy range above 35 MeV consists of two components, the Galactic and the Extragalactic. Obviously, the Galactic component results from the interactions of cosmic rays with interstellar matter and photon fields, and it is possible to separate these two components by using the information on the interstellar medium and cosmic rays. However, in the previous separations (Fichtel *et al.*, 1978; Thompson and Fichtel, 1982), the Inverse Compton γ-ray contribution to the Galactic component was ignored. This leads to a large value of the cosmic ray proton-HI emissivity and a high level of extragalactic background. For example, Fichtel *et al.* (1978) gave an emissivity, 3.0×10^{-26} photons cm^{-2} s^{-1} sr^{-1} H atom^{-1} (above 100 MeV) to be compared with the recent COS-B value of 1.8×10^{-26} photons s^{-1} sr^{-1} H atom^{-1} (Strong *et al.*, 1988). The derived extragalactic background was 1.0×10^{-5} photons cm^{-2} s^{-1} sr^{-1} above 100 MeV.

In the present work, all the contributors to the Galactic component of diffuse γ-rays at intermediate latitude are included. The atomic hydrogen data used here are from a summary of several surveys: Weaver and Williams (1973), Strong *et al.* (1982), Heiles and Cleary (1979) and Heiles and Habing (1974). The molecular hydrogen regions are avoided. The ionized hydrogen gas (HII) is assumed to be distributed over a uniform slab of radius 12 kpc and a vertical scale height (half-width) of 5 kpc, with a total column density in the polar direction of 2.0×10^{20} H ion cm^{-2}. The inverse Compton flux is taken from the last section. In this way, the observed diffuse γ-ray flux is expressed by

$$I_\gamma = (n_{HI} + n_{HII})q_p + I_{IC} + I_b \qquad (4.10)$$

where n_{HI} and n_{HII} are the atomic and ionized hydrogen column densities, respectively; q_p is the cosmic ray proton-hydrogen emissivity (including Bremsstrahlung), cited from Strong *et al.* (1988); I_{IC} is the inverse Compton flux of the new estimate in the last section; I_b is the extragalactic back-

ground. To derive the value of I_b, a least square fit is applied to SAS-II data at high latitudes ($|b| > 12.8°$). The fit yields $I_b = (0.81 \pm 0.3) \times 10^{-5}$ photons cm^{-2} s^{-1} sr^{-1} in the energy range above 100 MeV. This value is a little lower than the previous estimates, 1.0×10^{-5} photons cm^{-2} s^{-1} sr^{-1} by Fichtel *et al.* (1978) and 1.3×10^{-5} photons cm^{-2} s^{-1} sr^{-1} by Thompson and Fichtel (1982). The fit is also carried out in the energy range from 35 MeV to 100 MeV, resulting in $I_b = (3.9 \pm 1.0) \times 10^{-5}$ photons cm^{-2} s^{-1} sr^{-1} (to be compared with $I_b = 4.9 \times 10^{-5}$ photons cm^{-2} s^{-1} sr^{-1}, Fichtel *et al.*, 1978). If a power law spectrum is assumed, the differential index of the photon number spectrum is 2.7 (+0.4,-0.3). Figure 4.4 shows a comparison of the spectra between this work and that of Thompson and Fichtel (1982) and Bignami *et al.* (1979). Hereinafter, the term *background* refers to the new estimate.

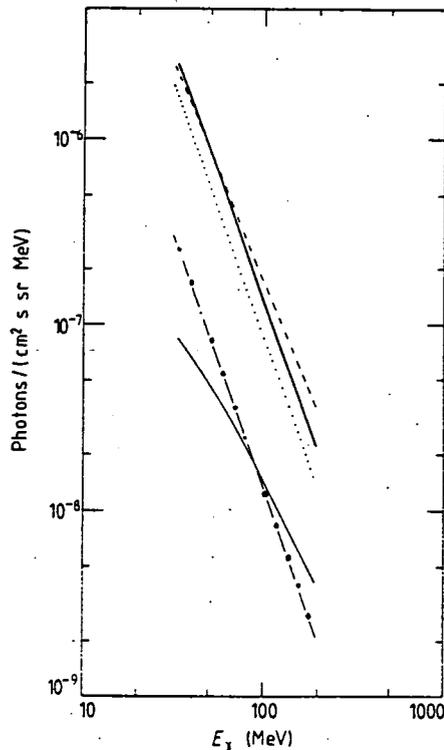Figure 4.4. Extragalactic γ-ray background. Dashed line: the γ-ray background estimated by Thompson and Fichtel (1982); thick solid line: the γ-ray background estimated in this work; dot line: the prediction from active galaxies by Bignami *et al.* (1979); dashed-dot line: the contribution from normal galaxies; thin solid line: the prediction of the Escaped Electron-Inverse Compton model.

4.3.3 Cosmic ray electrons escaping from normal galaxies

It is generally accepted that cosmic ray electrons are of Galactic origin, because the universal 2.7 K microwave radiation background acts as a natural barrier to prevent extragalactic electrons arriving at our Galaxy. As shown in Section 2.2, diffusive shocks by supernova remnants are a strong contender for the acceleration mechanism. The observed cosmic rays have undergone many complicated processes of propagation before reaching the earth. Various models of propagation have been proposed so far, in which the essential physical processes involve diffusion, convection, adiabatic deceleration, shock wave acceleration and energy loss. However, for the very high energy (above 100 GeV) cosmic ray electrons, the propagation process is thought to be simple, so that a diffusion model with energy loss is a good enough approximation (Lerche and Schlickeiser, 1980). The Galaxy cannot confine the very high energy cosmic rays (Cesarsky, 1980), although it slows down their escape.

Here, we use a one dimension diffusion model to derive the flux of cosmic ray electrons escaping from the Galaxy. The diffusion equation can be written as

$$D\frac{\partial^2 N(E,z)}{\partial z^2} + \frac{\partial(bN(E,z))}{\partial E} + Q(E,z) = 0 \qquad (4.11)$$

where $N(E,z)$ is the electron number density. D is the energy dependent diffusion coefficient, $D = D_0 (E/E_0)^{1/2}$, $D_0 = 1.1 \times 10^{29}\,\mathrm{cm^2\,s^{-1}}$, $E_0 = 1.0\,\mathrm{GeV}$, $Q(E,z)$ is the source function, b is the energy loss rate, here only synchrotron radiation and inverse Compton processes are considered, so that $b = a(z)(E/E_0)^2$, where

$$a(z) = 0.80 \times 10^{-16}\,(\mathrm{GeVs})^{-1}, |z| < 0.5\,\mathrm{kpc} \qquad (4.12)$$

$$a(z) = 0.27 \times 10^{-16}\,(\mathrm{GeVs})^{-1}, 0.5 < |z| < 5.0\,\mathrm{kpc} \qquad (4.13)$$

The source function $Q(E,z)$, is taken to have the usual power law form $K E^{-\Gamma}\delta(z)$. Our diffusion coefficient and halo size ensure the theoretical local lifetime to be $2.0 \times 10^7\mathrm{yr}$ as implied by isotope $^{10}\mathrm{Be}$ measurements (Garcia-Munoz et al., 1977a).

The boundary condition is that N=0 at the boundary, i.e. free escape. Solving the equation, we obtain the electron intensity in the Galaxy and the escaping flux, the latter is

$$I_{\mathrm{escaped}} = -D\frac{\partial N}{\partial z}|_{\mathrm{boundary}} \qquad (4.14)$$

N(E,z) and I_{escaped} are generally in series form of E and z, but they have roughly a power law form in E,

$$N(E,z) \sim E^{-(\Gamma+0.5)} \qquad (4.15)$$

$$I_{\text{escaped}} \sim E^{-\Gamma} \qquad\qquad (4.16)$$

except at very high energies (above 200 GeV) where the spectrum becomes slightly steeper due to energy losses. Obviously, the escaped electron spectrum has the same shape as the injected one, but the observed spectrum becomes steeper by 0.5 in the exponent owing to the diffusion being energy dependent.
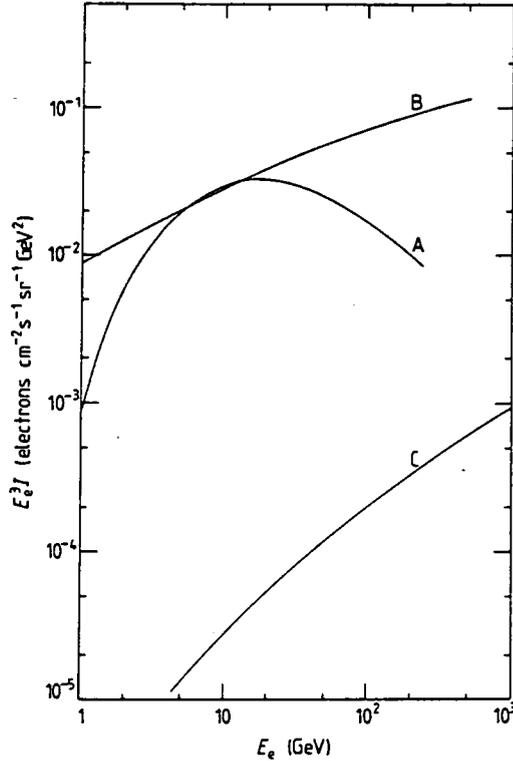

Figure 4.5. Cosmic ray electron spectrum. A: the local measured spectrum by Müller and Tang (1987); B: the local theoretical spectrum in this work; C: the escaped spectrum at the edge of the Galaxy in this work.

Before scaling the theoretical quantities to the measurements at the earth, it is necessary to look at the location of the solar system in the Galaxy. Although our local position is within the Galactic disk, very close to the Galactic plane (12 pc away), it is very probable that by chance there is a deficit of nearby sources (Giler *et al.*, 1978; Shapiro and Silberberg, 1971; Garcia-Munoz *et al.*, 1977b). Both very low energy and very high energy electrons will suffer heavy losses, the former due to ionization and the latter

due to the long transit times. The result is a bending occurred around 5 GeV in the observed spectrum. It is likely that the local spectrum is a special one, which may not represent the global spectrum in the Galaxy. Further evidence is provided by Galactic nonthermal radio observations, the power law index of the synchrotron radio emission of cosmic ray electrons is -0.7 from 408 MHz to 1.4 GHz (Lawson *et al.*, 1987; Reich and Reich, 1986), this value corresponds to a power law index -2.4 of the progenitor electron spectrum in the energy range 4 GeV — 10 GeV, assuming an interstellar magnetic field strength of 5 microgauss. Recognizing these facts, in this work, we take the input spectrum as $E^{-2.0}$, leading to a theoretical local spectrum of $E^{-2.5}$ (*local* yet remote from the earth) and the escaped spectrum is $E^{-2.0}$ except for very high energies. The theoretical electron spectrum is normalised to that measured at 5 GeV (Müller and Tang, 1987), assuming $z = 0$ for the local position. Figure 4.5 shows the electron spectrum measured locally, the local theoretical and the escaped flux at the edge of the Galaxy. To calculate the total electron output of the Galaxy, the size of the Galaxy is needed. Here we take the Galaxy as a slab with a height 10 kpc and a radius 20 kpc, the disk plane is in the middle height, on which the sources are uniformly distributed, the total output is $5.6 \times 10^{39}\,\mathrm{erg\,s^{-1}}$ for electrons above 1 GeV.

4.3.4 γ-rays produced by the escaped electrons

It is well known that normal galaxies are dominant in the Universe, at least by number. There is strong evidence that the processes in other galaxies are similar to those in ours, since linear correlations between radio luminosity and optical luminosity do exist among various galaxies (see Chapter 5). In particular, the rate of supernovae, dominant contributors of cosmic rays, is similar to ours in other galaxies (Cappellaro and Turatto, 1988). Hence, there is sufficient reason to assume that other normal galaxies are the same as ours, on average. The number density of normal galaxies is 0.02 Mpc^{-3} with $H_0 = 100\,\mathrm{km\,s^{-1}\,Mpc^{-1}}$. With these values, we can derive the average electron emitting rate of the Universe,

$$Q(E) = 8.7 \times 10^{-34}\,E^{-2.2}\,\mathrm{electrons\,cm^{-3}\,s^{-1}\,GeV^{-1}} \qquad (4.17)$$

at the present epoch.

After leaving the Galaxy, cosmic ray electrons undergo successive inverse Compton scatterings with the 2.7 K microwave radiation. This is the only way in which electrons lose their energy if the gas density and strength of magnetic field in the intergalactic space are negligible. The energy loss

equation describing this behavior is

$$Q(E) + \frac{\partial(b(E)N(E))}{\partial E} = 0 \tag{4.18}$$

where $N(E)$ is the electron number density, $b(E)$ is the energy loss rate of the electron and is taken as $b = 2.5 \times 10^{-17} E^2 \, \text{GeV s}^{-1}$. Solving the equation, the electron number density follows as

$$N(E) = 2.8 \times 10^{-17} E^{-3.2} \, \text{cm}^{-3} \, \text{GeV}^{-1} \tag{4.19}$$

and the intensity is

$$j(E) = 6.7 \times 10^{-8} E^{-3.2} \, \text{cm}^{-2} \, \text{s}^{-1} \, \text{sr}^{-1} \, \text{GeV}^{-1} \tag{4.20}$$

Since the energy of the 2.7 K microwave background photons is very small, here the Thompson cross-section can be used. Stecker (1975) has shown that the γ-ray emissivity, $q_c(E_\gamma)$, under the monochromatic approximation is given by

$$q_c(E_\gamma) = (8/3)\pi \, \sigma_T \, \rho_{ph} \, (mc^2)^{1-\Gamma} \, (4/3\bar{\epsilon})^{(\Gamma-3)/2} \, K \, E_\gamma^{-(\Gamma+1)/2} \tag{4.21}$$

where ρ_{ph} is the energy density of the microwave background ($0.24 \, \text{eV} \, \text{cm}^{-3}$), σ_T is the Thompson cross section ($6.65 \times 10^{-25} \, \text{cm}^2$), m is the mass of the electron, $\bar{\epsilon}$ is the average photon energy, K is the coefficient of the electron spectrum and Γ is the power law index of the electron spectrum.

Substituting the electron intensity in the above formula, the emissivity is,

$$q_c(E_\gamma) = 1.0 \times 10^{-34} E^{-2.1} \, \text{photons cm}^{-3} \, \text{s}^{-1} \, \text{GeV}^{-1} \tag{4.22}$$

To include contributions from early epochs (but not increasing the rate of electron production at early epochs), we adopt the treatment by Stecker (1971). The flux is given as

$$I_\gamma = c/(4\pi \, H_0) \, q_0(E_\gamma) \int_0^{z_{max}} (1+z)^{\Gamma-4}/(1+\Omega z)^{1/2} dz \tag{4.23}$$

where, H_0 is the Hubble constant, Ω is the density constant, z is the redshift and $q_0(E_\gamma)$ is the γ-ray emissivity at the present epoch. Here we take $H_0 = 100 \, \text{km s}^{-1} \, \text{Mpc}^{-1}$, $\Omega = 1$, $z_{max} = 4$ (where Galaxy formation occurs); the flux value is

$$I_\gamma = 1.0 \times 10^{-7} E^{-2.1} \, \text{cm}^{-2} \, \text{s}^{-1} \, \text{sr}^{-1} \, \text{GeV}^{-1} \tag{4.24}$$

For photons above 100 MeV, the flux is

$$I_\gamma(> 100 \, \text{MeV}) = 0.12 \times 10^{-5} \, \text{photons cm}^{-2} \, \text{s}^{-1} \, \text{sr}^{-1} \tag{4.25}$$

This accounts for 15% of the diffuse γ-ray background, as shown in Figure 4.4. Together with the contribution from normal galaxies themselves, the total contribution from normal galaxies amounts to 25%.

If a cosmological evolution is assumed, the contribution from normal galaxies will be considerably increased. For instance, the cascade model of Wdowczyk and Wolfendale (1990), in which γ-rays are produced by extragalactic cosmic ray cascades, can explain the background by including a cosmological evolution effect, i.e., $(1+z)^\beta$ in cosmic ray sources with $\beta = 3.7$. Accordingly, if we put a cosmological evolution factor $(1+z)^\beta$ in the discrete source (normal galaxies) model or the Escaped Electron-Inverse Compton model, we can explain the total background. The flux integrated over every epoch is given by

$$I = [cn/(4\pi H_0)] \int_0^{z_{max}} (1 + z)^\beta L_G[(1 + z)E] / [(1 + z)(1 + \Omega z)^{1/2}]dz \quad (4.26)$$
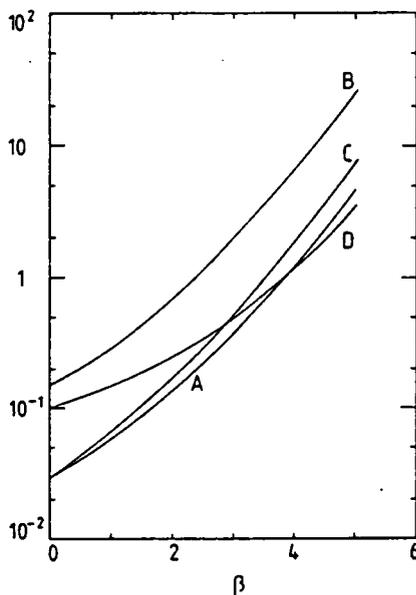

Figure 4.6. The fraction of the γ-ray background contributed by various models versus the cosmological evolutionary effect. A: the cosmic ray cascade model of Wdowczyk and Wolfendale (1989); B: electron escaping model (power law) where the escaping electron spectrum is related to the local *theoretical* one; C: electron escaping model (local measured) where the escaping electron spectrum is related to the local *measured* one; D: discrete source model where the source is normal galaxies.

where n is the number density of normal galaxies, L_G is the luminosity of

our Galaxy, H_0 is the Hubble constant. Figure 4.6 shows the fraction of γ-ray background contributed by these three kinds of model versus β. It is seen that these models are equally contenders and that we need $\beta = 3$. For comparison, it is worthwhile to examine how much evolutionary effect should be put in for other waveband backgrounds. We find that $\beta = 2 \sim 4$ for radio, far-infrared, UV and X-ray; while $\beta = -2$ for the visible light.

At the present stage, we cannot make a decisive choice among various models. The observations by GRO in the near future will improve the situation insofar as more precise measurements of spectra and luminosities will be achieved.

4.3.5 A brief summary

1. The extragalactic γ-ray background is found to be to 0.81×10^{-5} ph cm^{-2} s^{-1} sr^{-1} above 100 MeV; *i.e.* some $\simeq 40\%$ lower than the result of Thompson and Fichtel (1982).

2. The Escaped Electron-Inverse Compton mechanism contributes 15% of the γ-ray background above 100 MeV (without any evolutionary increase).

3. None of individual non-cosmological models considered here can explain the total γ-ray background. We need a strong cosmological increase:

   a) Normal galaxies totally, requires $\beta = 2.1$;

   b) W-W model, requires $\beta = 3.6$;

   c) these two together, requires $\beta = 2.0$.

   In comparison, for the other wavelengths (Radio, FIR, UV and X-ray), we need $\beta = 2 \sim 4$.

Chapter 5

Electrons in Other Normal Galaxies

In this chapter we discuss the origin and propagation of cosmic ray electrons in external galaxies. It is shown that cosmic rays play an important role in galactic evolution and dynamics, which leads to a tight correlation between radio continuum power and far infrared luminosity existing over a wide range of spiral galaxies.

5.1 Radio continuum observations

A major drawback in the study of the Galactic cosmic rays lies in our poor view along the Galactic Plane, within which the variation of Galactic magnetic field is not well known and there are ambiguities in determining the distances of radiations by cosmic rays. The accurate modelling of the three-dimensional distribution of cosmic rays and their sources in our Galaxy turns out to be difficult because of our being embedded in it. The study of cosmic rays in external galaxies is relevant to that in our Galaxy and has the advantage of better perspective in various ways. Face-on galaxies are ideal objects to study the global distributions of cosmic rays and their sources; while edge-on galaxies are ideal objects to study the distribution of cosmic rays in the perpendicular direction to the galactic plane. At the moment (and in the near future) the only observational window available for this purpose is the radio continuum radiation emitted by cosmic ray electrons gyrating in the galactic magnetic field. The other window, γ-rays, does not yet have the sensitivity to receive a great enough number of photons nor the resolution necessary to map the cosmic ray distribution.

A number of face-on galaxies have been mapped in radio continuum emission in the frequency range of a few GHz. Berkhuijsen and Klein (1984) found that the radial distributions of radio synchrotron radiation and blue

71

light have very different scale lengths in M31 and M51. They concluded that the distribution of cosmic ray electrons is a few kiloparsecs broader than that of the potential source—Population I stars. Beck *et al.* (1985) observed M82 at multi-frequency and found that if the distribution of cosmic ray electrons is established by outward diffusion through the disk, the diffusion speed is $\sim$150 km$\cdot$s^{-1} which is 5 times greater than the typical Alfvén speed in the ISM (Wentzel, 1974). If this interpretation is the case, energy losses will steepen the electron spectrum leading to a spectral index gradient in the synchrotron distribution. However, the observed spectral distribution, despite the large errors, shows a weak but opposite gradient. The observation of another face-on galaxy, M31, by Hummel *et al.* (1990) shows a nearly constant spectral index over the galaxy within the observational errors. The phenomenon of a nearly constant spectral index can be explained by our nonuniform propagation model (see Chapter 2), cosmic rays escape from the disk into the halo more quickly in the inner galaxy than in the outer galaxy and convection modifies the spectral variation.

Turning to edge-on galaxies, radio observations are able to provide the information on brightness and spectral index distributions perpendicular to the disk plane, specifically on the extension of the radio halo. Up till now about 20 edge-on galaxies have been observed. The first unambiguous detection of an extragalactic halo in NGC4631 was performed by Ekers and Sancisi (1977). This halo is the most extended (up to 10 kpc from the disk plane) found so far and has a full width at half power of 3.5 kpc (Hummel *et al.*, 1988a). The other observed edge-on galaxies do not generally show a very extensive, strong halo; their half power thickness ranges from 0.5 kpc to 1.5 kpc. Spectral index distributions in the z-direction are available only for NGC253, NGC891, NGC3556, NGC4631 and NGC 4666 (see the review by Hummel, 1989). The spectral steepening from the disk to the halo is very small and this may imply that the galactic wind compensates the steepening caused by energy losses. The best studied edge-on galaxy is NGC891, whose radio emission can be divided into two components: a thin disk and a thick disk (Allen *et al.*, 1978).

Very recently, polarization measurements of NGC891 and NGC4631 have been completed by Beck *et al.* (1990). The result has an interesting feature: the fraction of polarized emission, a measure of the regularity of the magnetic field, first increases with z and then falls down to zero at a few kpc from the disk (the detectable boundary of the radio emission). This variation clearly indicates that the magnetic field is irregular in the disk, becomes a little more regular in the halo and is turbulent at the boundary of the galaxy. It seems likely that the turbulence is probably excited by the termination of the galactic wind with the intergalactic medium.

5.2 The global correlation between radio continuum and far infrared emission

Soon after the completion of the IRAS survey, a tight correlation between the radio continuum power and the thermal far infrared luminosity for spiral galaxies over a wide range of luminosities was discovered by several groups (Dickey and Salpeter, 1984; de Jong et al., 1984; Helou et al., 1985). It is a striking fact, because it is the tightest of all the correlations between two global parameters of galaxies and exists among various morphological types and four orders of magnitude in luminosity. An interesting feature is that the exponent, δ, in the relation $P_\nu(\text{radio}) \propto L_{\text{FIR}}^\delta$, is not unity, but significantly greater. Specifically, $\delta = 1.20 \pm 0.03$ from the analysis by Devereux and Eales (1989). It is generally accepted that the radio continuum emission around 1 GHz from galaxies is dominantly non-thermal, being synchrotron emission by relativistic electrons (several GeV) moving in the interstellar magnetic field (several μG), while the electrons originate from supernovae which are related to the young stellar population. The far infrared emission on the other hand is thermal, coming largely from the interstellar dust heated by absorption of starlight, and mainly consisting of two components: a warm component related to recent star formation and a cool component related to the general interstellar radiation field. The physical mechanisms for the radio and the FIR are thus different in nature.

Many efforts have been made to reveal the underlying physical process for this correlation (Dickey and Salpeter, 1984; de Jong et al.,1985; Helou et al., 1985; Gavazzi et al., 1986; Ashton, 1987; Cox et al., 1988; Fitt et al., 1988; Hummel et al., 1988b; Völk, 1989; Unger et al., 1989; and Devereux and Eales, 1989). The general point of view is that the electrons responsible for radio emission and the dominant part (assumed to be the warm component) of FIR are both related to the young stellar population. Among them, a major analysis is that due to Völk (1989), who has put forward a calorimeter theory in which the source strength for relativistic electrons and energetic (ionizing) photons, respectively responsible for the radio synchrotron and the FIR emission, are both proportional to the supernova rate, and the electrons are trapped in the galaxy. However, his theory does not explain the non-unity slope in the correlation; nor give the observed value of the radio spectral index. The situation with the latter is as follows. It is very likely that the electron injection spectrum has a differential spectrum, γ, close to 2, say $2 + \varepsilon$ (where ε is $\ll 1$ and is determined by details of the acceleration mechanism and could be between 0.2 and 0.3, Völk et al., 1988). For complete trapping in the galaxy the equilibrium spectrum of the electrons will have $\gamma = 3 + \varepsilon$, leading to a radio spectrum with exponent $(\gamma - 1)/2 \simeq 1.1$. However, the

measured spectral index is 0.74 on average (Gioia *et al.*, 1982). It can be remarked that the model adopted by us where most of the electrons escape from the Galaxy, leads to the correct spectral index.

Fitt *et al.* (1988) and Devereux and Eales (1989), respectively, in different ways, separated the warm component of FIR from the cool component and recorrelated the warm component along with the radio emission to derive a unity slope in the correlation, to fulfil the physical picture that both cosmic ray electrons and the warm component of FIR are proportional to the star formation rate, while the interstellar magnetic field is nearly constant and the dust surrounding O, B stars is sufficient for converting the starlight into FIR. Unfortunately, the new correlation is less tight than the original one, *e.g.* the linear correlation coefficient decreases from 0.96 to 0.89 corresponding to a reduction in significance from 4σ to 2σ (Fitt *et al.*, 1988).

It seems to us that these approaches are too simple to work well. For example, the synchrotron radio emission is dependent on both the intensity of relativistic electrons and the strength of the interstellar magnetic field, the latter playing as important a role as the former and the magnetic field almost certainly varies from galaxy to galaxy. Similarly for the FIR, the optical depth for converting starlight into FIR is an important factor and the two component model is likely to be oversimple (Bally and Thronson 1989; Cox and Mezger 1989). It is not necessary that the FIR from molecular cloud regions should be warm and that from HI regions should be cool; these considerations were usually ignored in the previous analyses.

In the present work, we first propose a theory for the correlation, then present results from a sample of data. An extensive discussion is carried out to reveal the compensating factors leading to the correlation. We also examine the other global parameters of galaxies, such as optical luminosity, CO luminosity and radio spectral index, to search for any relation with the correlation. Finally, a conclusion and a prospect are made.

5.3 An energy equipartition theory for the correlation

The radio continuum emission at frequencies around 1 GHz is dominated by the synchrotron emission of cosmic ray electrons of several GeV moving in interstellar magnetic fields of several μG (Ginzburg and Syrovatskii, 1964). From the study of the Galactic cosmic rays in this energy region, we know that they almost certainly are accelerated by supernova remnants (Bhat *et al.*, 1984) and confined in the Galaxy for a long period of time ($\sim 10^7$ years) (Garcia-Munoz *et al.*, 1977) before escaping from the Galaxy; these remarks relate to nuclei, but are presumed to be also true for protons and, in

our model, also to relate to electrons in the GeV region (except for the very bright galaxies where losses are so great that most electrons are absorbed). The large-scale magnetic fields in spiral galaxies, which confine the cosmic rays, are mostly in the Bisymmetric Spiral configuration, the field lines are stretched along spiral arms and are probably connected to the intergalactic field. The field can be described by the induction-dynamo model, in which it is induced by the primordial intergalactic field and amplified by the turbulent dynamo—coupling between the galactic rotation and the turbulence which is related to star formation activity. Due to the turbulent diffusion, the magnetic field is liable to escape into the intergalactic space, the turbulent dynamo is the mechanism to maintain the field configuration and flux in a steady state (see *e.g.*, Sofue *et al.*, 1986).

The FIR is the reemitted product of starlight by way of the interstellar dust, which is also involved in the star formation activity. Young *et al.* (1989) have shown that the FIR luminosity is proportional to the CO luminosity and H_α luminosity for a sample of spiral galaxies. Since CO is an indicator of dust clouds where hydrogen atoms form molecules on dust surfaces which in turn form stars and where the young stars emit H_α as the sign of recent star formation, it can be concluded that the FIR luminosity is a measure of the star formation rate. Based on the above arguments, we make the following assumptions:

1. In a galaxy, global energy outputs of FIR and cosmic rays (protons and electrons) are proportional to the star formation rate, *i.e.* $W_p \propto W_e \propto L_{FIR}$, where L_{FIR} is the FIR luminosity and W is the cosmic ray energy output $W = \int Q(E)dE$, here Q is the energy dependent source function. We assume that the spectral exponents of cosmic rays at production are the same, thus $W_p \propto Q_p$ and $W_e \propto Q_e$, and accordingly $Q_p \propto Q_e \propto L_{FIR}$.

2. Averaged out over a galaxy there is near equality of the energy densities of cosmic ray protons, magnetic field and interstellar radiation field, $u_p \sim u_B \sim u_{rad}$. As is well known, there is this near equality locally in our own Galaxy; clearly the equality does not hold everywhere in the Galaxy (*e.g.* u_{rad} increases more rapidly than u_p as one nears the Galactic Centre) but the local position is in fact a roughly average position for the Galaxy as a whole. This average nature for the local position can be illustrated by considering the distribution of SN remnants with Galactocentric radius, the mean density $\int_0^{R_{max}} 2\pi R\sigma_{SN}(R)dR / \int_0^{R_{max}} 2\pi RdR$ is $\simeq \sigma_{SN}(R_\odot)$.

3. Most electrons, responsible for the radio emission, escape from their

parent galaxies, at least for galaxies which are not too large or very luminous.

The propagation of cosmic ray electrons is approximately described by

$$D\nabla^2 n_e + \frac{\partial}{\partial E}(bE^2 n_e) + q_e = 0$$
$$n_e|_{\text{boundary}} = 0$$

(5.1)

where n_e is the electron density; q_e is the source density function, related to Q_e by the spatial integral $Q_e = \int q_e dV$; D the energy dependent diffusion coefficient, $D = D_1(E/E_1)^\alpha$, $E_1 = 1$ GeV, α is assumed to be 0.5 (see *e.g.* Dogiel and Uryson, 1988); bE^2 is the energy loss rate via inverse Compton and synchrotron radiation, $b \propto (u_B + u_{\text{rad}})$.

Galaxies are assumed to be slab-like with radius R and scale height $z_{1/2}$ for cosmic ray confinement. This galaxy model is equivalent to the thick disk model of radio synchrotron emission within which most galactic radio emission is contained. Since $z_{1/2} \ll R$, the diffusion is predominantly in the z-direction. The sources are assumed to be in the central plane of the galactic disc. D and b are assumed to be independent of position. Following Giler's one-dimension solution (1988, private communication), in first-order approximation, the spatially averaged solution to the above equation can be written as

$$n_e \sim Q_e \frac{bE_1 z_{1/2}^3}{\pi D_1^2 R^2} [x - (1 - e^{-x})]$$

(5.2)

where $x = \frac{2D_1}{E_1 b z_{1/2}^2}(\frac{E}{E_1})^{-0.5}$; Q_e, the volume integrated electron production rate, has been taken as the normal expression for shock acceleration: KE^{-2} (a different expression would result from the adoption of a different form for Q_e).

This expression is an important one for the arguments advanced here and needs to be discussed in a little detail. The function $f(x) = [x - (1 - e^{-x})]$ is drawn out in Figure 5.1 and the extreme regimes of trapping and escape are indicated. As a check on its validity, the extremes can be considered in turn; it is necessary to show that the standard limiting forms are achieved. For $x \gg 1$ (mainly escape), we have

$$n_e \sim \frac{Q_e z_{1/2}}{\pi D_1 R^2}(\frac{E}{E_1})^{-0.5}$$

(5.3)

corresponding to the 'leaky box' model. For $x \ll 1$ (mainly trapping), we have

$$n_e \sim \frac{Q_e}{\pi R^2 z_{1/2} bE_1}(\frac{E}{E_1})^{-1}$$

(5.4)

76

corresponding to the 'closed box' model. We note that $n_e \propto E^{-3}$, since $Q_e \propto E^{-2}$.

Returning to the significance of equation (5.2) for the present situation, it will be apparent that if, as seems likely, $z_{1/2}$ and R are smoothy varying functions of W_e (and thus Q_e), and correspondingly of $L_{\rm FIR}$ and if the magnetic field also varies smoothly with $L_{\rm FIR}$ then the radio power P_ν vs $L_{\rm FIR}$ will have different slope below about $x \simeq 1$. Whether or not this is seen experimentally depends on the position of $x \sim 1$ with respect to the observational range (and, of course, to the precision of the data and other perturbing factors).
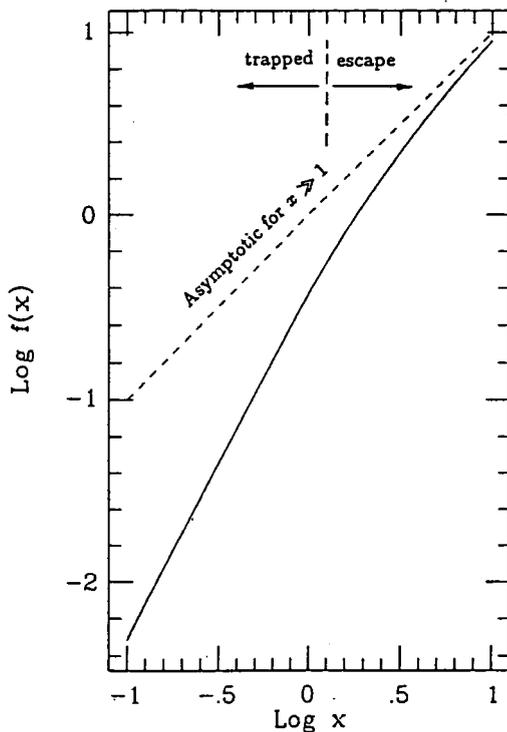

Figure 5.1. The function f(x) appearing in the expression for the cosmic ray electron intensity.

Turning to the radio power expected we note that the emissivity of the synchrotron emission of relativistic electrons moving in a magnetic field is given to sufficient accuracy by

$$q_\nu = n_e\left(-\frac{dE}{dt}\right)_{\rm syn}\frac{\partial E}{\partial \nu} \tag{5.5}$$

where q_ν is the emissivity, $(dE/dt)_{\rm syn}$ the energy loss rate via synchrotron radiation at the energy E corresponding to this frequency through $E =$

$1.65mc^2(2\pi mc/e)^{1/2}(\nu/B)^{1/2}$, in the present approximation. The emissivity follows as

$$q_\nu \propto n_e(E)BE \qquad (5.6)$$

where B is the strength of magnetic field. Integrating over the whole volume, we obtain the radio power,

$$P_\nu \propto R^2 z_{1/2} n_e(E)BE \qquad (5.7)$$

To relate P_ν with the FIR luminosity L_{FIR}, we need to utilise the expressions for the parameters in the equation. Obviously, $b \propto B^2$. For the dependence of diffusion coefficient on the magnetic field, we adopt $D_1 \propto B^2$ (see *e.g.*,Wentzel 1974). To calculate the magnetic field, we use the energy equipartition condition, *i.e.* $u_p \sim u_B$, since we have that $u_p \sim \frac{W_p z_{1/2}}{D_1 \pi R^2}$ (from simple diffusion arguments) and $u_B \sim B^2$, then $B^4 \propto \frac{W_p z_{1/2}}{R^2} \propto \frac{L_{FIR} z_{1/2}}{R^2}$.

It is now necessary to consider the dependence of $z_{1/2}$ and R on L_{FIR}. Insofar as the adopted model makes no predictions as to these dependences we take an empirical approach and write $z_{1/2} \propto L_{FIR}^{\beta_1}$ and $R \propto L_{FIR}^{\beta_2}$ (noting that $z_{1/2}$ and R relate to the radio emission, cosmic rays and magnetic field, but not those of FIR). Inspection of experimental data leads to identification of the values of β_1 and β_2, although it must be stressed that their accuracy is not great. The radio continuum survey of edge-on galaxies (Hummel *et al.*, 1984, 1989; Klein *et al.*, 1984; Harnett and Reynolds, 1985) yields $\beta_1 = 0.20 \pm 0.12$ and the high resolution radio continuum survey (Hummel *et al.*, 1985) yields $\beta_2 = 0.35 \pm 0.19$. The values of β_1 and β_2 can be considered further. β_1, a small value, is presumably a consequence of compensation mechanisms which are at work in determining the scale height of radio emissivity (the inflationary effects of the magnetic field, the cosmic ray pressure and the thermal motion of gas and the deflationary effect gravity acting on the ionized gas which is tied to the magnetic field). We note that the equivalent value of β_1 for the scale height of atomic hydrogen is also small (*e.g.*, van der Kruit and Searle (1981) find only a slow increase of $z_{1/2}$ for HI with increasing size for the edge-on galaxy sample studied). The philosophy to be adopted is presumably to use the empirical value of β_1 to (eventually) help to understand the relative roles of the various pressure components: cosmic rays, magnetic field, thermal and gravity. For the present purpose, however, β_1 is used as an input. Turning to the value of β_2, $\beta_2 = 0.35 \pm 0.19$ is not far from the value expected by simple scaling, $\beta_2 = 0.5$ (from $L_{FIR} \propto R^2$ for a constant scale height) for a similar reason. Combining the two empirical relations shows that the radio 'volume' ($\pi R^2 z^{1/2}$) is proportional to $L_{FIR}^{0.9 \pm 0.4}$—a not too unexpected result.

Using these two empirical relations, we have $B \propto L_{\text{FIR}}^{0.125}$. Substituting all the expressions into Equation(5.7), we obtain

$$P_\nu \propto L_{\text{FIR}}^{1.74} \nu^{-1/2}[x - (1 - e^{-x})] \tag{5.8}$$

where $x = c_0 L_{\text{FIR}}^{-0.37} \nu^{-1/4}$. Here c_0 is a constant $(= \frac{2D_1 k_B^{1/4}}{E_1 bk_z^2}(\frac{E_1}{1.65mc^2(2\pi mc)^{1/2}}))$, with $k_B = B/L_{\text{FIR}}^{0.125}$ and $k_z = z_{1/2}/L_{\text{FIR}}^{0.2}$), to be discussed in detail later. For $x \gg 1$ (*i.e.* L_{FIR} very small) equation (5.8) becomes

$$P_\nu \propto L_{\text{FIR}}^{1.37} \tag{5.9}$$

and for $x \ll 1$ (*i.e.* L_{FIR} very large) equation (5.8) tends to

$$P_\nu \propto L_{\text{FIR}} \tag{5.10}$$

note that here ν can be treated as a constant, since we are calculating the radio power at a single frequency.
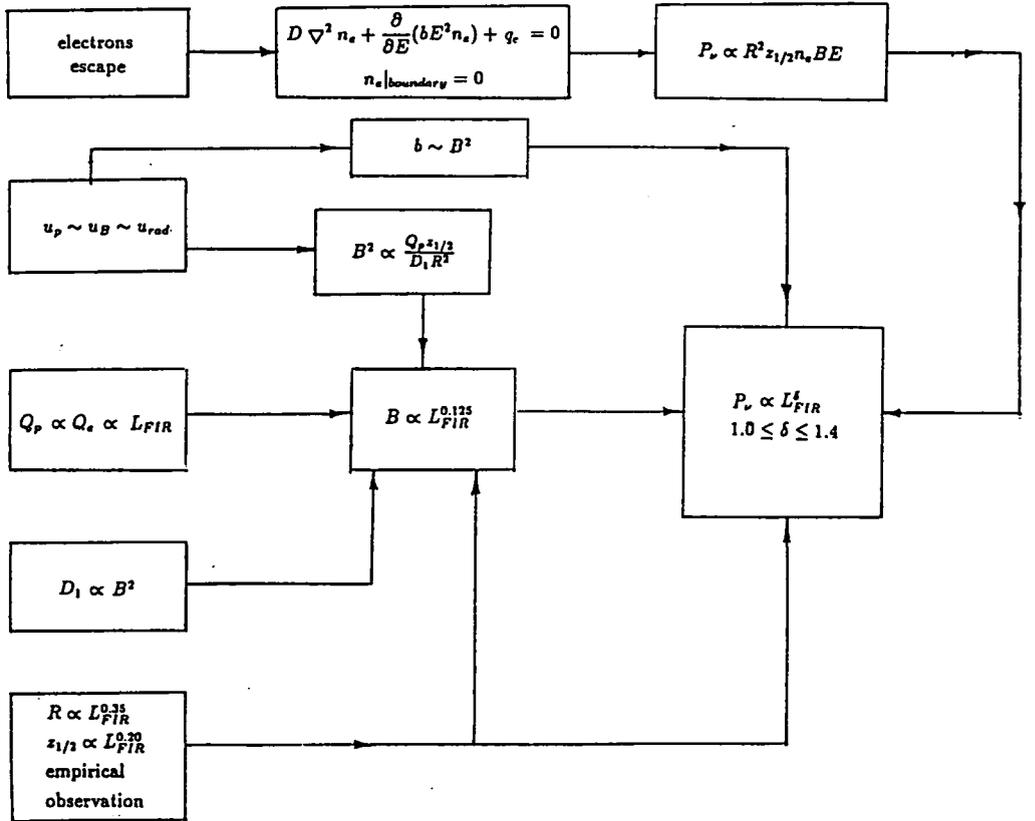

Figure 5.2. The flow diagram of our theory. The formula deduction process proceeds from left to right.

Figure 5.2 displays the flow diagram of our theory, the left-hand side is the assumption and the right-hand side is the result, the deduction process is towards the right. In the above formulae we have omitted all the coefficients, embedded a large number of constants into c_0 and taken the average values over a galaxy for simplicity. This approximation is reasonable because all the physical quantities are of the right orders of magnitude of energetics. To check this, we take the conventional values of the constants of our Galaxy to calculate a prior estimated value for c_0, i.e. $D_1 = 10^{29}\text{cm}^2 \cdot \text{s}^{-1}$, $E_1 = 1$ GeV, $b = 2 \times 10^{-16}$ (GeV $\cdot$ s)$^{-1}$, $L_{\text{FIR}} = 10^{10}L_{\odot}$, $B_{\perp} = (2/3)^{1/2}B = 5 \times 10^{-6}$ G and $z_{1/2} = 2$ kpc, accordingly $k_B = 0.28\mu\text{G} \cdot L_{\odot}^{-0.125}$ and $k_z = 6.18 \times 10^{19}\text{cm} \cdot L_{\odot}^{0.2}$. Then we obtain $c_0 = 5.1 \times 10^6\text{Hz}^{1/4} \cdot L_{\odot}^{0.37}$. We shall see in the next Section that this value is fairly consistent with the fitted value.

Figure 5.3 shows the numerical result of the radio-FIR correlation at radio frequency 1.49 GHz in arbitrary units; the numbers along the curve represent the trapping probability of cosmic ray electrons at about 10 GeV. The slope of the curve in the lower part is $\simeq 1.37$ (i.e as in equation (5.8)) and in the upper part is $\simeq 1.0$.
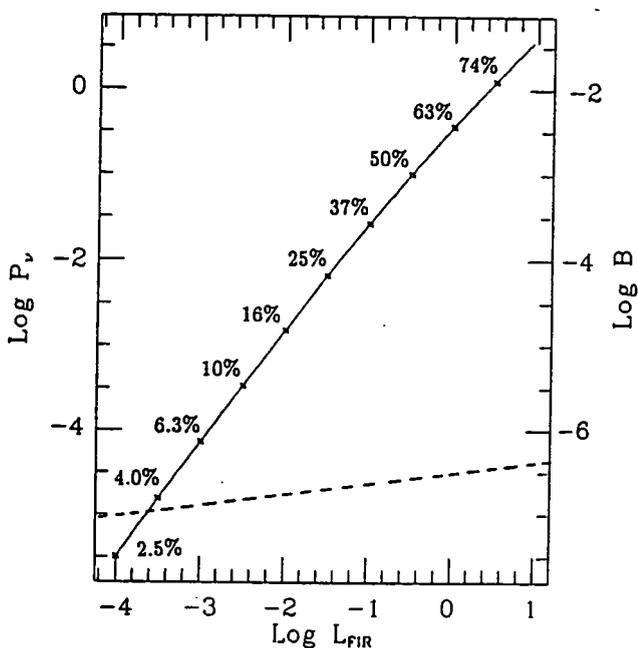

Figure 5.3. Solid line: theoretical correlation between radio power at 1.49 GHz and FIR luminosity predicted by our model, the numbers along the curve represent the trapping probability of electrons responsible for the observed radio emission ($viz \simeq 10$ GeV); Dashed line: variation of the strength of the magnetic field with FIR luminosity (all units are arbitrary).

Physically, the non-unity slope results from the variation of electron trapping probability from galaxy to galaxy, *i.e.* the trapping probability increases with the total output of the galaxy as shown in Figure 5.3. In this way an increase in the total electron output is automatically accompanied by an increase in the trapping probability so that a more rapid increase in the radio emission occurs although the energy losses slow down the increased rate a little. The above argument is valid in the regime where the electrons escape.

If the electrons are all trapped, the trapping probability is the same (equal to 1) for every galaxy, thus the radio emission will be just proportional to the total electron output, *i.e.*

$$P_\nu \propto \pi R^2 z_{1/2} n_e B^2 \propto \pi R^2 z_{1/2} [Q_e/(\pi R^2 z_{1/2} B^2)]B^2 \propto Q_e \propto L_{\text{FIR}} \quad (5.11)$$

(assuming an injected electron spectrum $j_e(E) \sim E^{-2}$).

5.4 Analysis of the correlation data

To test our theory, we have compiled a sample of 62 spiral galaxies, these galaxies being those for which both accurately measured radio data and FIR data are available. The radio continuum data are from Condon (1987). The FIR data are from Rice *et al.* (1988). For our own Galaxy, the FIR luminosity is taken from Cox and Mezger (1989) and the radio power from an extension of Broadbent *et al.* (1989) at 408 MHz by assuming the spectral index to be 0.75. The sample is listed in Table 5.1.

Figure 5.4 displays the radio power versus the FIR luminosity from the data. It is clearly shown that there is not only a tight correlation between radio and FIR, but also an interesting feature in the correlation, that is, the slope is steep (greater than unity) in the lower region and becomes flatter at the upper region. Fitting the correlation as a whole with a straight line yields $Log P_\nu = 1.17 Log L_{\text{FIR}} + 9.97$ with $r.m.s. = 0.22$. If we fit the correlation with the theoretical curve shown in Figure 5.1, it turns out to be an equal good fit ($r.m.s. = 0.22$) (In fact, inspection indicates that a bigger change of slope would give an even better fit). It is worth pointing out that our Galaxy is at the position where the electron trapping probability is 33% according to our model, a result consistent with the calculation by Ashton (1987). The goodness of the fit provides evidence for our theory (the fact that a simple straight line fit equally well is hardly an argument against the model in that the straight line slope (1.17) has no theoretical justification). Also, our fit gives a value for c_0: $c_0 = 6.3 \times 10^6$, being quite close to our prior estimate of 5.1×10^6.

Table 5.1. The sample of of galaxies. Column 1: the galaxy name; Column 2: the radio continuum emission power (W/Hz) at 1.49 GHz; Column 3: the FIR luminosity (in solar units $L_\odot$) integrated from 40μm to 120μm.

| GALAXY	Log P_ν	Log L_{FIR}	GALAXY	Log P_ν	Log L_{FIR}
Milky Way	21.51	9.99	NGC3623	20.30	9.22
NGC0045	19.41	8.61	NGC3627	21.89	10.21
NGC0055	20.66	9.17	NGC3628	22.12	10.30
NGC0134	22.37	10.63	NGC3718	21.19	8.92
NGC0224	20.73	8.96	NGC4192	21.63	9.90
NGC0247	19.46	8.27	NGC4216	20.89	9.55
NGC0253	22.07	10.48	NGC4236	19.36	7.90
NGC0300	18.42	8.48	NGC4244	19.42	8.42
IC1613	17.46	6.32	NGC4258	22.01	9.76
NGC0628	21.81	10.14	NGC4395	19.98	8.54
NGC0660	22.25	10.63	NGC4438	21.82	9.64
NGC0891	22.31	10.53	NGC4517	21.15	9.58
NGC0925	21.14	9.66	NGC4559	21.27	9.69
NGC1097	22.52	10.79	NGC4565	21.94	10.20
NGC1291	20.06	9.10	NGC4569	21.68	9.98
NGC1365	22.77	11.19	NGC4594	21.70	9.61
IC342	21.77	10.06	NGC4631	22.33	10.39
NGC1448	21.70	10.00	NGC4725	21.27	9.83
NGC1560	19.39	7.97	NGC4736	21.16	9.75
NGC2403	20.70	9.15	NGC4826	20.78	9.50
NGC2683	20.70	9.14	NGC5033	21.84	10.08
NGC2841	21.31	9.46	NGC5055	21.75	10.09
NGC2903	21.64	10.00	NGC5170	20.58	9.30
NGC3031	20.76	9.16	NGC5194	22.32	10.26
NGC3034	22.07	10.37	NGC5236	22.15	10.71
NGC3109	18.67	7.64	NGC5907	21.42	9.82
NGC3198	20.82	9.43	NGC6822	18.82	7.78
IC2574	19.20	7.91	NGC6946	21.88	10.09
NGC3521	21.83	10.17	NGC7331	22.35	10.61
NGC3556	21.96	10.21	NGC7640	20.80	9.17
NGC3621	21.25	9.70	NGC7793	20.33	9.27
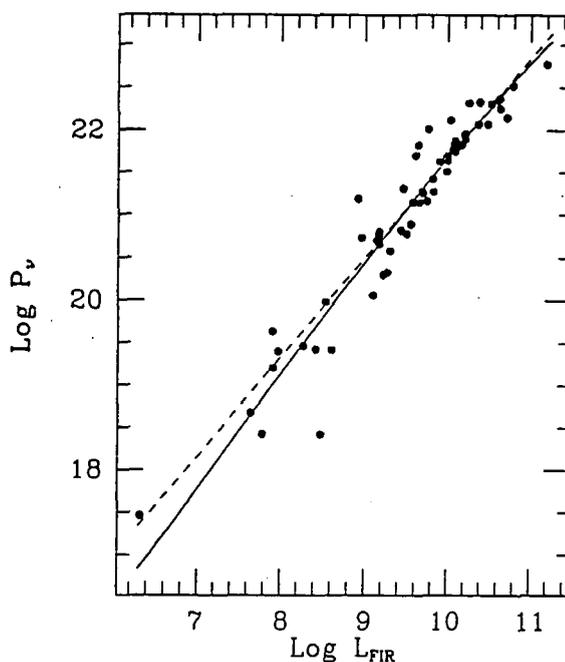
Figure 5.4. The correlation from the data listed in Table 5.1. The solid curve is our theoretical prediction; the dashed straight line is a linear fit having mathematical but no physical significance.

5.5 Implication of the correlation

The non-unity slope in the tight correlation between radio and FIR has been firmly established experimentally by a number of workers (Gavazzi *et al.*, 1986; Cox *et al.*, 1988; Devereux and Eales, 1989). Instead of trying to make the slope become unity by subtracting off a decreasing fraction of the FIR component with increasing L_{FIR}, we would rather show that the non-unity slope is itself reasonable. In fact, the underlying physics is not so simple as to make us expect that as the radio and FIR are from the same source, we might expect the slope to be unity. The reason is indirect: the FIR is determined by both starlight and dust, in a similar way the radio is determined by both

cosmic ray electrons and magnetic field. In the galactic evolution process, cosmic rays, interstellar magnetic field and dust are directly related to the star formation activity, meanwhile starlight and FIR are the direct product of it.

From observation we know that the energy densities of the kinetic energy of gas, cosmic rays, magnetic field and general interstellar radiation field are in the same order of magnitude globally. This is probably caused by Galactic dynamical factors. Although according to the traditional point of view the magnetic field and cosmic rays are instability agents of the Galactic dynamics (Parker 1966, 1969), with the increased knowledge of the interstellar gas and magnetic field in recent years we think that they are likely instead to be the stability agent, *i.e.* the propagation of cosmic rays is no longer as Parker described. The escape of cosmic rays from the galactic disk has the significance of balancing the pressures in the disk and in turn stabilizes the disk. Both cosmic rays and magnetic field are controlling factors in the star formation process via feedback actions. The cosmic rays, generated by supernova remnants, exert pressure on the interstellar gas against the gravitational contraction. The magnetic field, generated by a turbulent dynamo, suppresses the turbulence, resists the gravitational contraction of the gas and enhances the cross-section of cloud-cloud collisions.

The dust, associated with dark clouds and probably formed in them (Seab, 1987), shields the starlight and harbours chemical reactions to ensure that hydrogen atoms combine into molecules, promoting star formation. The FIR acts as a tracer of the star formation process, the more luminous the galaxy, the higher the star formation rate, more photons are emitted, more dust exists, more FIR is produced. Some authors argue that for the more luminous galaxies ($L_{\rm FIR} > 10^{10} L_\odot$), OB stars are the main heating source for FIR; while for less luminous galaxies ($L_{\rm FIR} < 10^{10} L_\odot$), the general interstellar radiation field is the main heating source (Wunderlich and Klein, 1988; Young *et al.*, 1989). However, this is just the consequence of the underlying physics. The nature of the main heating source is not important; the important factor is the underlying physical process: dynamical stability and a steady star formation rate in the galaxy.

We do not expect that a radio—FIR correlation exits from point to point within a galaxy as some authors have argued, although a correlation on a scale of several kpc may exist. It has been clearly shown that the distribution of the radio emission is different from that of FIR for two nearby galaxies NGC5236 and NGC6946 (Bicay *et al.*, 1989). The 'local' correlation for four nearby galaxies M31, M33, M101 and IC342 given by Beck and Golla (1988) is not very local in fact (it is averaged over a ring) nor is it good. The real local correlation is the one between the thermal radio and the FIR emission

(Broadbent *et al.*, 1989) which offers a method of separating the thermal and non-thermal radio emission.

Concerning the dispersion in the radio—FIR correlation, it should reflect some of the physics and different authors have given different physical explanations. For example, Ashton (1987) tried to related the dispersion to the probability of electron escape; Völk (1989) ascribed the dispersion to the FIR spectral variations among galaxies; Hummel *et al.* (1988b) argued that the dispersion is due to the variation in magnetic field strength among galaxies; Wunderlich and Klein (1988) even gave a list of reasons. All these seem to be reasonable, but proofs are needed. Because of the inaccuracy of measurements, at the moment, it has not proved possible to relate the dispersion with other parameters, such as Blue luminosity, CO luminosity, the size of galaxy, radio spectral index etc., and thereby to find clues. We have searched for all these correlations but found none. We think that the dispersion is due to a mixture of many physical and technical reasons. Condon and Broderick (1988) have studied the statistical properties of the dispersion of the points about the best line, and found that the distribution is Gaussian, the most random distribution, thereby also implying that many factors may contribute.

5.6 A brief summary of the correlation

The tight correlation between the radio and FIR with a non-unity slope for spiral galaxies can be explained by a model in which the total outputs of FIR and cosmic rays are proportional to the star formation rate, energy equipartition between cosmic rays and magnetic field being fulfilled. It is implied that cosmic rays are of galactic origin; the electrons which are responsible for the synchrotron radio emission at the observed frequencies escape from their parent galaxies except for the case of the biggest and brightest galaxies. Cosmic rays, the interstellar magnetic field and interstellar dust all play important roles in the star formation process and in the large-scale galactic dynamics. We have made a firm prediction for the shape of the $P_\nu - L_{\text{FIR}}$ relation (Figure 5.3) which will form the basis for comparison with new data as they appear and thereby offer a check on our model.

Chapter 6

The Local Galactic Magnetic Field

The propagation of cosmic rays is determined by the interstellar magnetic field and in this chapter we analyse pulsar rotation data to reveal some features of this field in the local region (within ~ 1 kpc). As an application of our result, the propagation of the highest energy protons is discussed.

6.1 Introduction

The basic reason why the origin of cosmic rays remains a problem nearly 80 years after their discovery is that the (charged) particles do not travel in straight lines but pursue a tortuous path in the Galaxy caused by the presence of the Galactic magnetic field. The relationship between the radius of curvature (the Larmor radius), $\rho(\text{cm})$, the momentum, $P(\text{eV}/c)$, and the magnetic field, $B(\text{Gauss})$, is well known:

$$\rho = Pc/(300B) \tag{6.1}$$

for a singly charged particle. A typical Galactic field is 3 micro-Gauss so that

$$\rho \simeq 10^3 Pc \quad \text{cm} \tag{6.2}$$

Changing units to parsecs (pc) we have

$$\rho \simeq 0.3 P_{15} c \quad \text{pc} \tag{6.3}$$

Typical values for the Larmor radius are thus $\sim 3 \times 10^{-7}$ pc for protons of momentum 10^9 eV/c; ~ 3 pc at 10^{16} eV/c; and ~ 30 kpc at 10^{20} eV/c. These radii can be compared with the linear dimensions of the Galaxy: distance to the Galactic Centre ~ 8.5 kpc, scale height of the gas locally ~ 150 pc, likely distance to the edge of the Galactic halo, beyond which particles escape, ~ 5 kpc.

It is apparent that the topography of the magnetic field is needed over an extraordinarily large distance range: from 10^{-7} pc to 10 kpc. In fact, progress has been very slow for a variety of reasons. For example, individual stars are separated by 2 pc so that techniques using stellar radiation give information averaged over such distances only. Indeed, at smaller distances the argument has been turned round (Kiraly *et al.*, 1979) and cosmic ray data have been used to draw conclusions about the local field geometry on scales below 1 pc.

It is on larger scales ($\simeq$ 1 kpc) that there has been some progress and this is the subject of the present work. We note that for a Larmor radius of 1 kpc the corresponding proton momentum is 3×10^{18} eV/c and this is certainly a region of considerable interest. Of particular importance is the propagation of protons of just a little higher momentum ($\geq 10^{19}$ eV/c) where there have been suggestions for a number of years that these particles are of extragalactic origin (see the review, *e.g.* Wdowczyk and Wolfendale, 1989). The crucial importance of a knowledge of the field at the kpc level can be appreciated by the fact that it is not inconceivable that the protons here are Galactic rather than extragalactic; the field *could* be sufficiently strong, coherent and extended for there to be trapping at these very high momenta.

Before turning to the measurements of the field, some remarks are necessary about the electron component. It is generally agreed that the diffuse Galactic radio radiation is due to cosmic ray electrons emitting synchrotron radiation as they gyrate in the Galactic magnetic field (typically, 10 GeV electrons produce synchrotron radiation of frequency of order 1 GHz in a field of 3 μG). Now the intensity of the radiation is approximately proportional to the product of the electron intensity, $j(E_e)$, and the square of the magnetic field, B_t^2, appropriately averaged along the line of sight. It is necessary to point out that this field B_t relates to the corresponding Larmor radius, 10^{-6} pc only, a fact of considerable importance in practice because the irregular component of the field is almost certainly much bigger than the regular part and it is the latter which is better known.

Returning to the main thrust of this work—the configuration and magnitude of the field on a large scale—there is general agreement that the regular component within a few kpc or so of the Sun is roughly aligned with the spiral arms and the irregular component is randomly oriented on various scales up to a few hundred pc. The irregular part is probably due in part, at least, to the perturbing effect of supernova remnants.

In the past, a variety of results have been given by different authors using various methods. Values for the strength of the regular field have ranged from 1 μG to 3.5 μG and the direction range is from (towards) longitude $l_0 = 45^0$ to $l_0 = 100^0$; while values for the strength of the irregular field have ranged

from 1 μG to 20 μG.

6.2 Review of previous work

There are several indirect methods of measuring the Galactic magnetic field. Historically, the existence of the field was deduced from the discovery of the linear polarization of starlight (Hall, 1949; Hiltner, 1949), the polarization being produced by the alignment of dust grains in the Galactic magnetic field. According to the theory of magnetic alignment, proposed by Jones and Spitzer (1967), a field strength of only 3 μG is needed to explain the observed polarization. Many studies have been made using this technique and a comprehensive review has been given by Ellis and Axon (1978). These authors examined a catalogue of stellar polarization data containing accurate stellar distances and estimated the direction of the regular field as being towards $l_0 \simeq 45^0$ within 500 pc and beyond this (but within 2 kpc) towards $l_0 \simeq 60^0$ in the solar vicinity. The disadvantage of this method is that the magnitude of the field cannot be determined from the observations, only the direction.

Another indirect way of measuring the Galactic field is by studying the diffuse Galactic synchrotron radio emission which is produced by relativistic cosmic ray electrons gyrating in the Galactic magnetic field. As remarked already, the Larmor radius of these electrons is only $\sim 10^{-6}$ pc and thus irregular field components down to very small scales indeed are responsible for the synchrotron radiation. The synchrotron radiation emissivity together with the measured cosmic ray electron spectrum can be used to determine the effective strength of the 'total field', $B_t \simeq < B^2 >^{1/2}$, which is sensitive to regions having higher than averaged field. Phillipps et $al.$ (1981) obtained a total strength $B_t \simeq 4$ μG; while Beuermann et $al.$ (1985) found $B_t \simeq 9$ μG by using different assumptions. The apparent difference in the field strength results from the use of different distributions of the synchrotron radiation emissivity; this topic has been discussed in Chapter 2.

The direction of polarization of the synchrotron radiation is perpendicular to the magnetic field and in the case of a uniform field the linear polarization is large, $\simeq 73\%$ (Ginzburg and Syrovatskii, 1969). However, the actually observed degree of polarization of the diffuse radio emission is low and thus difficult to measure, its low value being due to the large random field which dilutes the linear polarization arising from the large scale component. The result is that the polarization method does not work very well, and the results on the direction of the regular field from different workers are diverse: $l_0 \simeq 70^0$ by Mathewson and Milne (1965), $l_0 \simeq 60^0$ by Berkhuijsen (1971)

and $l_0 \simeq 45^0$ by Spoelstra (1984). Moreover, the detection range is limited to less than 500 pc.

The Zeeman splitting method is a standard technique for determining magnetic fields but it works only for cloud regions where the column density of gas is high and the emission line is narrow, for example the 21 cm HI line for HI clouds and the 18 cm OH line for molecular clouds. Because the filling factor of the clouds is small, this method cannot be used to measure the overall magnetic field. Nevertheless, the overall averaged magnetic field can be derived by properly extrapolating the relation of averaged field strength versus gas density in clouds, if, as we suppose, we know the appropriately averaged field strength in the clouds and if the mechanism causing the enhanced magnetic field in clouds is compression by gas condensation (although in fact the physical process involved is very complicated). Troland and Heiles (1986) have plotted the observed magnetic field strengths versus gas density (see Fig. 1 in their paper) and we have extrapolated down to an overall averaged gas density in the ISM of $1 \mathrm{cm}^{-3}$; the result is an average field strength of 5 μG.

It is likely that the Faraday rotation measure ($RM = \int n_e B_{||} dl$, where n_e is the thermal electron density and $B_{||}$ is the magnetic field component parallel to the line of sight, the path of integration being along the line of sight), provides the best approach for determining the Galactic magnetic field since the involved parameters can be measured by other techniques and thus both the magnitude and direction of the field can be derived. If Galactic pulsars are used the detection range extends to several kpc; averages over this scale and greater come from extragalactic Faraday rotation data. Early complete surveys of extragalactic Faraday rotation measures showed that the field was directed towards $l_0 \simeq 80^0$ (Gardner *et al.*, 1969). With a more complete sample of extragalactic Faraday rotation data, Simard-Normandin and Kronberg (1980) concluded that the direction of the field is towards $l_0 = 76^0$ and that there is a reversal of the field direction between spiral arms. Inoue and Tabara (1981), however, found $l_0 = 100 \pm 10^0$ and no evidence for a reversal of the field direction.

Pulsars have a number of advantages over extragalactic objects for Faraday rotation measures. Firstly, pulsars show no intrinsic Faraday rotation. Secondly, the electron density along the line of sight toward a pulsar is reasonably well known. Thirdly, the electron-density-weighted magnetic field along the line of sight can be directly derived from the rotation measure and dispersion measure (we will examine this topic in detail later). Manchester (1974) used a sample of 38 pulsars with distances less than 2 kpc from the Sun to derive a strength $B_{reg} = 2.2 \pm 0.4$ μG and direction $l_0 = 94 \pm 11^0$ for the regular field. In his least-square fitting, $cos^2 b$ (b is the Galactic latitude)

was taken to be the weighting factor. He also concluded that the irregular component has the same strength. Thomson and Nelson (1980) used 48 pulsars within 3 kpc and a five-parameters model, including the scale height, to derive $B_{\text{reg}} = 3.5 \pm 0.3$ μG and $l_0 = 74 \pm 10^0$ with a surprisingly low scale height of 75 pc for the regular field (note the contrast with the synchrotron radiation results where $z_{1/2}$ is considered to be several kpc, *viz* twenty times bigger). Thomson and Nelson also found a reversal of the field toward the inner Galaxy at a distance of $d_{\text{rev}} = 170 \pm 90$ pc. They estimated the irregular field to have a strength from 4 μG to 14 μG assuming its scale length to be from 100 pc to 10 pc. Recently, Rand and Kulkarni (1989) have used about 200 (118 within 3 kpc) pulsar rotation measures, mainly from the observations of Hamilton and Lyne (1987), to perform a comprehensive analysis. Assuming no variation in the z-direction, they find that the local regular field (within 3 kpc) has a strength $B_{\text{reg}} = 1.6 \pm 0.2$ μG and is towards $l_0 = 96 \pm 4^0$, with a reversal of field at a distance $d_{\text{rev}} = 600 \pm 80$ pc toward the inner Galaxy. They suggest, therefore, that the Galactic magnetic field has a concentric-ring geometry on a large scale with the field reversing from one ring to the next. In their analysis, the variance and covariance of the best-fit residuals were used with a single-cell-size model for the irregular magnetic field to yield a strength of 5 μG and a cell length of 55 pc.

It is clear from the above that there are many inconsistencies in previous treatments, which come from the complexity of the actual magnetic field configuration and the defects of the available methods. Whiteoak (1974) and Heiles (1976) have pointed out that one need not necessarily expect the same result since different methods sample different regions of the interstellar medium. As we have seen above, the radio polarization method samples the very nearby region, within 500 pc of the Sun; the optical polarization method samples the region within 1 kpc; while the Faraday rotation can sample not only the nearby region but also those far away. With this knowledge in mind, we have enough reason to speculate that the discrepancy in the field direction comes from the effect of large scale irregularities ($\sim$ 1 kpc) in the Galactic magnetic field. There is also other evidence for large scale irregularities. It is well known that the patterns of interstellar gas form distorted spirals and the magnetic field is lined up with the spiral arms to some extent, and it is natural to imagine that its pattern will also be distorted. Indeed, the radio synchrotron structure of the Galaxy, recently deduced by Broadbent (1989), bears out this expectation. In view of the distortion and the likely field reversal the results have been sensitive to sample selection; most previous studies having assumed a uniform field.

In the present work we will use the pulsar rotation measures to derive the features of the local Galactic magnetic field, for example, to see whether

the regular field lines up with the spiral arms and if there is any difference between the field in the arm and in the interarm regions. Further, to cope with the complexity of the irregular field, we invent a multi-cell-size model by invoking the Kolmogorov spectrum of interstellar turbulence and determine the effective total field.

6.3 Faraday rotation measure, data and fitting model

6.3.1 Faraday rotation measure

If a weak magnetic field is present, the propagation of electromagnetic waves in a plasma is 'quasi-longitudinal' in essentially all directions and normal modes of propagation are circularly polarized (one mode is that in which the electric vector is in the same direction as the electron gyrates around the magnetic field lines, the other mode has the electric vector in the opposite direction). Because of the slightly different indexes of refraction for these two modes (see, *e.g.* Ginzburg, 1970), the plane of polarization of a linearly polarized wave rotates along the wave vector direction. This effect is known as Faraday rotation. The angle of rotation after traversal of a distance d is

$$\Delta\psi = \frac{2\pi e^3}{m^2 c^2 \omega^2} \int_0^d n_e B cos\theta dl \qquad (6.4)$$

where B is the strength of the magnetic field and θ is the angle between the direction of the wave vector and the direction of the magnetic field. The rotation measure RM is then defined by

$$\Delta\psi = RM\lambda^2 \qquad (6.5)$$

so that

$$RM = \frac{e^3}{2\pi m^2 c^4} \int_0^d n_e B cos\theta dl \qquad (6.6)$$

The rotation measure is positive for a field directed toward the observer and negative for a field directed away. Numerically,

$$RM = 0.812 \int_0^d n_e B cos\theta dl \ \text{rad} \cdot \text{m}^{-2} \qquad (6.7)$$

where n_e is in units of cm^{-3}, B is in μG and dl is in pc.

From the above equation we can see that the rotation measure represents a mean value of the parallel component of the magnetic field along the line of sight to the pulsar, weighted by the electron density. For pulsars the

normalization factor is at least approximately known because the dispersion measure is proportional to the integral of n_e, and as discussed in Chapter 3, n_e is found to be reasonably constant over a large scale in the Galaxy. Hence, the mean parallel component of the magnetic field is given by

$$< B cos\theta > = \frac{\int_0^d n_e B cos\theta \, dl}{\int_0^d n_e \, dl} = \frac{1.232 RM}{DM} \tag{6.8}$$

where B is in units of μG, RM is in rad $\cdot$ m^{-2} and DM is in pc $\cdot$ cm^{-3}.

6.3.2 Data

The sample is selected from data published by Manchester (1974) and Hamilton and Lyne (1987) with distances less than $D \leq 1.4$ kpc to avoid the problem of the curvature of the spiral arms and the likely large scale irregularity. The sample contains 51 pulsars in total, listed in Table 6.1.

In deciding upon the manner of analysis of the Galactic data, we are influenced by interesting features of magnetic fields in external galaxies which have been recently discovered: the ordered magnetic fields line up roughly along the spiral arms and the polarized synchrotron radiation is (remarkably) found to be stronger from the interarm region than from the arm region (Krause *et al.*, 1989; Sukumar and Allen, 1989). Our solar system is located on the inner edge of the Orion-Perseus arm and about 1 kpc away from the Sagittarius arm toward the inner Galaxy, with an interarm region inbetween. In order to see if there are similar features in our Galaxy, we divide our sample into two sets: the Inner Galaxy Subsample which contains 22 pulsars in the interarm region and the Outer Galaxy Subsample which contains 29 pulsars in the arm region.

The North Polar Spur has anomalous rotation measures and this region has been excluded from our sample. This region forms part of Loop I which is thought to be a nearby supernova remnant (SNR). The SNR has compressed the magnetic field (and probably rotated its direction) and although this region, which is obvious, has been removed, the effect of unidentified weak SNR, which must be manifold, is to cause the irregular component of the field.

Table 6.1. Dispersion measures and rotation measures of the data sample. Column 1 gives the pulsar name; Columns 2, 3 give the Galactic longitude l and latitude b, respectively; Column 4 gives the dispersion measure; and Column 5 gives the rotation measure.

Pulsar	$l(^0)$	$b(^0)$	$DM(\text{pc} \cdot \text{cm}^{-3})$	$RM(\text{rad} \cdot \text{m}^{-2})$
0031-07	110.4	-69.8	10.9	14
0105+65	124.6	3.3	30.1	-24
0138+59	129.1	-2.1	34.8	-48
0148-06	160.4	-65.0	25.1	2
0149-16	179.3	-72.5	11.9	15
0154+61	130.6	0.3	25.7	-29
0301+19	161.1	-33.3	15.7	-6
0320+39	152.2	-14.3	25.8	58
0329+54	145.0	-1.2	26.8	-54
0450+55	152.6	7.5	14.7	10
0655+64	151.6	25.2	8.9	-7
0656+14	201.2	8.2	14.0	22
0809+74	140.0	31.6	5.8	-12
0820+02	222.0	21.2	23.9	13
0823+26	197.0	31.7	19.5	2
0833-45	263.6	-2.8	69.1	37
0834+06	219.7	26.3	12.9	15
0906-17	246.1	19.8	15.7	-36
0919+06	225.4	36.4	27.2	32
0940+16	216.6	45.4	20.0	53
0942-13	249.1	28.8	12.6	-7
0950+08	228.9	43.7	3.0	2
1010-23	262.2	26.3	26.5	52
1039-19	265.5	33.7	32.1	-16
1112+50	154.4	60.4	9.9	-4
1133+16	241.9	69.2	4.8	3
1237+25	252.5	86.5	9.3	1
1508+55	91.3	52.3	19.6	0
1612-29	347.2	14.9	40.0	-30
1717-29	356.5	4.2	42.8	21
1749-28	1.5	-1.0	50.9	114
1839+56	86.1	23.9	26.2	-3
1845-19	14.8	-8.3	18.3	7
1857-26	10.3	-13.5	37.6	-3

continued

Pulsar	$l(^{0})$	$b(^{0})$	$DM(\mathrm{pc} \cdot \mathrm{cm}^{-3})$	$RM(\mathrm{rad} \cdot \mathrm{m}^{-2})$
1905+39	70.9	14.2	30.1	7
1929+10	47.4	-3.9	3.2	-7
1940-12	27.3	-17.2	29.1	-10
1944+17	55.3	-3.5	16.3	-44
1952+29	65.9	0.8	7.9	-18
1953+50	84.8	11.6	31.8	-22
2003-08	34.1	-20.3	26.0	-52
2016+28	68.1	-4.0	14.2	-37
2020+28	68.9	-4.7	24.6	-78
2021+51	87.9	8.4	22.6	-2
2043-04	42.7	-274	35.9	-1
2045-16	30.5	-33.1	11.5	-9
2110+27	75.1	-13.9	24.8	-65
2152-31	15.8	-51.6	14.4	21
2310+42	104.4	-16.4	17.3	7
2315+21	95.8	-36.1	20.5	-37
2327-20	49.4	-70.2	8.4	16

6.3.3 Fitting model

The model of the regular magnetic field which we use here is essentially the bisymmetric spiral model, in which the field reverses from one *field* spiral arm to the next. The direction of the arm is not defined but the local region is divided into Inner Galaxy and Outer Galaxy regions by a line through the Sun parallel to the *stellar* spiral arm, at $l = 76^{0}$. It is assumed that there is no field reversal in the Outer region but one is allowed in the Inner region at some distance, d_{rev}. It is also assumed that the field direction in the Inner Galaxy up to the reversal distance is antiparallel to that beyond the distance. The data are therefore used to determine the following parameters

l_{0O}, $B_{\mathrm{reg,O}}$: direction and strength of the regular field in the Outer Galaxy region.

l_{0I}, $B_{\mathrm{reg,I}}$: direction and strength of the regular field in the Inner Galaxy region.

·The method has validity if l_{0O} and l_{0I} are not too different from 76^{0}. Here, it is necessary to point out that the model is not a prior one, but a posterior one, of which the assumptions are obtained from iterative analyses of the data. Our model is similar to that adopted by Thomson and Nelson

(1980) and considered, but not favoured, by Rand and Kulkarni (1989).

Following Inoue and Tabara's (1981) analysis of the rotation measures of extragalactic objects, we assume the vertical scale height of the regular component to be much greater than several times the pulsar scale height. The radio synchrotron surveys of our Galaxy (Phillipps *et al.*, 1981; Beuermann *et al.*, 1985) also suggest a large scale height for the total field, as discussed earlier in Section 2.4. The pulsar rotation measures cannot be used to determine the scale height of the magnetic field; in our model there is no vertical variation in the field over the region studied: $z \leq 0.5$ kpc.

The dispersion of the observed rotation measures about the best line is assumed to be due to an irregular field and its value is determined from this dispersion. It is expected, and assumed, that this irregular field has a large scale height as well.

6.4 Statistical analysis

6.4.1 The regular component

We derive the regular component by applying a weighted least square fit to our data sample. The weighting scheme is essentially the same as that used by Thomson and Nelson (1980) and Rand and Kulkarni (1989), that is, the weight goes down with distance d as d^{-1}; this procedure assumes that the variance is caused by the irregular field component as has been mentioned. Our χ^2 analysis gave the following results: the regular magnetic field has a strength $B_{reg,O} = 1.0 \pm 0.4$ μG and direction towards $l_{oO} = 80 \pm 19^0$ in the Outer Galaxy; while $B_{reg,I} = 3.2 \pm 1.0$ μG, $l_{oI} = 57 \pm 14^0$ and a reversal of the field direction at $d_{rev.} = 190 \pm 90$ pc in the Inner Galaxy. It is evident that l_{oO} and l_{oI} are near enough to 76^0, as required. Figure 6.1.a shows a plan view of the pulsar data sample; and Figs. 6.1.b and 6.1.c give their rotation measure vs. distance in the Inner Galaxy and the Outer Galaxy, respectively. Figure 6.2 shows a plan view of the field in the local region derived in this work.

Insofar as the 'Outer' region is mainly in a stellar spiral arm and the 'Inner' region beyond 190 pc is mainly in an inter-arm region, it is apparent that the regular magnetic field is stronger in the interarm region than in the arm region. This result is consistent with the observations of external galaxies, *e.g.* M81 by Krause *et al.* (1989) and M83 by Sukumar and Allen (1989), which are of similar type to our Galaxy and which have been mentioned already in Section 6.3. The results are in contradiction with the simple si-

nusoidal model of Simard-Normandin and Kronberg (1980) and Rand and Kulkarni (1989), however, in which the field strength variation with galacto-centric radius is sinusoidal (equal strength but opposite sign for the reversed regions) and the field spirals (or circles) have no obvious connection with the stellar structure, although it is appreciated that the assumption of simple sinusoidal form was made for reasons of simplicity.
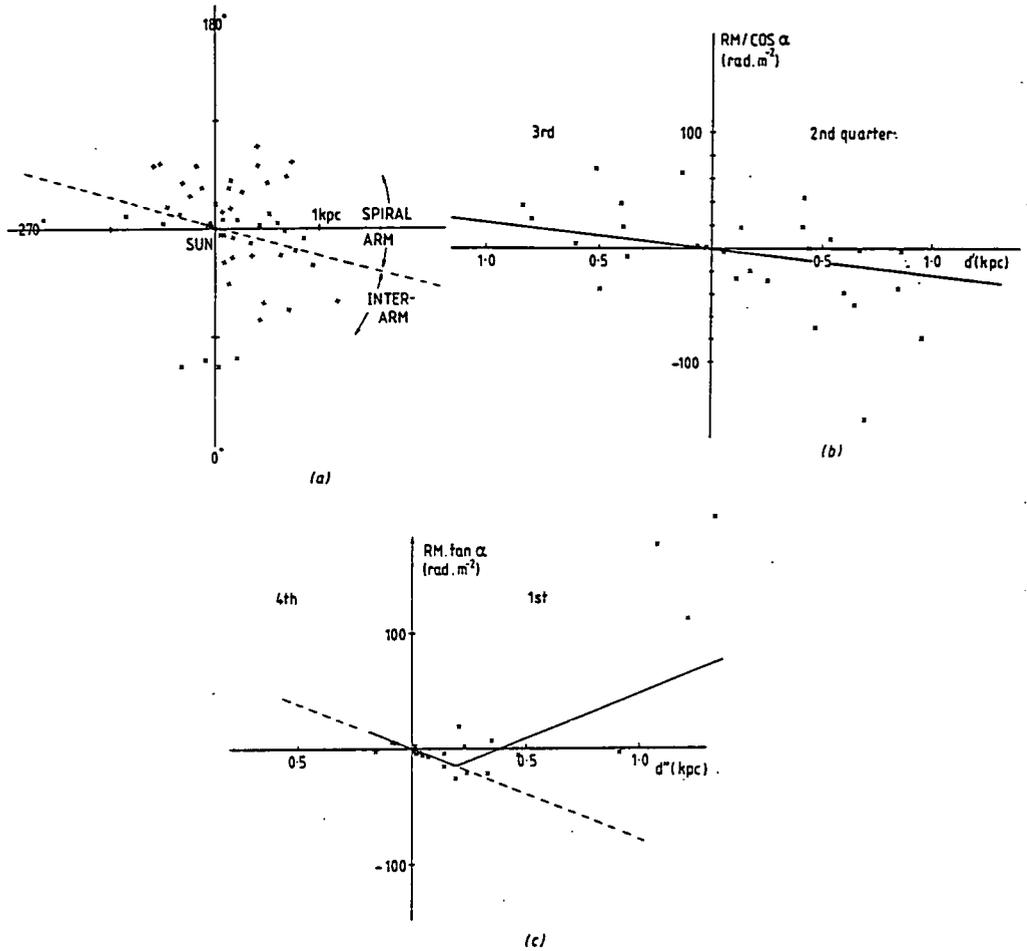

Figure 6.1. (a) A plan view of the pulsars in our sample. (b) $RM/cos(\alpha)$ versus $d'(= dcosb)$ for the Outer Galaxy subsample, where α is the angle between the direction of the regular field and the direction of the line of sight towards the pulsar. (c) $RM\ tan(\alpha)$ versus $d''(= dcosb\ sin\alpha)$ for the Inner Galaxy sub-sample.

We believe that the reason for a smaller regular field in the arm is that there are more disturbances by star formation activity and star destruction

(SNR) in arm regions than in interarm regions, although the density wave action, which is trying to compress the field into order, is stronger in the arm than in the interarm. It is also apparent that the field direction is roughly lined up along the spiral arms of stars and interstellar gas and consistent with the radio synchrotron emission pattern (Broadbent, 1989). These two facts together with a reversal of the field suggest that the large scale magnetic field can be represented by a bisymmetric spiral rather than a concentric ring (the latter would require $l = 90^\circ$ in both regions).
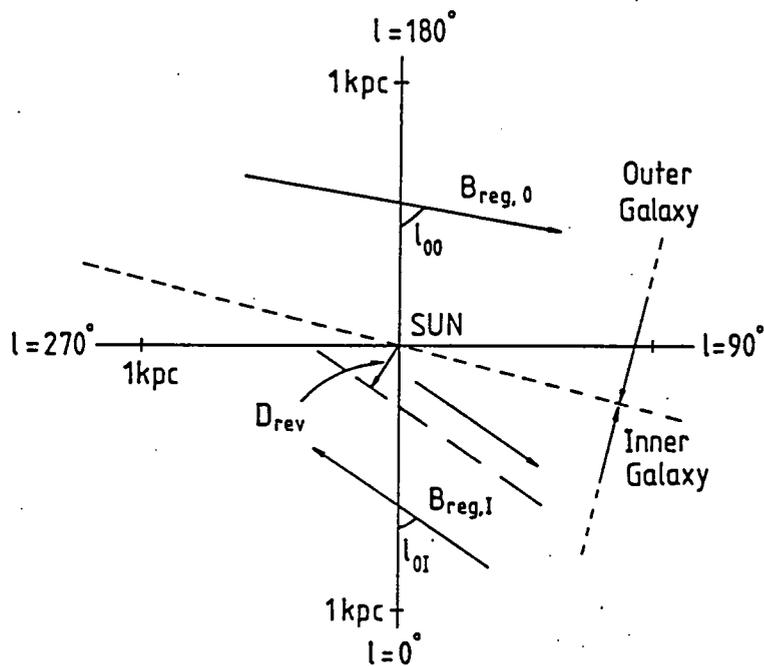
Figure 6.2. A plan view of the regular magnetic field in the solar vicinity as, derived in Section 6.4.1.

6.4.2 The irregular component

All previous analyses of the irregular field were based on the 'single-cell-size' model in which the field strength is constant over a cell and the field direction is randomly oriented from cell to cell. We start by following the same procedure and use it as a first-order approximation and calculate the variance

and covariance of best-fitting residuals of magnetic field, as formulated by Rand and Kulkarni (1989). If the median values are taken to interpret the variance and covariance and B_{ir} and L are used to denote the irregular field strength and the cell-size, respectively, we find: $B_{ir}^2 L = 1.3 \times 10^3$ $\mu G^2 pc$ and $B_{ir}^2 L^2 = 6.5 \times 10^4$ $\mu G^2 pc^2$, yielding $B_{ir} = 5.1$ μG and $L = 50$ pc for the Outer Galaxy; for the Inner Galaxy, $B_{ir}^2 L = 1.5 \times 10^3$ $\mu G^2 pc$ and $B_{ir}^2 L^2 = 9.0 \times 10^4$ $\mu G^2 pc^2$, yielding $B_{ir} = 5.0$ μG and $L = 60$ pc. Our result is similar to that of Rand and Kulkarni (1989), *i.e.* $B_{ir} = 5$ μG and $L = 55$ pc.

We now proceed to a more realistic model involving a range of cell sizes. We invoke the Kolmogorov spectrum of interstellar turbulence and adopt energy equipartition between kinetic energy of turbulence and energy of magnetic field on every scale size. Our multi-cell-size model contains the following assumptions:

1. the interstellar medium is full of turbulent energy sources of scale size L_0.

2. there are sub-scales of linear dimension l inside each L_0 which obey the Kolmogorov spectrum $v_l \simeq (\omega l)^{1/3}$, where v_l is the velocity on scale l and ω is the energy transfer rate.

3. energy equipartition between the kinetic energy of turbulence and the energy of the irregular magnetic field holds on every scale size, that is, $B_l^2/8\pi = \rho v_l^2/2$ or $B_l = \sqrt{4\pi\rho}v_l$, where ρ is the density of the interstellar medium.

4. the spatial distribution of the irregular field direction is isotropic on every scale size.

The largest scale L_0 is probably related to the SNR radius (a few hundred pc) at which energy input occurs. Systems such as SNR have considerable substructures which are thought to obey the Kolmogorov distribution and where energy equipartition between the kinetic energy of motion and the energy of magnetic field holds.

In the case where there are multi-scale irregularities in the magnetic field, the effective field contributing to the radio synchrotron emission is different from the field seen by the pulsar rotation measure, the former is the total field while the latter is the averaged field over the line of sight. Inside the largest scale L_0 there are many scales. In order to derive the average field we have performed a Monte-Carlo simulation. The scale lengths are quantized into $L_0/2$, $L_0/4$, $L_0/8$, $L_0/16$, $L_0/64$ and $L_0/128$ units. On each scale l, the strength of the irregular field is $B_l = \sqrt{4\pi\rho}(\omega l)^{1/3}$ by combining *Assumptions 2 and 3* and the direction is randomly oriented according to *Assumption 4*.

In our numerical simulation, the field strength on the scale L_0 is taken to be 5 units and thus on scale l is $5(l/L_0)^{1/3}$. Figure 6.3 shows the result of our Monte-Carlo simulation, *i.e.* the distribution of the averaged field. The distribution is close to Gaussian and is peaked at 5 units (it was not obvious that it would be of Gaussian shape). Therefore, the direction of the field on the largest scale L_0 can be used to represent that of the averaged field, *i.e.* they have the same effect on the pulsar rotation measure.
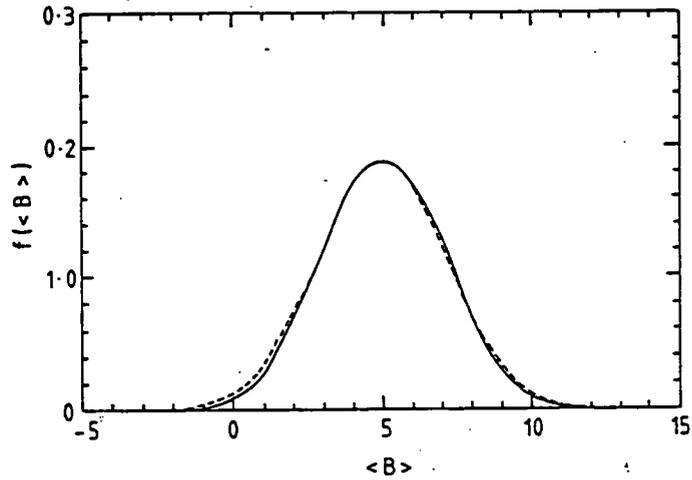
Figure 6.3. The distribution of the line of sight averaged field strength in the largest scale cell from the Monte-Carlo simulation. A Gaussian with the same peak value and same standard derivation value is indicated (the dashed line). The field is given in arbitrary units.

According to the Kolmogorov spectrum and the energy equipartition assumption (*Assumption 3*), the energy density of the irregular magnetic field on scale of wave number $k(= 1/l)$ is

$$E_k dk = \omega^{2/3} k^{-5/3} dk \qquad (6.9)$$

so the total energy density (of the effective field contributing to the radio synchrotron radiation) of all scales is the integral

$$E_t = \omega^{2/3} \int_K^\infty k^{-5/3} dk = (3/2)\omega^{2/3} L_0^{2/3} \qquad (6.10)$$

where $K = 1/L_0$. The energy density on largest scale E_0 is

$$E_0 = v_{L_0}^2 = \omega^{2/3} L_0^{2/3} \qquad (6.11)$$

leading to

$$E_t/E_0 = 3/2 \quad . \tag{6.12}$$

therefore the effective strength of the total field is $\sqrt{3/2}$ times that of the field on scale L_0 (the value derived above), *i.e.* $\sqrt{3/2} \times 5\mu G = 6.1\mu G$.

6.5 Application to the propagation of energetic protons

In the Introduction it was pointed out that the Larmor radius for a proton of 10^{20} eV is 30 kpc in a magnetic field of 3 μG; correspondingly the Larmor radius at 10^{19} eV is 3 kpc. The question to be asked now is: could the magnetic field distribution be such that protons in this energy band are generated in our Galaxy and have such paths that their origin would not be recognized as such? The evidence supporting extragalactic origin includes the observation that particle trajectories above 10^{19} eV favour large latitudes (such as might be expected by propagation from sources in the Virgo cluster of galaxies) but a large coherent halo field *could* allow a Galactic origin.

To demonstrate this argument quantitatively, we perform a trajectory calculation, of the type first used by Thielheim and Langhoff (1968). The technique is to numerically trace the paths of energetic antiprotons propagating in the Galactic magnetic field. The procedure of tracing an antiproton starts at the Earth and terminates at the boundary of the Galaxy where the particle escapes, to simulate the inverse problem of proton propagation in the Galaxy and arrival at the Earth. Our model of the magnetic field consists of two components: a regular component with spiral pattern, a pitch angle 13^0 and a strength of 2 μG; and an irregular component of random oriented single-size cells with a cell-size of 55 pc and a strength of 6 μG. Apparently, this model is an irregular component dominated model, being different from those used in previous calculations. Figure 6.4 displays our results in two dimension for antiproton energies of 10^{18} eV, 5×10^{18} eV and 10^{19} eV, respectively, in each case eight trajectories being calculated. We can see that: (1) at 10^{18} eV the trajectories are completely randomized by the irregular field, being consistent with the observed, highly isotropic arrival directions; (2) at 5×10^{18} eV the trajectories are largely bent by both the regular field and the irregular field; and (3) at 10^{19} eV the trajectories are only weakly influenced by the presence of the fields and are hence close to straight lines.

The present work indicates reversals of the regular field on the scale of spiral arms so that certainly for this reason the particle trajectories will be straightened by those field reversals, *i.e.* the deflections by fields in different arms will cancel. Also, presumably for this reason alone, the mean regular

100

field at heights above the Galactic plane of greater than 2—4 kpc will be very small (oppositely directed fields cancel). As seen already the evidence from synchrotron data (Section 2.4) is that the total field probably has a scale height of no more than 5 kpc so that, again, significant halo fields which could deflect back 10^{19} eV particles are most unlikely. Thus, it seems most unlikely that protons above 10^{19} eV are of Galactic origin. It is not impossible that the primaries of this energy are not protons but heavier nuclei, in which case the magnetic rigidity (pc/Ze) is reduced and with it the Larmor radius. However, other problems then appear (Wdowczyk and Wolfendale, 1989).
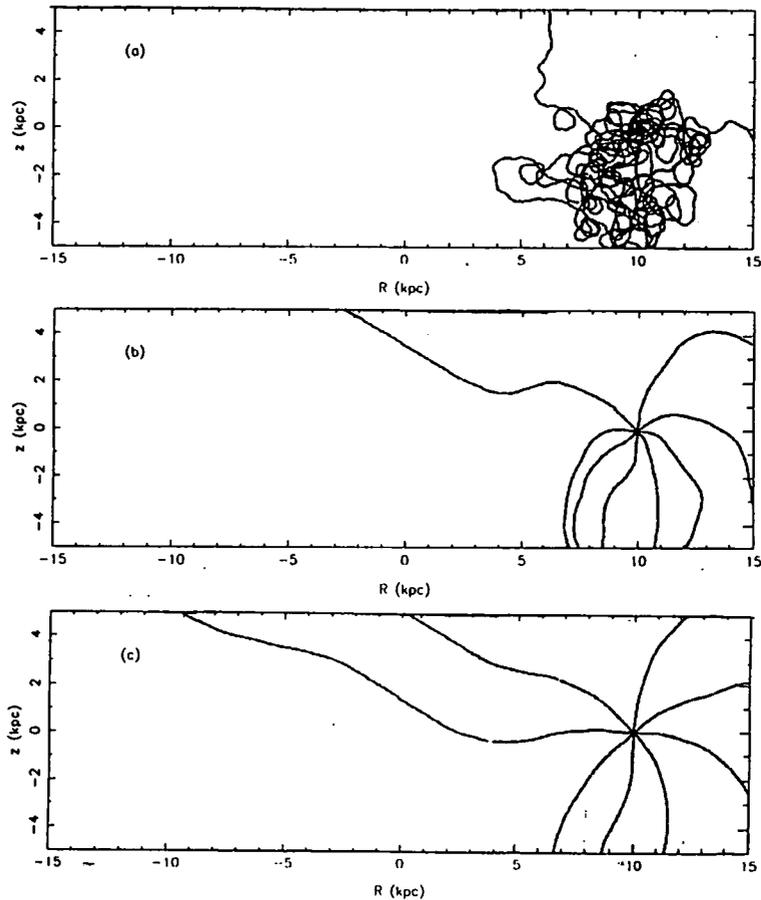
Figure 6.4. Trajectories of highest energies protons in the Galactic magnetic field with energies (a) 1×10^{18} eV; (b) 5×10^{18} eV; and (c) 1×10^{19} eV.

101

6.6 Discussion and summary

It is important to use an adequate model in deriving the local magnetic field structure since it is impossible to obtain the field configuration by performing a direct deconvolution of the pulsar rotation measure data. The major difference between our analysis and previous ones is that we distinguish the arm region and the interarm region and fit data with the model separately in these two regions. This leads to our conclusion that the regular field is stronger in the interarm region than in the arm region and the field runs roughly along the spiral arms. Rand and Kulkarni (1989) obtain a different conclusion by fitting a model in which the field follows concentric rings and is not associated with the Galactic spiral arms.

The reversal of the regular field can be predicted by the induction-and-dynamo theory (Krause, 1987; Ruzmaikin, 1987), which was originally developed by Parker (1971). In such a theory, a primordial field was amplified and then the field maintained by the $\alpha - \Omega$ dynamo, caused by the coupling between the helical turbulence of interstellar gas and the Galactic differential rotation. Since the strength of the dynamo depends on Galactic rotation, the spiral density wave should have an important effect on the dynamo strength. Lesch *et al.* (1988) have looked into this problem in some detail. They found that the dynamo strength goes up with increasing the strength of the density shock wave and that weak dynamos correspond to an axisymmetric field and strong dynamos correspond to a bisymmetric field. Applying their criterion for the density wave strength, $\omega_\perp/c_s$ (where c_s is the effective acoustic speed of the ionized gas; $\omega_\perp$ is given by $\omega_\perp = \bar{r}(\overline{\Omega} - \Omega_p)\sin i$, i is the pitch angle of the density wave pattern, $\bar{r}$ is the mean value of the radius, $\overline{\Omega}$ is the mean galactic rotation frequency and Ω_p is the angular speed of the bisymmetric spiral pattern), to our Galaxy, it turns out that $\omega_\perp/c_s = 1.2$. This value is moderately strong and thus indicates that the large scale Galactic magnetic field is probably bisymmetric.

Turning to the irregular field, we can remark that the interstellar medium is full of turbulent shock waves stimulated by star formation activities, particularly by supernova explosions. There is sufficient observational evidence for an approximate energy density equipartition among the thermal motion of interstellar gas, cosmic rays and the Galactic magnetic field locally, and the well-established observational evidence for the enhancement of the magnetic field strength by interstellar shocks (Heiles, 1987), to allow us to conclude that the assumptions we made in Section 6.4.2 are reasonable. It must be said, however, that direct observational evidence for the Kolmogorov spectrum has not appeared yet.

To summarise, the regular component of the local Galactic field appears

to be aligned along the local spiral arms, there is a reversal of field direction in the interarm region and the regular field strength is stronger in the interarm region than in the arm region. The results imply that the large scale structure of the Galactic magnetic field can be represented by a bisymmetric spiral. The effective strength of the total irregular field component is found to be 6 μG in both the arm regions and the interarm regions by using a multi-cell-size model. The results strengthen the view that cosmic rays protons above 10^{19} eV are extragalactic; they also imply that the Galactic distribution of cosmic electrons in the GeV region can be understood.

Chapter 7

Conclusions

7.1 Summary

In this thesis we have shown the importance of cosmic ray electrons in the cosmic radiation. An interesting feature of the radiations emitted by the electrons is that they are significant mainly at the two extreme wavebands of the electromagnetic spectrum: in radio and in γ-rays. Both regions are important and are the subject of much contemporary research.

The radio continuum emission of our Galaxy and that from external galaxies is dominantly produced by cosmic ray electrons gyrating in the galactic magnetic field and is widely used as a probe to detect galactic structure and the cosmological evolution of distant galaxies.

The γ-ray continuum emission is at least partly produced by cosmic ray electrons interacting with interstellar matter via bremsstrahlung and with interstellar radiation field via inverse Compton scatterings. The diffuse γ-ray emission has found its application, at the moment, very largely only in probing the large scale structure of our Galaxy, due to the limitation of techniques. Because of the existence of the 2.7 K microwave background radiation, the electrons, generated in individual galaxies and even permitted to escape from their parent galaxies, are localized to the vicinities ($\sim$ 40 Mpc) of their parent galaxies by the background photons via inverse Compton scattering. As a result X-ray and γ-ray radiations are emitted in the process and they contribute to the cosmic X-ray and γ-ray background radiations.

An understanding of the mode of acceleration and propagation of cosmic ray electrons in our Galaxy is a key to the study of their radiation. In Chapter 2 we have demonstrated that cosmic ray electrons are of Galactic origin, almost certainly being accelerated in the diffusive shocks of supernova remnants. It is estimated that, in our Galaxy, the supernova rate is 1/30 yr^{-1}, the average supernova shock energy output is 10^{51} ergs and the cosmic

ray (proton) acceleration efficiency is 10%, then the energy input into cosmic rays therefore follows as: $0.1 \times 10^{51}/(30 \times 3.15 \times 10^7) \sim 10^{41}$ ergs $\cdot$ s^{-1}, of which about 3% goes into electrons. The propagation of cosmic rays in the Galactic Disk is one of mainly diffusive motion and the diffusion coefficient is a function of Galactocentric radius, being greater towards the Inner Galaxy because of more turbulent nature so that the smoothness of the distribution and the smallness of the cosmic ray gradient—both protons and electrons—can be understood, although convection may also play a role in manifesting the spectral variation. We have proposed a convection associated diffusion propagation model to explain the spectral variation of the Galactic radio synchrotron emission and the γ-ray continuum emission. The radio spectral flattening with Galactic latitude is caused by convection—the Galactic wind; whereas the γ-ray spectral variation over the Galaxy is complicated and caused by many factors, such as the inverse Compton halo, the local Orion arm and unresolved point sources.

The 'seed' population—MeV and hundred keV cosmic ray electrons—not only play an important role in the cosmic radiation, but also in the Galactic dynamical process and chemical process. The interstellar flux of these electrons derived from the diffuse γ-ray data is surprisingly high. The standard diffusive shock acceleration by SNR is insufficient to account for the ambient electron intensity and an extra source is required. We have put forward the idea that the low frequency turbulence due to the lower hybrid instability in a magnetized plasma is the working acceleration mechanism, being operated by massive star-initiated shocks. The spatial distribution of these electrons in the Galaxy has a relatively large Galactocentric gradient, the intensity being higher in the Inner Galaxy than in the Outer Galaxy, and therefore the electrons exert more pressure in the Inner Galaxy. We regard this pressure as important in keeping a constant scale height of the HI gas layer.

An important consequence of the presence of the proposed high flux of MeV electrons is their contribution to the extragalactic γ-ray background radiation in the hundred keV energy range if, as is very likely, external spiral galaxies also produce considerable fluxes of MeV electrons. Another important consequence is the interstellar ionization and heating by the electrons—the three decade mystery of the source of ionization in HI regions may now be revealed; the heating also keeps the interstellar medium warm ($\sim 10^4$ K). We presume that, if the MeV electrons are able to penetrate interstellar clouds or are produced inside them, many important chemical processes will take place and this in turn provides a test of our model.

The global distribution of cosmic rays in the Galaxy is characterized by the presence of an extensive halo above the stellar and gas disks, this halo

being first seen through the radio synchrotron emission of cosmic ray electrons. An analysis of the grammage measurement together with life-time measurement of cosmic ray nuclei leads to the conclusion that cosmic rays spend most their life-time in the halo after being produced in the disk. The coexistence (incidentally?) of the extensive halo of the starlight radiation field facilitates an inverse Compton halo. Our detailed calculation has shown that up to 60% of the diffuse Galactic γ-ray flux at intermediate latitudes can be contributed by the γ-ray halo and accordingly the SAS-II estimate of the extragalactic γ-ray background can be lowered by 30%. Since dynamical studies conclude that the cosmic ray halo is dynamically unstable, we have considered the possibility (a likelihood, in fact) of cosmic rays escaping from our Galaxy and found consequently that $\sim 15\%$ of the extragalactic γ-ray background flux can be produced by the escaping electrons via inverse Compton scattering off the 2.7 K microwave background photons if other normal galaxies have the same number of escaping electrons as our Galaxy. However, all the known contributors of the γ-ray background are insufficient to account for the observed flux, so that some type of cosmological model should be employed; we have specified such models.

External spiral galaxies bear a similar evolutionary process to that in our Galaxy, star formation and destruction activities are continuously occurring and supernova events frequently happen. The generation of cosmic rays in external galaxies is a common phenomenon. The study of cosmic rays in other galaxies is relevant to that of our Galaxy because we can have a better perspective view, particularly for those galaxies possessing similar properties to our own. The tight correlation between radio continuum power and far infrared luminosity which exists over a wide range of sizes and powers of spiral galaxies is an eminent representation of the similarity in star formation and destruction. Based on empirical results, we have proposed an energy equipartition theory to account for the correlation, in which the total outputs of far infrared emission and cosmic rays in a galaxy are assumed to be proportional to the star formation rate in that galaxy. A success of our model is the prediction of the observed non-unity slope of the correlation. Our statistical study leads to the conclusion that the majority of the cosmic ray electrons emitting radio synchrotron radiation escape from our Galaxy. A significant implication of our model is that cosmic rays play an indispensible role in the evolution and large scale dynamics of galaxies.

A knowledge of the Galactic magnetic field is certainly required in the study of cosmic ray astrophysics although it is very difficult to achieve and is still scanty at the moment. Pulsar rotation measure provides the best approach to the solution of this problem because it probes the magnetic field on both large scales and small scales. Our detailed analysis of the local pulsar

rotation data clears away the confusion over the conclusions on the large scale configuration of the Galactic magnetic field. We conclude that the large scale regular field in our Galaxy is bisymmetric, there being a directional reversal of the regular field between spiral arms. Since there is less perturbation of star formation and destruction activities in the interarm regions than in the arm regions, we can see that the regular field is stronger in the interarm regions than in the arm regions. On a small scale, we found, amazingly, that the irregular field is stronger than the regular field, the former is $\sim 6~\mu$G and the latter is $\sim 2~\mu$G. This implies that the interstellar medium is full of turbulence and accordingly the diffusive nature of cosmic ray propagation in the Galaxy can be easily understood.

7.2 Prospects

Observationally, great achievements are expected in the 1990's. The launch of space observatories working in various wavebands, headed by the Hubble Space Telescope, and the construction of ground-based grand telescopes, will yield fruitful data and solve many key problems in astrophysics. Relating to the study of cosmic rays and the interstellar medium, the Soviet-French-Polish satellite 'GAMMA-1' has already started operation and this will be followed in early 1991 by the US-FRG's Gamma Ray Observatory (GRO). Both will carry out accurate measurements of the large scale distribution of cosmic ray intensity and spectrum over the whole Galaxy and will surely discover many new γ-ray sources. The X-ray observatory ROSAT will provide accurate data in the important X-ray/UV band which will lead to stringent constraints on interstellar heating and cooling structures. Ground-based radio telescopes will continue high resolution surveys and polarization measurements of nearby spiral galaxies and complete the all-sky radio spectral measurement of our Galaxy. Meanwhile, direct measurements of the cosmic ray spectrum, grammage and life-time near the Earth will accumulate more data and give more accurate results.

Theoretically, a unified 3-dimensional model of cosmic ray propagation in the Galaxy (as well as in other galaxies) will be built up; this model will reconcile all the available experimental facts including the spectrum, grammage, life-time and halo extension. The problem of continuous acceleration of cosmic rays in the interstellar medium will be clarified, thereby answering such questions as, how efficient is it and how does it influence the secondary to primary ratio? The dynamical role of cosmic rays in supporting the interstellar medium in the Galaxy will be studied further, particularly in the halo. The detailed structure of cosmic ray ionization, heating and the conse-

quent cooling processes will be determined. Our knowledge of the manner of generation and maintenance of the Galactic magnetic field will be improved, specifically the field structure in the halo will be worked out; such structure determines cosmic ray propagation on the one hand and is modified by the presence of cosmic rays on the other. Finally, a global model of the Galactic dynamics and evolution, which incorporates the interstellar gas, gravity, magnetic field, cosmic rays, interstellar shocks and star formation activity, will be established.

Appendix A

The Interstellar Radiation Field

A.1 Introduction

The study of the Interstellar Radiation Field (ISRF) in the Galaxy is both
an old astronomical topic and a new one. In 1926, Eddington made the
first attempt to answer the question of its magnitude when he was gathering
evidence for the existence of diffuse interstellar matter (gas). By assuming
the ISRF to be equivalent to a black-body radiation in equilibrium, he found
the mean energy 'density' of the ISRF to be 3.2 K. Four years later, the
discovery of interstellar extinction by Trumpler (1930) raised a real difficulty
in determining the ISRF: the interstellar dust absorbs starlight very effec-
tively and reemits photons at far infrared wavelengths; our optical view of
the Galaxy is therefore limited. In order to determine the distribution of the
ISRF in the Galaxy, both the stellar distribution and that of the dust have
to be known first and only now are they becoming available.

In the past four decades, all electromagnetic wavelengths (from radio
to γ-rays) have been explored and this has greatly enlarged our view of
the Galaxy. Prominent examples include the 21-cm emission line surveys of
neutral atomic hydrogen, which yields information on the distribution of this
diffuse gas component, and the broadband infrared surveys which trace the
interstellar dust. Knowledge of dust is important because of its absorbing
effects on optical radiation; its distribution must be known so that both the
distribution of stars may be inferred in distant regions and the absorption
effects on the received radiation allowed for.

The all-sky survey of the infrared astronomical satellite (IRAS) launched
in the early 1980's has yielded fruitful information on the interstellar dust
distribution on a large scale in the Galaxy. By correlating the flux of infrared
emission with the column density of interstellar gas, Boulanger and Pérault
(1988) concluded that locally the diffuse infrared emissions are dominantly

from the HI associated dust heated by the ISRF, and that the dust is uniformly mixed with the gas. Since the interstellar gas distribution is quite well known (see *e.g.*, Burton and Gordon, 1978; Kulkarni and Heiles, 1987), the local dust distribution can be directly derived.

For the distribution of stars in the Galaxy and their contribution to the ISRF, many studies have been made (see *e.g.*, Freeman, 1970; Hayakawa et al., 1978; Mezger, 1978; Güsten, 1980) and a detailed model has been proposed by Mathis *et al.* (1983). In this model, there are four stellar components contributing to the interstellar radiation field, (1) OB stars; (2) and (3) disk stars and (4) giant (and super giant) stars. Each of these components follows an exponential distribution in radial direction (with a low R-cutoff in some cases) which is suggested by the observed distribution of stars in the disks of external spiral galaxies; in the direction perpendicular to the disk plane an exponential distribution is also indicated mainly by observations of the distribution of stars in the solar vicinity.

The interstellar radiation field has importance not only in optical astronomy but in other astronomical areas, too, particularly in γ-ray astronomy. Previous studies (Kniffen and Fichtel, 1981; Riley and Wolfendale, 1984; Bloemen, 1985) in the γ-ray field show that a substantial fraction of the Galactic diffuse γ-rays is produced via the inverse Compton process, in which relativistic cosmic ray electrons interact with the ISRF photons. However, since the ISRF was not well known before the IRAS results on the dust distribution appeared, there was a wide difference in the estimates of the fraction of the diffuse γ-rays contributed by the inverse Compton process, specifically from 5% by Bloemen to 35% by Riley and Wolfendale. It is true that part of the difference arises from uncertainty in the intensity of cosmic ray electrons as a function of height above the Galactic Plane, and this will remain for some time, but it should now be possible to make a more accurate study of the important ISRF.

The imminent launch of NASA's Gamma Ray Observatory with an unprecedented sensitivity and resolution has focussed on the need to provide up to date estimates of the energy density of interstellar radiation away from the Galactic Plane, this parameter being a prerequisite for calculation of the flux of gamma rays coming from the inverse Compton interactions of cosmic ray electrons.

A.2 A new analysis

A.2.1 Assumptions

The stellar model used in this work is the same as that given by Mathis *et al.* (1983). It consists of four stellar components contributing to the ISRF in the 0.1~ 8.0 μm wavelengths range:

1. UV emission from early type stars, which dominates the ISRF between 0.09 μm and 0.25 μm. Its spectrum and local flux was derived from Gondhalekar (1980), with adjustments from the measurements of Henry *et al.* (1980) and Lillie (1968).

2. and 3. Optical emission due to disk stars, described by diluted blackbody radiation with temperature $T_2 = 7500$ K, dilution factor $W_2 = 1.0 \times 10^{-14}$, and $T_3 = 4000$ K, $W_3 = 1.0 \times 10^{-13}$, respectively. The dilution coefficients are slightly different from those of Werner and Salpeter (1969) with which the ISRF is considerably underestimated longward of 1 μm (Jura, 1979) if the near infrared emission from the Galactic Plane as observed by different Japanese groups (see *e.g.*, review by Okuda, 1981) is properly taken into account. With these parameters the derived spectrum is in good agreement with the synthetic spectrum of Mattila (1980a,b).

4. Red and near infrared emission due to Red Giants (and Supergiants), described by blackbody radiation with $T_4 = 3000$ K (as suggested by Price, 1981) and $W_4 = 4.0 \times 10^{-13}$.

The proportion of each component contributing to the ISRF is mainly determined by observations of the stellar population with a minor adjustment to match the observed spectral shape of the ISRF.

The spatial distribution of the volume emissivities of the stellar components $j_i(\lambda, R, z)$ (i=1,2,3,4) in the model is (valid for R greater than some minimum value, R_c):

$$j_i(\lambda, R, z) = j_i(\lambda, R_\odot, 0) exp(-z/h_i - (R - R_\odot)/H_i) \qquad (A.1)$$

where R is the Galacto centric distance and z is the distance perpendicular to the Plane, $R_\odot$ is the Galactocentric distance of the Sun and $j_i(\lambda, R_\odot, 0)$ stands for the local emissivity. The scale heights H_i and h_i are different for the different components. The model adopts radial symmetry about the Galactic Centre (this point is returned to later). In its first form we adopt $R_\odot = 10$ kpc; later analysis relates to the adoption of $R_\odot = 8.5$ kpc.

The stellar component 1 (OB stars) shows a strong concentration around $R = 5$ kpc (Mezger, 1978) corresponding to $R_c = 4$ kpc. The scale lengths of components 2 and 3 (disk stars) were derived from the observed surface brightness of spiral galaxies (Freeman, 1970) corrected for dust absorption, and here $R_c = 0$. For component 4, the scale parameters were derived from fitting the 2.4 μm and 3.4 μm Galactic-ridge intensity observed by Hayakawa *et al.* (1978). This stellar component is concentrated between Galactocentric distances 4 kpc and 8 kpc and again a cut-off at $R_c = 4$ kpc is applied. Table

A.1 lists the parameters in the model. It is considered reasonable to ignore the spiral arm structure of the Galaxy since it affects only component 1, from which the contribution to the ISRF is a small fraction.

Table A.1. Parameters of the 4-component stellar model.

i	h_i(pc)	H_i(kpc)	R_c(kpc)	$j_i(R_\odot, z = 0)$ $L_\odot \mathrm{pc}^{-3}$
1	60	2.5	4.0	0.022
2	190	4.0	0.0	0.061
3	270	4.0	0.0	0.044
4	50	1.3	4.0	0.033

Most important (and not very realistically) it is assumed that the dust is distributed smoothly throughout the Galaxy. The likely errors caused by this assumption will be discussed later. The dust model adopted here is a simplified one. We do not distinguish the various components such as silicates, amorphous carbon, graphite, organic refractories and metallic oxides, but just take their total extinction $k(\lambda)$ to account for absorption. The values of $k(\lambda)$ at various wavelengths are taken directly from Table C1 of Mathis *et al.* (1983) and are given here in Table A.2 for the four wavelength regions into which we have divided the 'optical' range (defined by us as 0.1 μm $< \lambda < 8$ μm: 'OPT', actually UV+V+NIR); the region with $\lambda > 8\mu$m, for which extinction is negligible, is referred to as 'FIR'). The absolute values in the Table relate to the local region under specific assumptions which may or may not be applicable in the present case. For this reason we proceed by including a normalization factor (applied in this case to the scale height of the dust component(s)) to ensure that the standard total Galactic luminosity (by Mathis *et al.*, 1983) of OPT and FIR is achieved. The measured mean extinction from the Sun to the Galactic Centre is then used to check the adopted extinction values.

Table A.2. The adopted average values of visual extinction in different wavelength intervals for the 'local' region from the work of Mathis *et al.* (1983).

$\lambda(\mu$m)	$0.13 \sim 0.25$	$0.25 \sim 0.7$	$0.7 \sim 1.8$	$1.8 \sim 8.0$
$k_v(R_\odot, 0)$(mag/kpc)	2.8	1.2	0.42	0.06

112

In the model the dust-to-gas ratio is assumed to be the same for both HI-
and H_2-associated dust and to fall with increasing Galactocentric distance
as does the metallicity (see later).

Concerning the z-dependence of the HI-associated dust density, we take
the distribution to be the same as that of the HI gas, which has roughly a
constant volume density and a constant scale height (at least over the region
of importance here):

$$n_{HI}^d(R, z) = n_{HI}^d(R_\odot, 0) exp(-\frac{z^2}{(0.17)^2}) \qquad (A.2)$$

where $n_{HI}^d(R_\odot, 0)$ is the local dust density and the scale height parameter,
0.17 kpc, is chosen to given the 'correct' total absorption (see above). The
metallicity gradient $(Z/Z_\odot)$ is taken to be the same as that for the [O/H]
abundance, given by Güsten and Mezger (1983) and has the form

$$Z/Z_\odot = exp(-0.12(R - 10)) \qquad (A.3)$$

The visual extinction of the HI-associated dust between $R = 4$ kpc and
$R = 10$ kpc calculated from the above formulae is 8.8 mag in the disk plane.

In a similar way, the dust associated with molecular hydrogen H_2 follows
the H_2 distribution as

$$n_{H_2}^d(R, z) = n_{H_2}^d(R) exp(-(\frac{z}{\Delta_{H_2}})^2) \qquad (A.4)$$

where the scale height Δ_{H_2} is also a function of R, given by $\Delta_{H_2} = 0.036 +$
0.004 R kpc in the range 4 kpc $\leq R \leq$ 12 kpc (see $e.g.$, Scoville and Sanders,
1987). The resulting visual extinction of the H_2-associated dust is 18.9 mag
from $R = 4$ kpc to $R = 10$ kpc in the Disk.

Adopting the results given already and the arguments of Bhat et $al.$
(1986), concerning the surface density of H_2, $\sigma_{H_2}(R)$, we have:

$$\sigma_{H_2}(R)/\sigma_{HI}(R) = \begin{cases} 1, & 4 \text{ kpc} \leq R \leq 6 \text{ kpc} \\ 2 - R/6, & 6 \text{ kpc} < R \leq 12 \text{ kpc} \\ 0, & R > 12 \text{ kpc} \end{cases} \qquad (A.5)$$

For $R < 4$ kpc, we take the dust surface density, $\sigma_d(R)$, to be proportional
to R and to join the surface density function referred to above beyond 4 kpc.
Its spatial distribution for $R < 4$ kpc follows as

$$n^d(R < 4kpc) = 2(R/4kpc) n_{HI}^d(R = 4kpc, z = 0) exp(-\frac{z^2}{(0.17)^2}) \qquad (A.6)$$

The visual extinction between the Galactic Centre and $R = 4$ kpc is 8.2 mag,
$i.e.$ 23% of the total from the G.C. to the Sun.

113

With the above parameters, our model ensures that, following our datum input from Mathis *et al.* (1983), the total input of radiation is $5 \times 10^{10} L_\odot$ and the far infrared output luminosity is $1 \times 10^{10} L_\odot$; the corresponding OPT output luminosity is $4 \times 10^{10} L_\odot$, these values being based on $R_\odot = 10$ kpc.

The infrared emission from HII regions is not dealt with separately, but is effectively included in the infrared emission from molecular clouds. In this way, the total visual extinction between the Sun and the Galactic Centre is 36 mag by our model, only a little higher than the observed value of 34 mag quoted by Henry *et al.* (1984).

For the FIR energy density, we use a simple model in which absorption is neglected—the procedure being to take the radial variation of the FIR surface luminosity of the 'cold dust' curve in Figure 11.b of Cox *et al.* (1986), assume that the scale height is given by $\Delta_{\text{FIR}} = 120$ pc and normalize the total luminosity to $1 \times 10^{10} L_\odot$, the canonical value of the FIR of the Galaxy.

A.2.2 Manner of calculation

The energy density of the interstellar radiation field at position (R', z') and wavelength λ, due to the emission of the four stellar components, is defined by

$$\varepsilon(\lambda, R', z') = \sum_{i=1}^{4} \int \int \int \frac{j_i(\lambda, R, z) g R dR dz d\theta}{4\pi c l^2} \qquad (A.7)$$

where the integration is over the whole Galaxy ($0 \leq R \leq 13$ kpc and $|z| \leq 2$ kpc). l is the distance from each position (R, z) in the Galaxy to (R', z') and is given by

$$l^2 = R^2 + R'^2 - 2RR'\cos\theta + (z - z')^2 \qquad (A.8)$$

where θ is the azimuthal angle of position (R', z') to the Galactic Centre $(0,0)$. The function g describes the dust absorption

$$g = exp(-\frac{1}{1.082} \int_{(R,z)}^{(R',z')} k_v(\lambda, R, z) dl) \qquad (A.9)$$

where k_v is the visual extinction per unit path length, related to the value in Table A.2 by $k(R, z) = k(R_\odot, 0) n_H^d(R, z) / n_H^d(R_\odot, 0)$. In this expression, n_H^d is the appropriate summed density of H-atoms in the form of HI and H_2. The integral path is along the line of sight.

A.3 Results

A.3.1 z-dependence at the solar radius, $R_\odot$

A.3.1.1 Scope of the calculations

It is sensible to check the model by calculating the predicted OPT energy density at the solar radius $R_\odot$ and comparing it with observation, the point being that the model used the observed local value as an input. The $R_\odot$ value has been changed from 10 kpc to 8.5 kpc recently, but in the following calculation we first use $R_\odot = 10$ kpc to enable comparisons with previous results to be made; $R_\odot = 8.5$ kpc is then adopted so that what is presumably a more accurate result for the OPT may be achieved.

A.3.1.2 Results for $R_\odot = 10$ kpc

In order to see the impact of dust absorption on the OPT energy density, we start with the case of no dust absorption. The dashed curve in Figure A.1 shows the result; the total output of the four stellar components contributing to the OPT is normalised to $4 \times 10^{10} L_\odot$, our standard ($R_\odot = 10$ kpc) value.
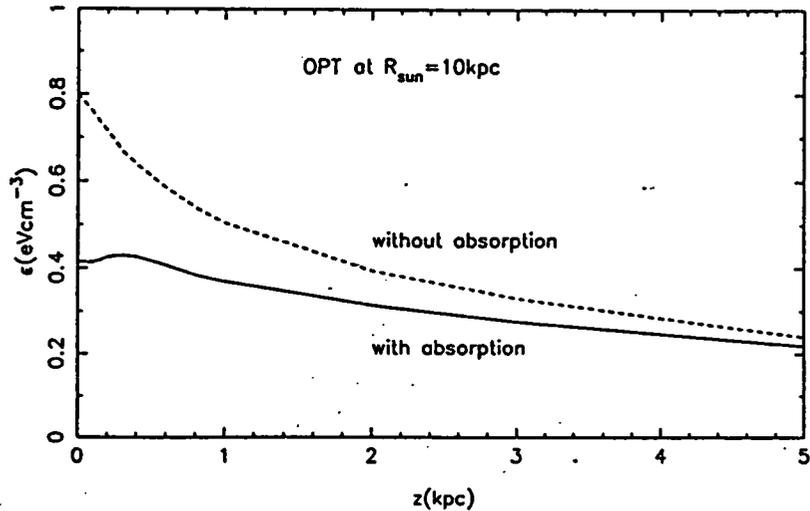
Figure A.1. The OPT energy density versus z at $R_\odot = 10$ kpc, with the total luminosity $L_{OPT} = 4 \times 10^{10} L_\odot$. The dashed curve

shows the result in the case without dust absorption and the solid curve shows the result in the case with absorption. The asymptotic limits, reached for $z \gg 10$ kpc will be the same. ('OPT' is defined as the range $0.1\mu m < \lambda < 8\mu m$ and thus includes part of UV and IR wavelengths as well as the whole of the visible region; the median wavelength, from the standpoint of energy is $\lambda_m \simeq 1\mu m$).

For the case in which dust absorption is included the solid curve shows the result. Here the total output from the four stellar components is normalised to $5 \times 10^{10} L_\odot$, 20% of it is absorbed and reemitted at far infrared wavelengths, to keep the starlight luminosity at $4 \times 10^{10} L_\odot$ and the FIR luminosity at $1 \times 10^{10} L_\odot$. It is necessary to examine the features of the curve in detail. In the solar vicinity ($z = 0$) the energy density is calculated to be 0.42 eV·cm^{-3}, which is in agreement with that of Mathis et al. (1983). Then it falls a little until $z = 0.1$ kpc, rises to a peak at $z = 0.3$ kpc, afterwards falling slowly. This variation can be understood in term of the dust distribution in the z-direction following a Gaussian, the dust concentration in the Disk close to its central plane being greater than that for the exponential case as used by Bloemen (1985) and Chi et al. (1989) where no such variation was obtained.
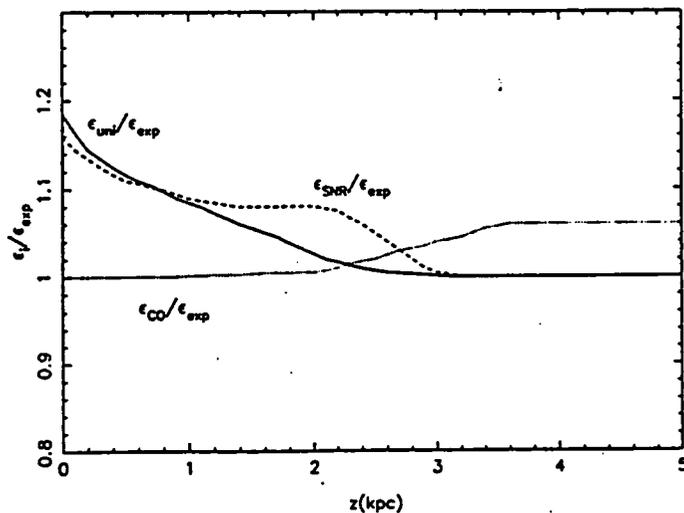
Figure A.2. The sensitivity of the OPT energy density (at $R_\odot = 10$ kpc) to the radial distribution of stellar emissivity.

Comparing the two curves in Figure A.1, the impact of dust absorption

is clearly seen. In the Disk the energy density of OPT is decreased to half by absorption whereas in the Galactic halo (large z) it is decreased by only a little. There are two reasons for this: (1) the dust resides mainly in the Disk so that it blocks the lines of sight lying in the Disk effectively but does not block the lines of sight perpendicular to the Disk plane very much; (2) due to the geometrical shape of the Galaxy, the energy density at a position in the Disk is dominantly contributed from the nearby regions while at a position in the halo it is contributed from almost all regions of the Galaxy.
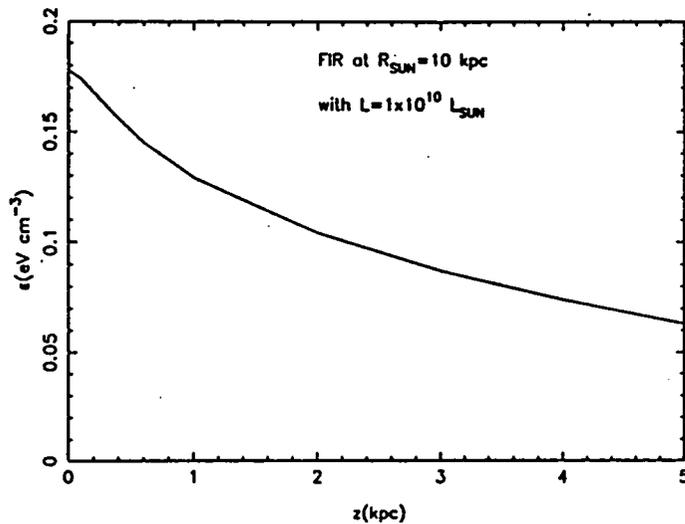
Figure A.3. The FIR energy density versus z at $R_\odot = 10$ kpc for a total luminosity $L_{FIR} = 1 \times 10^{10} L_\odot$.

In order to demonstrate this latter point, we have studied the sensitivity of $\varepsilon(z)$ to the stellar emissivity. Firstly, we tested the sensitivity to the radial distribution of emissivity. The following radial forms were examined: (1) uniform; (2) exponential; (3) CO distribution; and (4) SNR distribution. With the same luminosity, $4 \times 10^{10} L_\odot$, for all the cases, Figure A.2 shows the result for the OPT energy density ($R_\odot = 10$ kpc) with respect to the exponential distribution. It is interesting to note that the sensitivity is not marked. Secondly, we tested the sensitivity of the distance within which half of the radiation is contributed; the result is that, at a position in the Disk, more than half of the radiation comes from the region within 1 kpc and this value is also insensitive to the form of the radial distribution.

It is obvious that the derived energy density is proportional to the adopted total Galactic luminosity. We consider that the total UV and visible light

input to the Galaxy, $5 \times 10^{10} L_\odot$, and the total OPT luminosity output from the Galaxy $4 \times 10^{10} L_\odot$, are reasonable figures. This can be confirmed by comparing our Galaxy with other spiral galaxies of similar radio continuum luminosity, FIR luminosity, etc. and noting that the OPT luminosities are similar.

Figure A.3 shows the FIR energy density versus z at $R_\odot = 10$ kpc with total luminosity $1 \times 10^{10} L_\odot$ for our standard $j_i(R)$. An interesting feature of this distribution is that the scale height is quite large.

Figure A.4 shows the OPT density contour map on the R-z plane. Two features should be noted: (1) the variation in the z direction is rather slow; in other words, the energy density in the Galactic halo is substantial; (2) at small z the variation in the R direction is quite fast; the energy density in the Galactic Centre is about 10 times that in the solar vicinity.
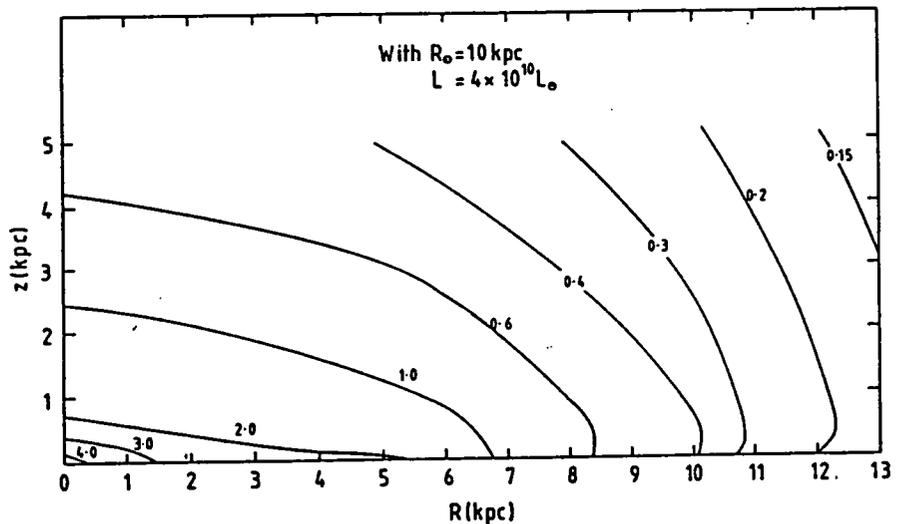
Figure A.4. The distribution of the OPT energy density in the Galaxy, with $R_\odot = 10$ kpc and $L_{OPT} = 4 \times 10^{10} L_\odot$. The units for the numbers on the contour map are $eV \cdot cm^{-3}$. The data are given in Table A.3 and the contours are derived, in an approximate manner, from these data.

Table A.3. The OPT energy densities for $R_\odot = 10$ kpc and $L_{OPT} = 4 \times 10^{10} L_\odot$. The energy density units are in eV $\cdot$ cm^{-3} and the distance units are in kpc.

$z \backslash R$	0.00	2.00	4.00	5.00	6.00	8.00	10.0	12.0	13.0
0.0	4.36	2.20	2.29	2.09	1.33	0.68	0.42	0.20	0.16
0.1	4.14	2.15	2.01	1.91	1.28	0.68	0.41	0.21	0.17
0.2	3.71	2.17	1.86	1.77	1.26	0.69	0.43	0.22	0.17
0.4	3.01	2.08	1.74	1.59	1.20	0.69	0.43	0.23	0.18
0.6	2.47	1.87	1.56	1.42	1.10	0.65	0.41	0.22	0.17
1.0	1.81	1.51	1.28	1.15	0.93	0.58	0.37	0.22	0.17
3.0	0.80	0.76	0.67	0.61	0.53	0.39	0.28	0.19	0.16
5.0	0.48	0.47	0.42	0.39	0.36	0.28	0.22	0.16	0.14

A.3.1.3 Results for $R_\odot = 8.5$ kpc

Since $R_\odot = 8.5$ kpc is the new convention recommended by the International Astronomical Union, and becoming more and more popular with astronomers, it is appropriate to adopt it in our calculation to obtain the 'best' result for the OPT distribution in the Galaxy. With $R_\odot$ changed from 10 kpc to 8.5 kpc, the total output of UV and visible light is clearly smaller. In addition to the purely geometrical change, we take account of more recent work, following Cox and Mezger (1989), and adopt $4 \times 10^{10} L_\odot$ for the total (UV and visible) energy input (these workers actually quote 3-4$\times 10^{10} L_\odot$; we adopt the value at the top of the range). Again, following these workers we adopt a FIR luminosity of $1 \times 10^{10} L_\odot$. This means that 25% of the UV and visible light output is now absorbed and turned into FIR, the resultant OPT luminosity output is $3 \times 10^{10} L_\odot$ and the total FIR luminosity is $1 \times 10^{10} L_\odot$. An adjustment to the dust model is necessary to allow more dust absorption, the fraction of energy absorbed being now somewhat larger; the scale height of HI-associated dust is increased to $\Delta_{HI} = 0.18$ kpc and the visual extinction from the Sun to the Galactic Centre is changed from 36 mag to 30 mag due to the change of $R_\odot$. With these new parameters, we recalculate the OPT and FIR energy density in the Galaxy.

Figure A.5 shows the OPT energy density versus z at $R_\odot = 8.5$ kpc. While the overall variation is similar to that in Figure A.1, the local value ($z = 0$) is increased to 0.47 eV $\cdot$ cm^{-3} and the value at $z = 5$ kpc is decreased by 10%, compared with the case of $R_\odot = 10$ kpc. Figure A.6 shows the FIR energy density versus z at $R_\odot = 8.5$ kpc. The local value is increased by 37%, to 0.27 eV$\cdot$cm^{-3}, and the high z value is increased by a little, compared

with the case of $R_\odot = 10$ kpc. This local value is higher than the observed value (~ 0.3 eV·cm^{-3} from our approximate estimate). The reason, is likely
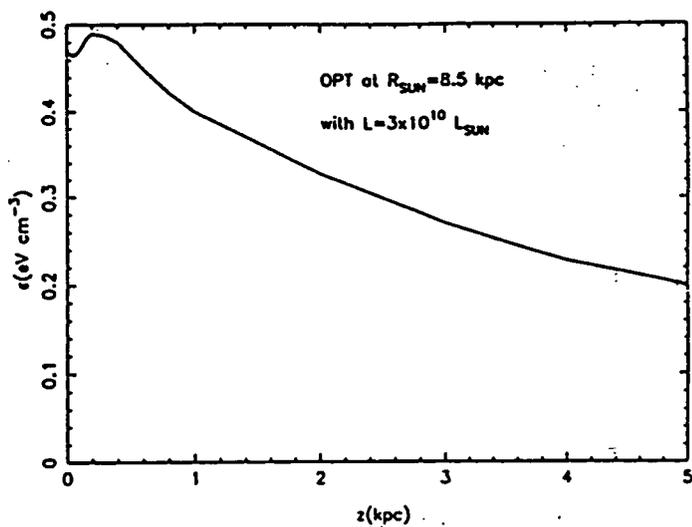

Figure A.5. The OPT energy density versus z at $R_\odot = 8.5$ kpc for a total luminosity $L_{OPT} = 3 \times 10^{10} L_\odot$.
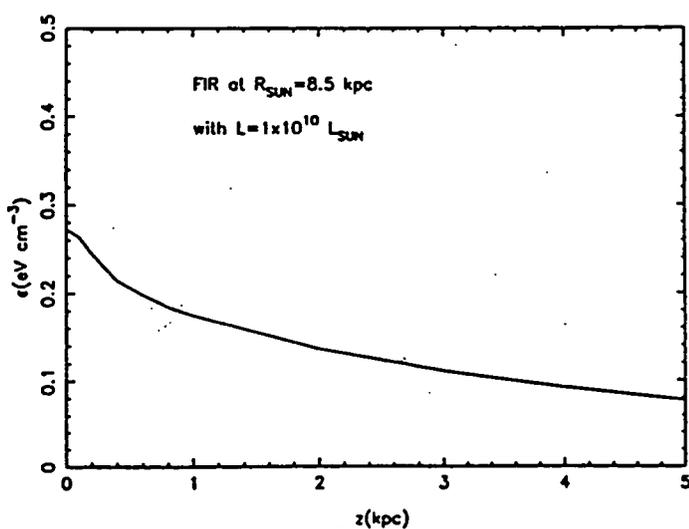

Figure A.6. The FIR energy density versus z at $R_\odot = 8.5$ kpc for $L_{FIR} = 1 \times 10^{10} L_\odot$.

to be the extraordinarily low FIR emissivity in the solar vicinity, as pointed out by Bloemen *et al.* (1990); Our model is not detailed enough to take account of this feature insofar as it assumes axial symmetry. Inspection of the clumpiness of (optical) emission from other galaxies reveals that departures from axial symmetry to this extent are not surprising. Finally, Figure A.7 shows the OPT density contour map on the R-z plane. We notice, that the R-variation becomes slower and the z-variation faster compared with the case of $R_\odot = 10$ kpc. All these results confirm the conclusion about the impact of dust absorption on the OPT energy density distribution reached in the last subsection.
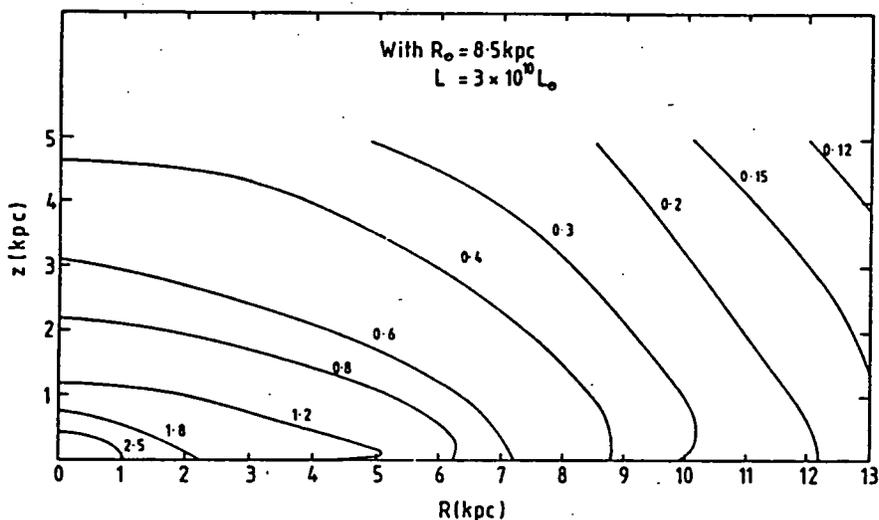

Figure A.7. The distribution of the OPT energy density in the Galaxy, with $R_\odot = 8.5$ kpc and $L_{OPT} = 3 \times 10^{10} L_\odot$. The wavelength range is $0.1\mu m < \lambda < 8\mu m$. The units for the numbers on the contour map are $eV \cdot cm^{-3}$. The data are given in Table A.4 and the contours are derived, in an approximate manner, from these data. This Figure is our best-estimate at the present time; as described in the text, the uncertainty overall is probably about 30%, except locally, where it is smaller. Energy density values for $z > 5$ kpc may be easily obtained to sufficient accuracy using the technique described in Subsection A.3.2, the 0.266 factor being replaced by 0.20.

121

Table A.4. The OPT energy densities for $R_\odot = 8.5$ kpc and $L_{OPT} = 3 \times 10^{10} L_\odot$. The energy density units are in $eV \cdot cm^{-3}$ and the distance units are in kpc.

$z \setminus R$	0.00	2.00	4.00	5.00	6.00	8.50	10.0	12.0
0.0	3.70	1.85	1.39	0.98	0.86	0.47	0.28	0.23
0.1	3.50	1.79	1.31	1.22	0.89	0.47	0.35	0.23
0.2	3.15	1.78	1.26	1.17	0.89	0.49	0.35	0.22
0.4	2.51	1.70	1.23	1.09	0.86	0.48	0.35	0.21
0.6	2.05	1.52	1.12	0.99	0.79	0.45	0.33	0.20
1.0	1.49	1.21	0.93	0.82	0.67	0.40	0.29	0.18
3.0	0.62	0.59	0.50	0.45	0.39	0.27	0.21	0.15
5.0	0.37	0.35	0.32	0.29	0.27	0.20	0.16	0.12

A.3.2 Asymptotic behavior

As a further check on our calculations, we have examined the asymptotic behavior of $\varepsilon(z)$ for the OPT at $R_\odot = 10$ kpc. At $z \gg R_\odot$, the Galaxy can be approximated as a point source. Therefore, it is convenient and reasonable to situate an OPT source of emissivity $4 \times 10^{10} L_\odot$ at the Galactic Centre and to neglect the dust absorption. In this way, an approximate expression for $\varepsilon(z)$ at $R_\odot = 10$ kpc is derived as

$$\varepsilon(z) = \frac{0.266}{1 + (z/10\text{kpc})^2} \, eV \cdot cm^{-3} \tag{A.10}$$

A comparison of the result from the above formula with that from our accurate calculation is shown in Figure A.8. The correct asymptotic behavior of our accurate result confirms the correctness of our calculations.

For the sake of completeness we can derive an approximate expression, accurate to within 5% beyond $z = 5$ kpc by normalizing the asymptotic expression at $z = 5$ kpc and ensuring that it gives the correct value for $z \gg 5$ kpc. The error will thus be essentially zero at $z = 5$ kpc and $z \gg 5$ kpc but rise to a few percent in between. Thus, we write, for any R,

$$\varepsilon(z) = \frac{0.266}{f(R) + (z/10\text{kpc})^2} \, eV \cdot cm^{-3} \tag{A.11}$$

where $f(R)$ is chosen to ensure that ε (5 kpc) is equal to the actually calculated value given in the Figures. As examples we find that $f(R = 0) = 0.304$

and $f(R = 5\,\text{kpc}) = 0.432$. At $R = 10$ kpc, $f(R = 10\,\text{kpc}) = 0.959$ and thus very close to 1.0 as expected from the arguments leading to Equation A.10.
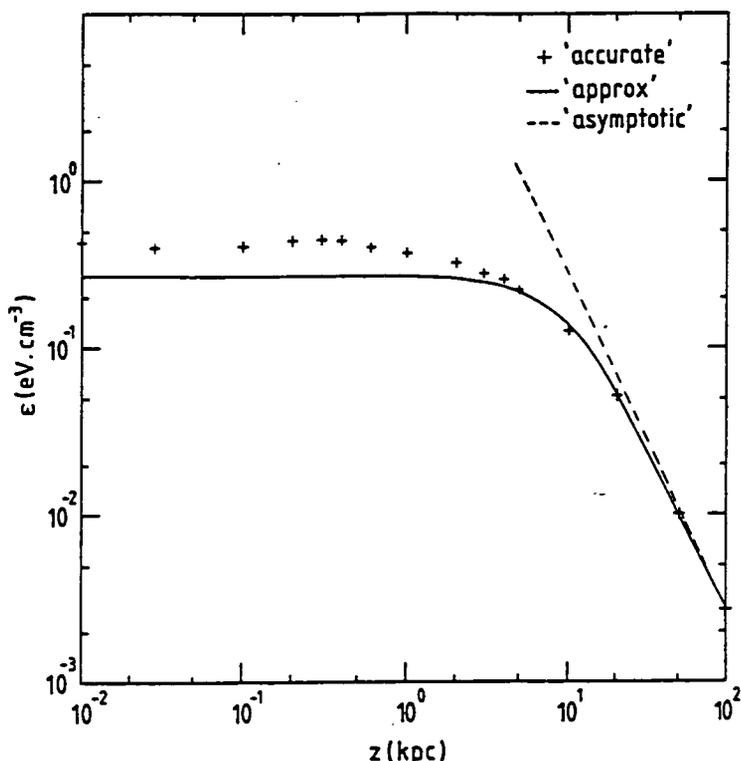

Figure A.8. The asymptotic behavior of the OPT energy density for $z \gg R_\odot$ with $R_\odot = 10$ kpc and $L_{\text{OPT}} = 4 \times 10^{10} L_\odot$.

A.3.3 The spectral shape of the radiation

Due to the substantial consumption of computing time, we did not calculate the spectral variation of the OPT at every position in the whole Galaxy, but only at $R = 10$ kpc and $z = 2$ kpc. Here the spectrum is approximated by the ratios 0.03: 0.27: 0.50: 0.20 for the energy densities in the four wavelength ranges: $0.13 \sim 0.25\mu\text{m}$, $0.25 \sim 0.7\mu\text{m}$, $0.7 \sim 1.8\mu\text{m}$, $1.8 \sim 8\mu\text{m}$. For the use of gamma ray astronomy, the position considered, is representative since the interesting regions are at $|b| \geq 10^0$ where the form of the OPT spectrum is expected to be rather stable.

A.4 Comparison with the results of other workers

A number of γ-ray astronomers have tackled the problem of determining the OPT and FIR energy density as a function of position in the Galaxy for the reason mentioned in Section A.1. Kniffen and Fichtel (1981) realised the difficulty of taking account of the dust absorption effect on UV and visible light and adopted an approximate approach by using a lower emissivity value (about half that observed) and neglecting dust absorption. In this way, the derived OPT energy density in the solar vicinity is a little higher than the observed value, but it is seriously underestimated in the Galactic halo. Their FIR result has the same problem of being too high in the Disk plane and too low in the halo. This problem arises due to the fact that whereas they adopted the same emissivity as that deduced by Boissé *et al.* (1981) their assumed scale height (125 pc) was considerably larger than that (65 pc) used by those workers.

Bloemen (1985) developed a fairly detailed model which, like ours, is based on the four stellar component model of Mathis *et al.* (1983) to calculate the OPT energy density. His result in the solar vicinity is in agreement with the observed value but is considerably less than ours in the Galactic Centre region and in the halo. The reason for this appears to be that he normalized the local energy density to the observed value by using a lower emissivity value (compared with that of Mathis *et al.* (1983)) and neglected the contribution from the Galactic Centre region ($R \leq 3$ kpc). In this way, the total radiation input is only $3 \times 10^{10} L_\odot$, compared with the 'correct' total of $5 \times 10^{10} L_\odot$. Moreover, there is, in our view, an inadequacy in his dust absorption: the absolute value of extinction is too low to achieve enough absorption and its variation in the z-direction is too fast for sufficient dust concentration in the Disk, so that the OPT energy density versus z falls continuously and does not show a dip in the Disk as does ours. There is a similar problem with the FIR: the total luminosity is probably underestimated, leading to a rapid fall in the z direction.

A.5 Discussion and Conclusions

A number of factors give rise to uncertainties in our result. An important one is the considerable clumpiness in the dust distribution in the Galaxy. This affects both the inferred stellar distribution and the derived energy densities. The effect largely cancels locally but not, of course, elsewhere. If we take the uncertainty of the stellar emissivity to be 20% and that of dust density to be also 20%, an approximate estimate leads to a random error of 30% in

our OPT result away from $R = R_\odot$ and $z = 0$ (and for $R \geq 13$ kpc where we have ignored the presence of dust—see Section A.2.1).

Turning to the differences among the various estimates, the questions are, essentially, (1) how fast is the OPT energy density decreasing with z and (2) where is the dominant FIR from ? Actually, these two questions are closely related. While all the previous analyses reach a reasonable value for the OPT energy density in the solar vicinity, they diverge in the energy density in the halo. From the analysis described in Section A.3, it is clear that the energy density in the Disk depends mainly on the local emissivity whereas the energy density in the halo depends mainly on the total luminosity and the correction for absorption. The 'proper' model should lead to not only the correct value in the solar vicinity, but also the correct value in the halo at large z, where its calculation becomes trivial (see Figure A.8). As for the differences in the FIR, they result from the fact that there were no accurate observations to rely on until the advent of the IRAS results, there was even no proper local emissivity value. All the pre-IRAS models of the FIR are thus more or less imperfect in some way.

As for the application to the diffuse Galactic γ-rays, the differences in the contribution due to inverse Compton interactions largely results from the differences of the OPT in the halo since cosmic ray electrons have been assumed by most workers to have a large scale height. Bloemen's model (Bloemen, 1985) considerably underestimated the inverse Compton contribution (only 5% of the the total γ-ray luminosity) because of the underestimated OPT (and also the adoption of a rather small electron scale height, in fact). Kniffen and Fichtel (1981) underestimated the inverse Compton contribution from the OPT again by underestimating the OPT in the halo, but overestimated the inverse Compton contribution from the FIR by using a large FIR energy density and a surprisingly flat electron spectrum. In our recent work (Chi et al., 1989), the OPT used is very close to the present result but the FIR used is only half of the present value. Since the γ-rays produced via inverse Compton collisions are mainly contributed by the OPT, we would not expect a significant change in our previous work; the conclusion reached there appears to be still valid.

References

Chapter 1

Alfvèn, H.: 1950, *Phys. Rev.* **77**, 1169.

Anderson, C.D.: 1932, *Phys. Rev.* **41**, 405.

Axford, W.I., Leer, E., and Skadron, G.: 1977, *Proc. 15th Int. Cosmic Ray Conf.*, Plovdiv, **11**, p.132.

Bell, A.R.: 1978a, *Mon. Not. Roy. astr. Soc.* **182**, 147.

Bell, A.R.: 1978b, *Mon. Not. Roy. astr. Soc.* **182**, 443.

Bhat, C.L., Mayer, C.J., Rogers, M., Wolfendale, A.W., and Zan, M.: 1986, *J. Phys. G: Nucl. Part. Phys.* **12**, 1087.

Blake, P.R., Hembrow, K.P., and Nash, W.F.: 1990, *21th Int. Cosmic Ray Conf., Adelaide* **9**, 106.

Blandford, R.D., and Ostriker, J.P.: 1978, *Astrophys. J.* **221**, L29.

Blandford, R.D., and Ostriker, J.P.: 1980, *Astrophys. J.* **237**, 793.

Bloemen, J.B.G.M.: 1987, *Astrophys. J.* **317**, L15.

Bothe, W., and Kolhörster, W.: 1928, *Naturmiss.* **16**, 1044.

Bradt, H.L., and Peters, B.: 1948, *Phys. Rev.* **74**, 1828.

Brecher, K., and Burbidge, G.R.: 1972, *Astrophys. J.* **174**, 253.

Burbidge, G.R.: 1956, *Phys. Rev.* **101**, 906.

Chevalier, R.A., and Fransson, C.: 1984, *Astrophys. J.* **279**, L43.

Chi, X., Issa, M.R, Richardson, K.M., Szabelski, J., Wdowczyk, J., and Wolfendale, A.W.: 1989, *J. Phys. G: Nucl. Part. Phys.* **15**, 1495.

Clay, J.: 1927, *Proc. Acad. Amsterdam* **30**, 1115.

De Shong, J.A., Hildbrand, R.H., and Meyer, P.: 1964, *Phys. Rev. Lett.* **12**, 3.

Dodds, D., Strong, A.W., and Wolfendale, A.W.: 1975, *Mon. Not. Roy. astr. Soc.* **171**, 569.

Earl, J.A.: 1961, *Phys. Rev. Lett.* **6**, 125.

Fermi, E.: 1949, *Phys. Rev.* **75**, 1169.

Fichtel, C.E., Simpson, G.A., and Thompson, D.J.: 1978, *Astrophys. J.* **222**, 833.

Fichtel, C.E., and Linsley, J.: 1986, *Astrophys. J.* **300**, 474.

Freier, P. et al.: 1948a, *Phys. Rev.* **74**, 213.

Freier, P. et al.: 1948b, *Phys. Rev.* **74**, 1818.

Fujimoto, Y., Hasegawa, H., and Taketani, M.: 1964, *Prog. Theor. Phys. Suppl.*, **30**, 32.

Garcia-Munoz, M., Mason, G.M., and Simpson, J.A.: 1977, *Astrophys. J.* **217**, 859.

Garcia-Munoz, M., Simpson, J.A., Guzik, T.G., Wefel, J.P., and Margolis, S.H.: 1987, *Astrophys. J. Suppl.* **64**, 269.

Gawin, J., Kempa, J., Wdowczyk, J.: 1984, *Acta Univ. Lodziensis Folia Physica* **7**, 57.

Giler, M., Osborne, J.L, Ptuskin, V.S., Szabelska, B., Wdowczyk, J., and Wolfendale, A.W.: 1989, *Astron. Astrophys.* **217**, 311.

Ginzburg, V.L.: 1951, *Dokkl. Akad. Nauk. USSR* **76**, 377.

Ginzburg, V.L.: 1953, *Sov. Phys. Uspekhi* **51**, 343.

Ginzburg, V.L., and Syrovatskii, S.I.: 1964, *The origin of cosmic rays*, Pergamon, Oxford.

Hartquist, T.W., and Morfill, G.E.: 1986, *Astrophys. J.* **311**, 518.

Haslam, C.G.T., Klein, U., Salter, C.J., Stoffel, H., Wilson, W.E., Cleary, M.N., Cooke, D.J., ,and Thomasson, P.: 1981a, *Astron. Astrophys.* **100**, 209.

Haslam, C.G.T., Klein, U., Salter, C.J., Stoffel, H., and Wilson, W.E.: 1981b, *Astron. Astrophys. Suppl.* **47**, 1.

Hess, V.F.: 1912, *Phys. Zeits.* **13**, 1084.

Hillas, A.M.: 1968, *Can. J. Phys.* **46**, 623.

Hoyle, F.: 1947, *Mon. Not. Roy. astr. Soc.* **106**, 384.

Ipavich, F.M.: 1975, *Astrophys. J.* **196**, 107.

Johnson, T.H.: 1933, *Phys. Rev.* **43**, 307.

Jokipii, J.R., and Parker, E.N.: 1969, *Astrophys. J.* **155**, 799.

Jokipii, J.R.: 1976, *Astrophys. J.* **208**, 900.

Kiepenheuer, K.O.: 1950, *Phys. Rev.* **79**, 738.

Klein, O.: 1944, *Arkiv Mat. Astron. Fys.* **31A**, No. 14.

Lattes, C.M.G., Occhialini, G.P.S., and Powell, C.F.: 1947, *Nature* **160**, 486.

Lee, L.C., and Jokipii, J.R.: 1976, *Astrophys. J.* **206**, 735.

Lerche, I., and Schlickeiser, R.: 1982, *Astron. Astrophys.* **107**, 148.

Letaw, J.R., Silberberg, R., Tsao, C.H., Eichler, D., Shapiro, M.M., Wandel, A.: 1987, *Proc. 20th Int. Cosmic Ray Conf.*, Moscow, 2, p.222.

Meyer, P., and Vogt, R.: 1961, *Phys. Rev. Lett.* **6**, 193.

Millikan, R.A., Neher, V.H., and Pickering, W.H.: 1942, *Phys. Rev.* **61**, 397.

Müller, D., and Tang, K.K.: 1987, *Astrophys. J.* **312**, 183.

Neddermeyer, S.H., and Anderson, C.D.: 1937, *Phys. Rev.* **51**, 884.

Parker, E.N.: 1973, *Astrophys. Space Sci.* **24**, 279.

Phillipps, S., Kearsey, S., Osborne, J.L., Haslam, C.G.T., and Stoffel, H.: 1981, *Astron. Astrophys.* **103**, 405.

Piddington, J.: 1972, *Cosmic Electrodynamics*, Vol.3, 129.

Rasmussen, I.L., and Peters, B.: 1975, *Nature* **258**, 412.

Richtymer, R.D., and Teller, E.: 1949, *Phys. Rev.* **75**, 1929.

Rochester, G.D., and Butler, C.C.: 1947, *Nature* **160**, 855.

Rossi, B.: 1934, *Ric. Sci.* **5**, 569.

Skilling, J.: 1971, *Astrophys. J.* **170**, 265.

Skobeltzyn, D.V.: 1927, *Z. Physik* **43**, 354.

Street, J.C., and Stevenson, E.C.: 1937, *Phys. Rev.* **52**, 1003.

Wandel, A., Eichler, D., Letaw, J.R., Silberberg, R., and Tsao, C.H.: 1987, *Astrophys. J.* **316**, 676.

Webber, W.R.: 1983, in *Composition and Origin of Cosmic Rays*, ed. M.M. Shapiro, Reidel, Dordrecht, p.83.

Wenztel, D.G.: 1974, *Ann. Rev. Astron. Astrophys.* **12**, 71.

Wdowczyk, J., and Wolfendale, A.W.: 1989, *Ann. Rev. Nucl. Sci.* **39**, 43.

Chapter 2

Asarov, A.I., Dogiel, V.A., Guseinov, O.H., and Kasumov, F.K.: 1990, *Astron. Astrophys.* **229**, 196.

Banday, A.J., Giler, M., Szabelska, B., Szabelski, J., and Wolfendale, A.W.: 1990, preprint, University of Durham.

Bell, A.R.: 1978, *Mon. Not. Roy. astr. Soc.* **183**, 443.

Beuermann, K., Kanbach, G., and Berkhuijsen, E.M.: 1985, *Astron. Astrophys.* **153**, 17.

Bhat, C.L., Issa, M., Houston, B.P., Mayer, C.J., and Wolfendale, A.W.: 1985, *Nature* **314**, 511.

Bhat, C.L., Issa, M.R., Mayer, C.J., Wolfendale, A.W., and Zan, M.: 1986a, *J. Phys. G: Nucl. Phys.* **12**, 1067.

Bhat, C.L., Mayer, C.J., Rogers, M., Wolfendale, A.W., and Zan, M.: 1986b, *J. Phys. G: Nucl. Phys.* **12**, 1087.

Bloemen, J.B.G.M., Bennett, K., Bignami, G.F., Blitz, L., Caraveo, P.A., Gottwall, M., Hermsen, W., Lebrun, F., Mayer-Hasselwander, H.A., and Strong, A.W.: 1984, *Astron. Astrophys.* **135**, 12.

Bloemen, J.B.G.M.: 1985, *Ph. D. Thesis*, University of Leiden.

Bloemen, J.B.G.M., 1987, *Astrophys. J.* **317**, L15.

Bloemen, J.B.G.M., Reich, P., Reich, W., and Schlickeiser, R.: 1988, *Astron. Astrophys.* **204**, 88.

Bloemen, J.B.G.M.: 1989, *Ann. Atron. Astrophys. Rev.* **27**, 469.

Blumenthal, G.R., and Gould, R.J.: 1970, *Rev. Mod. Phys.* **42**, 237.

Breitschwerdt, D., Völk, H.J., and McKenzie, J.F.: 1987, *Proc. 20th Int. Cosmic Ray Conf.*, Moscow, **2**, 115.

Broadbent, A.: 1989, *Ph. D. Thesis*, University of Durham.

Brown, J.C.: 1971, *Solar Phys.* **18**, 489.

Cavallo, G.: 1982, *Astron. Astrophys.* **111**, 368.

Chi, X., Issa, M.R, Richardson, K.M., Szabelski, J., Wdowczyk, J., and Wolfendale, A.W.: 1989, *J. Phys. G: Nucl. Part. Phys.* **15**, 1495.

Dodds, D., Strong, A.W., and Wolfendale, A.W.: 1975, *Mon. Not. Roy. astr. Soc.* **171**, 569.

Dröge, W., Lerche, I., and Schlickeiser, R.: 1987, *Astron. Astrophys.* **178**, 252.

Drury, L. O'C.: 1987, *Proc. 20th Int. Cosmic Ray Conf.*, Moscow, **2**, 161.

Ellison, D.C., Jones, F.C., and Ramaty, R.: 1990, *Proc. 21st Int. C osmic Ray Conf.*, Adelaide, **4**, 68.

Evenson, P., Krawczyk, L., Moses, D., and Meyer, P.: 1981, *Proc. 17th Int. Cosmic Ray Conf.*, Paris, **10**, 77.

Fanselow, J.L., Hartman, R.C., Hildebrand, R., H., and Meyer, P.: 1969, *Astrophys. J.* **158**, 771.

Giler, M., Kearsey, S., Osborne, J.L., and Freeman, I.: 1979, *16th Int. Cosmic Ray Conf., Kyoto*, **2**, 131.

Ginzburg, V.L., and Syrovatskii, S.I.: 1964, *The Origin of Cosmic Rays*, Oxfoed: Prergamon Press.

Gould, R.J.: 1969, *Phys. Rev.* **185**, 72.

Haslam, C.G.T., Klein, U., Salter, C.J., Stoffel, H., Wilson, W.E., Cleary, M.N., Cooke, D.J., ,and Thomasson, P.: 1981a, *Astron. Astrophys.* **100**, 209.

Haslam, C.G.T., Klein, U., Salter, C.J., Stoffel, H., and Wilson, W.E.: 1981b, *Astron. Astrophys. Suppl.* **47**, 1.

Haslam, C.G.T., and Osborne, J.L.: 1987, *Nature* **327**, 211.

Hayakawa, S.: 1979, *16th Int. Cosmic Ray Conf., Kyoto*, **2**, 177.

Heitler, W.: 1960, *The Quantum Theory of Radiation*, Oxford Press, London.

Ipavich, F.M.: 1975, *Astrophys. J.* **196**, 107.

Jauch, J.M., and Rohrlich, F.: 1955, *The Theory of Photons and Electrons*, Addison-Wesley Publ. Co., Inc., Reading, Mass.

Jokipii, J.R.: 1976, *Astrophys. J.* **208**, 900.

Jones, F.C.: 1968, *Phys. Rev.* **167**, 1159.

Kniffen, D.A., and Fichtel, C.E.: 1981, *Astrophys. J.* **250**, 389.

Koch, H.W., and Motz, J.W.: 1959, *Rev. Mod. Phys.* **31**, 921.

Lawson, K.D., Mayer, C.J., Osborne, J.L., and Parkinson, M.L.: 1987, *Mon. Not. Roy. astr. Soc.* **225**, 307.

Lerche, I., and Schlickeiser, R.: 1982, *Astron. Astrophys.* **107**, 148.

McKenzie, J.F., and Völk, H.J.: 1982, *Astron. Astrophys.* **116**, 191.

Müller, D., and Tang, K.: 1987, *Astrophys. J.* **312**, 183.

Nishimura, J., et al.: 1981, *Proc. 17th Int. Cosmic Ray Conf.*, Paris, **2**, 94.

Owens, A.J., and Jokipii, J.R.: 1977, *Astrophys. J.* **215**, 685.

Phillipps, S., Kearsey, S., Osborne, J.L., Haslam, C.G.T., Stoffel, H.: 1981a, *Astron. Astrophys.* **86**, 286.

Phillipps, S., Kearsey, S., Osborne, J.L., Haslam, C.G.T., Stoffel, H.: 1981b, *Astron. Astrophys.* **103**, 405.

Prince, T.A.: 1979, *Astrophys. J.* **254**, 391.

Reich, P., and Reich, W.: 1988, *Astron. Astrophys.* **196**, 211.

Riley, P.A., and Wolfendale, A.W.: 1984, *J. Phys. G:Nucl. Phys.* **10**, 1149.

Rogers, M.J., Sadzinska, M., Szabelski, J., van der Walt, D.J., and Wolfendale, A.W.: 1988, *J. Phys. G: Nucl. Phys.* **14**, 1147.

Sacher, W., and Schönfelder, V.: 1984, *Astrophys. J.* **279**, 817.

Strong, A.W., Bloemen, J.B.G.M., Dame, T.M., Grenier, I., Hermsen, W., Lebrun, F., Nyman, L. -Å., Pollock, A.M.T., and Thaddeus, P.: 1988, *Astron. Astrophys.* **207**, 1.

Tang, K.: 1984, *Astrophys. J.* **278**, 881.

van der Walt, D.J., and Wolfendale, A.W.: 1988, *Space Sci. Rev.* **47**, 1.

van der Walt, D.J.: 1990, *Proc. 21st Cosmic Ray Conf.*, Adelaide, **3**, 233.

Völk, H.J., Zank, L.A., and Zank, G.P.: 1988, *Astron. Astrophys.* **198**, 274.

Wolfendale, A.W.: 1986, in *Cosmic Radiation in Contemporary Astrophysics*, ed. M.M. Shapiro, Reidel, Dordrecht, p.83.

Chapter 3

Bahcall, J.N., Schmidt, M., and Soneira, R.M.: 1983, *Astrophys. J.* **265**, 730.

Cesarsky, C., Paul, J.A., and Shukla, P.G.: 1978, *Astrophys. Space Sci.* **59**, 73.

Cox, D.P.: 1989, in *IAU Colloquium 120, Structure and Dynamics of the Interstellar Medium*, ed. G. Tenorio-Tagle, M. Moles, and J. Melnick, Springer, New York.

Cummings, A.C., Stone, E.C., and Vogt, R.E.: 1973, *Proc. 13th Int. Cosmic Ray Conf.*, Denver, **1**, p.335.

Eraker, J.H., and Simpson, J.A.: 1981, *Proc. 17th Int. Cosmic Ray Conf.*, Paris, **3**, p.279.

Evenson, P., Krawczyk, L., Moses, D., and Meyer, P.: 1981, *Proc. 17th Int. Cosmic Ray Conf.*, Paris, **10**, p.80.

Fichtel, C.E., Simpson, G.A., and Thompson, D.J.: 1978, *Astrophys. J.* **222**, 833.

Giler, M., Kearsey, S., Osborne, J.L., Freeman, I.: 1979, *16th Int. Cosmic Ray Conf., Kyoto*, **2**, 131.

Ginzburg, V.L.: 1970, *The Propagation of Electromagnetic Waves in Plasmas*, 2nd. ed., Pergamon, New York.

Ip, W-H., and Axford, W.I.: 1985, *Astron. Astrophys.* **149**, 7.

Kundu, M., Gopalswamy, N., White, S., Cargill, P., Schmahl, E.J., and Hildner, E.: 1989, *Astrophys. J.* **347**, 505.

Israel, F.P., and Mahoney, M.J.: 1990, *Astrophys. J.* **352**, 30.

Lampe, M., and Papadopoulos, K.: 1977, *Astrophys. J.* **212**, 886.

Lavigne, J.M., Mandrou, P., Niel, M., Agrinier, B., Bonfand, E., and Parlier, B.: 1986,, *Astrophys. J.* **308**, 370.

Lockman, F.: 1984, *Astrophys. J.* **283**, 90.

Lyne, A.G.: 1990, private communication.

Manchester, R.N. and Taylor, J.H.: 1981, *Astron. J.* **86**, 1953.

Marshall, F.E., Boldt, E.A., Holt, S.S., Miller, R.B., Mushotzky, R.F., Rose, L.A., Rothschild, R.E., and Serlmitsos, P.J.: 1980, *Astrophys. J.* **235**, 4.

Mathis, J.S., Mezger, P.G., and Panagia, N.: 1983, *Astron. Astrophys.* **128**, 212.

McBride, J.B., Ott, E., Boris, J.P., and Orens, J.H.: 1972, *Phys. Fluids* **15**, 2367.

Pandey, A.K., Bhatt, B.C., and Mahra, H.S.: 1990, *Astron. Astrophys.* **234**, 128.

Paul, J.A., Bennett, K., Bignami, G.F., Buccheri, R., Caraveo, P., Hermsen, W., Kanbach, G., Mayer-Hasselwander, H.A., Scarsi, L., Swanenburg, B.N., and Wills, R.D.: 1978, *Astron. Astrophys.* **63**, L31.

Peterson, L.E., Gruber, D.E., Jung, G.V., and Matteson, J.L.: 1990, *Proc. 21st Int. Cosmic Ray Conf.*, Adelaide, 2, p.44.

Pikel'ner, S.B., and Tsytovich, V.N.: 1969, *Soviet Astr.* **13**, 5.

Protheroe, R.J., and Wolfendale, A.W.: 1980, *Astron. Astrophys.* **92**, 175.

Reynolds, R.J.: 1983, *Astrophys. J.* **268**, 698.

Reynolds, R.J.: 1984, *Astrophys. J.* **282**, 191.

Reynolds, R.J.: 1985, in *Gaseous Halos of Galaxies*, ed. J.N. Bregman and F.J. Lockman, Green Bank, NRAO, p.53.

Reynolds, R.J.: 1989, *Astrophys. J.* **339**, L29.

Reynolds, R.J.: 1990a, *Astrophys. J.* **348**, 153.

Reynolds, R.J.: 1990b, *Astrophys. J.* **349**, L17.

Rothschild, R.E., Mushotzky, R.F., Baity, W.A., Gruber, D.E., Matteson, J.L., and Peterson, L.E.: 1983, *Astrophys. J.* **269**, 423.

Sacher, W., and Schönfelder, V.: 1984, *Astrophys. J.* **279**, 817.

Schönfelder, V., von Ballmoos, P., and Diehl, R.: 1988, *Astrophys. J.* **335**, 748.

Sciama, D.W.: 1990, *Nature* **346**, 40.

Silk, J., and Werner, M.W.: 1969, *Astrophys. J.* **158**, 185.

Spitzer, L., Jr.: 1978, *Physical Processes in the Interstellar Medium*, John Wiley & Sons, New York.

Spitzer, L., Jr., and Tomasko, M.G.: 1968, *Astrophys. J.* **152**, 971.

Spitzer, L., Jr., and Jenkins, E.B.: 1975, *Ann. Rev. Astron. Astrophys.* **13**, 133.

Strong, A.W., Wolfendale, A.W., and Worrall, D.M.: 1976, *Mon. Not. Roy. astr. Soc.* **175**, 23.

Strong, A.W., and Wolfendale, A.W.: 1978, *J. Phys. G.* **7**, 1123.

Sunyaev, R.A.: 1969, *Astr. Zh.* **46**, 929.

Vaisberg, O.L., Galeev, A.A., and Zastenker, G.N.: 1983, *Soviet Phys.—JETP Lett.* **85**, 1232.

Vlahos, L., Gergely, T., and Papadopoulos, K.: 1982, *Astrophys. J.* **258**, 812.

Webber, W.R., Simpson, G.A., and Cane, H.V.: 1980, *Astrophys. J.* **236**, 448.

Werner, M.W., Silk, J., and Rees, M.J.: 1970, *Astrophys. J.* **161**, 965.

Wu, C.S., et al.: 1984, *Space Sci. Rev.* **36**, 63.

Chapter 4

Bhat, C.L., Mayer, C.J., Rogers. M.J., Wolfendale, A.W.,.and Zan, M.A.: 1986, *J. Phys. G:Nucl. Phys.* **12**, 1087.

Bignami, G.F., Lichti, G.G., and Paul, J.A.: 1978, *Astron. Astrophys.* **68**, L15.

Bignami, G.F., Fichtel, C.E., Hartmann, R.C., and Thompson, D.J.: 1979, *Astrophys. J.* **232**, 649.

Bloemen, J.B.G.M.: 1985, *Ph.D. Thesis*, University of Leiden.

Bloemen, J.B.G.M., Reich, P., Reich, W., and Schlickeiser, R.: 1988, *Astron. Astrophys.* **204**, 88.

Bloemen, J.B.G.M.: 1989, *Ann. Rev. Astron. Astrophys.* **27**, 469.

Cappellaro, E., and Turatto, M.: 1988, *Astron. Astrophys.* **190**, 10.

Cesarsky, C.J.: 1980, *Ann. Rev. Astron. Astrophys.* **18**, 289.

Chevalier, R.A., and Fransson, C.: 1984, *Astrophys. J.* **279**, L43.

Dame, T.M., Ungerechts, H., Cohen, R.S., de Guess, E.J., Grenier, A., May, J., Murphy, D.C., Nyman, L.A., and Thaddeus, P.: 1987, *Astrophys. J.* **322**, 706.

Dermer, C.D.: 1986, *Astron. Astrophys.* **157**, 223.

Fichtel, C.E., Hartmann, R.C., Kniffen, D.A., Thompson, D.J., Ögelmann, H.B., Özel, M.E., Tümer, T.: 1977, *Astrophys. J.* **217**, L9.

Fichtel, C.E., Simpson, G.A., and Thompson, D.J.: 1978, *Astrophys. J.* **222**, 833.

Gao, Y-T, Cline, D.B., and Stecker, F.W.: 1990, *Astrophys. J.* **357**, L1.

Garcia-Munoz, M., Mason, G.M., and Simpson, J.A.: 1977a, *Astrophys. J.* **217**, 859.

Garcia-Munoz, M., Mason, G.M., and Simpson, J.A.: 1977b, *Proc. 15th Int. Cosmic Ray Conf.*, Plovid, **1**, p.224.

Giler, M., Wdowczyk, J., and Wolfendale, A.W.: 1978, *J. Phys. G:Nucl. Phys.* **4**, L269.

Grindlay, J.E.: 1978, *Nature* **273**, 211.

Hartquist, T.W., and Morfill, G.E.: 1985, *Astrophys. J.* **311**, 518.

Heiles, C., and Habing, H.J.: 1974, *Astron. Astrophys. Suppl.* **14**, 1.

Heiles, C., and Cleary, M.N.: 1979, *Aust. J. Phys. Astrophys. Suppl.* **14**, 1.

Kniffen, D.A., and Fichtel, C.E.: 1981, *Astrophys. J.* **250**, 389.

Ko, C.M., Dougherty, M.K., and McKenzie, J.F.: 1990, *Astron. Astrophys.*, in press.

Lawson, K.D., Mayer, C.J., Osborne, J.L., and Parkinson, M.L.: 1987, *Mon. Not. R. astro. Soc.* **225**, 307.

Lerche,I., and Schlickeiser, R.: 1980, *Astrophys. J.* **239**, 1089.

Müller, D., and Tang, K.K.: 1987, *Astrophys. J.* **312**, 183.

Phillips, S., Kearsey, S., Osborne, J.L., Haslam, C.G.T., Stoffel, H.: 1981, *Astron. Astrophys.* **103** 405

Reich, P., and Reich, W.: 1986, *Astron. Astrophys. Suppl.* **63**, 205.

Riley, P.A., and Wolfendale, A.W.: 1984, *J. Phys. G:Nucl. Phys.* **10**, 1149.

Rudaz, S., and Stecker, F.W.: 1988, *Astrophys. J.* **325**, 16.

Savage, B.D., and de Boer, K.S.: 1979, *Astrophys. J.* **230**, L77.

Schönfelder, V.: 1978, *Nature* **273**, 344.

Shapiro, M.M., and Silberberg, R.: 1971, *Proc. 12th Int. Cosmic Ray Conf.*, Hobart, 1, p.64.

Simpson, J.A.: 1983, in *Composition and Origin of Cosmic Rays*, ed. M.M. Shapiro, Reidel, Dordrecht, p.1.

Spitzer, L.: 1956, *Astrophys. J.* **124**, 20.

Stecker, F.W.: 1971, *Cosmic Gamma Rays*, Mono Book Corp., Baltimore.

Stecker, F.W.: 1975, in *Origin of Cosmic Rays*, ed. J.L. Osborne and A.W. Wolfendale, Reidel, Dordrecht, p.267.

Strong, A.W., Wolfendale, A.W., and Worrall, D.M.: 1976, *Mon. Not. R. astro. Soc.* **175**, 23.

Strong, A.W., Riley, P.A., Osborne, J.L., and Murray, J.D.: 1982, *Mon. Not. R. astr. Soc.* **201**, 495.

Strong, A.W.: 1985, *Astron. Astrophys.* **145**, 81.

Strong, A.W., Bloemen, J.B.G.M., Lebrun, F., Hermsen, W., Mayer-Hasselwander, H.A., and Buccheri, R.: 1987, *Astron. Astrophys. Suppl.* **67**, 283.

Strong, A.W., Bloemen, J.B.G.M., Dame, T.M., Grenier, I.A., Hermsen, W., Lebrun, F., Nyman, L. -Å., Pollock, A.M.T., and Thaddeus, P.: 1988, *Astron. Astrophys.* **207**, 1.

Thompson, D.J., and Fichtel, C.E.: 1982, *Astron. Astrophys.* **109**, 352.

Völk, H.J.: 1990, in *IAU Sym. 144: Interstellar Disk-Halo Connections in galaxies*, ed. H. Bloemen, Kluwer Academic Publishers, Dordrecht.

Wdowczyk, J., and Wolfendale, A.W.: 1989, *Astrophys. J.* **349**, 35.

Weaver, H., and Williams, D.R.W.: 1973, *Astron. Astrophys. Suppl.* **8**, 1.

Webber, W.R.: 1983, in *Composition and Origin of Cosmic Rays*, ed. M.M. Shapiro, Reidel, Dordrecht, p.83.

Webber, W.R., Golden, R.L., and Stephens, S.A.: 1987, *Proc. 20th Int. Cosmic Ray Conf.*, Moscow, 1, 325.

Chapter 5

Allen, R.J., Baldwin, J.E., and Sancisi, R.: 1978, *Astron. Astrophys.* **62**, 397.

Ashton, F.: 1987, *Proc. 20th Int. Cosmic Ray Conf.*, Moscow, 2, p.100.

Bally, J., and Thronson Jr., H. A.: 1989, *Astron. J.* **97**, 69.

Beck, R., Klein, U., and Krause, M.: 1985, *Astron. Astrophys.* **152**, 237.

Beck, R., and Golla, G.: 1988, *Astron. Astrophys.* **191**, L9.

Beck, R., et al.: 1990, in *The Interstellar Disk-Halo Connection in Galaxies, IAU Sym. 144*, Leiden, ed. H. Bloemen, Kluwer Academic Publishers, Dordrecht.

Berkhuijsen, E.M., and Klein, U.: 1985, in *The Milky Way Galaxy*, eds. H van Woerden, R.J. Allen and W.B. Burton, p431.

Bhat, C. L., Mayer, C. J., and Wolfendale, A. W.: 1984, *Astron. Astrophys.* **140**, 284.

Bicay, M. D., Helou, G., and Condon, J. J.: 1989, *Astrophys. J.* **338**, L53.

Broadbent, A., Haslam, C. G. T., and Osborne, J. L.: 1989, *Mon. Not. R. astr. Soc.* **237**, 381.

Condon, J. J.: 1987, *Astrophys. J. Suppl.* **65**, 485.

Condon, J. J., and Broderick, J. J.: 1988, *Astron. J.* **96**, 30.

Cox, M. J., Eales, S. A., Alexander, P., and Fitt, A. J.: 1988, *Mon. Not. R. astr. Soc.* **235**, 1227.

Cox, P., and Mezger, P. G.: 1989, *Astron. Astrophys. Rev.* **1**, 49.

de Jong, T., Klein, U., Wielebinski, R., and Wunderlich, E.: 1985, *Astron. Astrophys.* **147**, L6.

Devereux, N. A., and Eales, S. A.: 1989, *Astrophys. J.* **340**, 708.

Dickey, J. M., and Salpeter, E. E.: 1984, *Astrophys. J.* **284**, 461.

Dogiel, V. A., and Uryson, V.: 1988, *Astron. Astrophys.* **197**, 335.

Ekers, R.D., and Sancisi, R.: 1977, *Astron. Astrophys.* **54**, 196.

Fitt, A. J., Alexander, P., and Cox, M. J.: 1988, *Mon. Not. R. astr. Soc.* **233**, 907.

Garcia-Munoz, M., Mason, G. M., and Simpson, J. A.: 1977, *Astrophys. J.* **217**, 859.

Gavazzi, G., Cocito, A., and Vettolani, G.: 1986, *Astrophys. J.* **305**, L15.

Ginzburg, V. L., and Syrovatskii, S. I.: 1964, *Origin of Cosmic Rays*, Pergamon Press, Oxford.

Gioia, I. M., Gregorini, L., and Klein, U.: 1982, *Astr. Astrophys.* **116**, 164.

Harnett, J. I., and Reynolds, J. E.: 1985, *Mon. Not. R. astr. Soc.* **215**, 247.

Helou, G., Soifer, B. T., and Rowan-Robinson, M.: 1985, *Astrophys. J.* **298**, L7.

Hummel, E., Sancisi, R., and Ekers, R. D.: 1984, *Astron. Astrophys.* **133**, 1.

Hummel, E., Pedlar., A., van der Hulst, J. M., and Davies, R. D.: 1985, *Astron. Astrophys. Suppl.* **60**, 293.

Hummel, E., Lesch, H., Wielebinski, R., and Schlickeiser, R.: 1988a, *Astron. Astrophys.* **197**, L31.

Hummel, E., Davies, R. D., Wolstencroft, R. D., van der Hulst, J. M., and Pedlar, A.: 1988b, *Astron. Astrophys.* **199**, 91.

Hummel, E.: 1989, in *Windows on Galaxies*, Erice, eds. G. Fabbiano et al.

Hummel, E., and van der Hulst, J.M.: 1989, *Astron. Astrophys. Suppl.* **81**, 51.

Hummel, E., et al.: 1990, in *The Interstellar Disk-Halo Connection in Galaxies, IAU Sym. 144*, Leiden, ed. H. Bloemen, Kluwer Academic Publishers, Dordrecht.

Klein, U., Beck, R., and Wielebinski, R.: 1984, *Astron. Astrophys.* **133**, 19.

Parker, E. N.: 1966, *Astrophys. J.* **145**, 811.

Parker, E. N: 1969, *Space Sci. Rev.* **9**, 651.

Rice, W., Lonsdale, C. J., Soifer, B. T., Neugebauer, G., Kopan, E. L., Lloyd, L. A., de Jong, T., and Habing, H. J.: 1988, *Astrophys. J. Suppl.* **68**, 91.

Seab, C. G.: 1987, in *Interstellar Processes*, p.491, eds. Hollenbach, D. J. and Thronson Jr., H. A., Reidel, Dordrecht.

Sofue, Y., Fujimoto, M., and Wielebinski, R.: 1986, *Ann. Rev. Astr. Astrophys.* **24**, 459.

Unger, S. W., Wolstencroft, R. D., Pedlar, A., Savage, A., Clowes, R. G., Leggett, S. K., and Parker, Q. A.: 1989, *Mon. Not. astr. Soc.* **236**, 425.

van der Kruit, P. C., and Searle, L.: 1981, *Astron. Astrophys.* **95**, 105.

Völk, H. J., Zank, L. A., and Zank, G. P.: 1988, *Astron. Astrophys.* **198**, 274.

Völk, H. J.: 1989, *Astron. Astrophys.* **218**, 67.

Wentzel, D. G.: 1974, *Ann. Rev. Astron. Astrophys.* **12**, 71.

Wunderlich, E., and Klein, U.: 1988, *Astron. Astrophys.* **206**, 47.

Young, J. S., Xie, S., Kenney, J. D. P., and Rice, W.: 1989, *Astrophys. J. Suppl.* **70**, 699.

Chapter 6

Berkhuijsen, E.M.: 1971, *Astron. Astrophys.* **14**, 359.

Beuermann, K., Kanbach, G., and Berkhuijsen, E.M.: 1985, *Astron. Astrophys.* **153**, 17.

Broadbent, A.: 1989, *Ph. D. Thesis*, University of Durham.

Ellis, R.S., and Axon, D.J.: 1978, *Astrophys. Space Sci.* **54**, 425.

Gardner, F.F., Morris, D., and Whiteoak, J.B.: 1969, *Australian J. Phys.* **22**, 813.

Ginzburg, V.L., and Syrovatskii, S.I.: 1969, *Ann. Rev. Astron. Astrophys.* **7**, 375.

Ginzburg, V.L.: 1970, *The Propagation of Electromagnetic Waves in Plasmas*, 2nd. ed., Pergamon, New York.

Hall, J.S.: 1949, *Science* **109**, 166.

Hamilton, P.A., and Lyne, A.G.: 1987, *Mon. Not. R. astr. Soc.* **224**, 1073.

Heiles, C.: 1976, *Ann. Rev. Astron. Astrophys.* **14**, 1.

Heiles, C.: 1987, in *Interstellar Processes*, p.171, eds. D.J. Hollenbach and H.A. Thronson Jr., Reidel, Dordrecht.

Hiltner, W.A.: 1949, *Astrophys. J.* **109**, 471.

Inoue, M., and Tabara, H.: 1981, *Publ. Astron. Soc. Japan* **33**, 813.

Jones, R.V. and Spitzer, L.: 1967, *Astrophys. J.* **147**, 943.

Kiraly, P., Kóta, J., Osborne, J.L., Stapley, N.R., and Wolfendale, A.W.: 1979, *Lett. Nuovo Cimento* **24**, 249.

Krause, F.: 1987, in *Interstellar Magnetic Fields*, eds. R. Beck, R. Gräve, Springer, Heidelberg, p.8.

Krause, M., Beck, R., and Hummel, E.: 1989, *Astron. Astrophys.* **217**, 17.

Lesch, H., Sawa, T., Krause, M., Beck, R., Fujimoto, and Biermann, P.L.: 1988, *Astron. Astrophys.* **192**, 19.

Manchester, R.N.: 1974, *Astrophys. J.* **188**, 637.

Mathewson, D.S., and Milne, D.K.: 1965, *Austr. J. Phys.* **18**, 635.

Phillipps, S., Kearsey, S., Osborne, J.L., Haslam, C.G.T., and Stoffel, H.: 1981, *Astron. Astrophys.* **103**, 405.

Parker, E.N.: 1971, *Astrophys. J.* **163**, 255.

Rand, R.J., and Kulkarni, S.R.: 1989, *Astrophys. J.* **343**, 760.

Ruzmaikin, A.A.: 1987, in *Interstellar Magnetic Fields*, eds. R. Beck, R. Gräve, Springer, Heidelberg, p.16.

Simard-Normandin, M., and Kronberg, P.P.: 1980, *Astrophys. J.* **242**, 74.

Spoelstra, T.A.T.: 1984, *Astron. Astrophys.* **135**, 238.

Sukumar, S., and Allen, R.J.: 1989, *Nature* **340**, 537.

Thielheim, K.O., and Langhoff, W.: 1968, *J. Phys. A.* **1**, 694.

Thomson, C.R., and Nelson, A.H.: 1980, *Mon. Not. R. astr. Soc.* **191**, 863.

Troland, T.H., and Heiles, C.: 1986, *Astrophys. J.* **301**, 339.

Wdowczyk, J., and Wolfendale, A.W.: 1989, *Ann. Rev. Nucl. Part. Sci.* **39**, 43.

Whiteoak, J.B.: 1974, *IAU Symp. No. 60*, p.137.

Appendix A

Bhat, C.L., Mayer, C.J., and Wolfendale, A.W.: 1986, *Phil. Trans. Roy. Soc. London* **319**, 249.

Bloemen, J.B.G.M.: 1985, *Ph. D. Thesis*, University of Leiden.

Bloemen, J.B.G.M., Deul, E.R., and Thaddeus, P.: 1990, *Astron. Astrophys.*, in press.

Boissé, P., Gispert, R., Coron, N., Wijinbergen, J.J., Serra, G., Ryter, C., and Puget, J.L.: 1981, *Astron. Astrophys.* **94**, 265.

Boulanger, F., and Pérault, M.: 1988, *Astrophys. J.* **332**, 328.

Burton, W.B., and Gordon, M.A.: 1978, *Astron. Astrophys.* **63**, 7.

Chi, X., Issa, M.R., Richardson, K.M., Szabelski, J., Wdowczyk, J., and Wolfendale, A.W.: 1989, *J. Phys. G: Nucl. Part. Phys.* **15**, 1495.

Cox, P., Krügel, E., and Mezger, P.G.: 1986, *Astron. Astrophys.* **155**, 380.

Cox, P., and Mezger, P.G.: 1989, *Astron. Astrophys. Rev.* **1**, 49.

Eddington, A.S.: 1926, *Proc. Roy. Soc. A.* **11**, 423.

Freeman, K.C.: 1970, Astrophys. J. **160**, 811.

Gondhalekar, P.M., Phillips, A.P., and Wilson, R.: 1980, *Astron. Astrophys.* **85**, 272.

Güsten, R.: 1980, *Ph. D. Thesis*, University of Bonn.

Güsten, R., and Mezger, P.G.: 1983, *Vistas in Astronomy* **26**, 159.

Hayakawa, S., Ito, K., Matsumoto, T., and Uyama, K.: 1978, *Publ. Astron. Soc. Japan* **30**, 369.

Henry, R.C., Anderson, R.C., and Fastie, W.G.: 1980, *Astrophys. J.* **239**, 859.

Henry, J.P., DePoy, D.L., and Becklin, E.E.: 1984, *Astrophys. J.* **285**, L27.

Jura, M.: 1979, *Astrophys. Lett.* **20**, 89.

Kniffen, D.A., and Fichtel, C.E.: 1981, *Astrophys. J.* **250**, 389.

Kulkarni, S.R., and Heiles, C.: 1987, in *Interstellar Processes*, eds. Hollenbach, D.J., Thronson Jr., H.A., Reidel, Dordrecht, p.87.

Lillie, C.F.: 1968, *Ph. D. Thesis*, University of Wisconsin.

Mathis, J.S., Mezger, P.G., and Panagia, N.: 1983, *Astron. Astrophys.* **128**, 212.

Mattila, K.: 1980a, *Astron. Astrophys. Suppl.* **39**, 53.

Mattila, K.: 1980b, *Astron. Astrophys.* **82**, 373.

Mezger, P.G.: 1978, *Astron. Astrophys.* **70**, 565.

Okuda, H.: 1981, in *Infrared Astronomy*, eds. Wynn-Williams, C. G., Cruikshank, D.P., Reidel, Dordrecht, p.247.

Price, S.D.: 1981, *Astron. J.* **86**, 193.

Riley, P.A., and Wolfendale, A.W.: 1984, *J. Phys. G: Nucl. Phys.* **10**, 1149.

Scoville, N.Z., and Sanders, D.B.: 1987, in: *Interstellar Processes*, eds. D.J. Hollenbach and H.A. Thronson Jr., Reidel, Dordrecht, p.21.

Trumpler, R.J.: 1930, *Publ. Astr. Soc. Pac.* **42**, 267.

Werner, M.W., and Salpeter, E.E.: 1969, *Mon. Not. R. astr. Soc.* **145**, 249.

Acknowledgements